# ISIAC 2025

**29th International Symposium on Ion-Atom Collisions**

July 25-27, 2025 / Uji, Kyoto, Japan

# SCIENTIFIC PROGRAM

# Scope and Mission

**The International Symposium on Ion-Atom Collisions (ISIAC)** is a biennial satellite of the International Conference on Photonic, Electronic and Atomic Collisions (ICPEAC). This year the ICPEAC34 will be held shortly after the ISIAC in Sapporo, Japan.

The ISIAC brings together world-leading experts in the field of atomic collision physics involving heavy projectiles (ions). The scope includes the following topics:

- Fundamental processes in ion-atom and ion-molecule collisions
- Ion-surface and ion-solid interactions
- Fragmentation of molecules and clusters
- Ion-biomolecule interactions
- Laser-assisted collisions
- Atomic collision processes
- New developments, techniques and instrumentation
- Applications, including hadron therapy

Previous ISIAC meetings were held in Rolla(2023), Cluj/online (2021), Paris (2019), Palm Cove (2017), Barcelona (2015), Beijing (2013), Caen (2011), Norfolk (2009), Agios Nikolaos (2007), Rio de Janeiro (2005), ...

# Website

https://ion-beam.jp/isiac2025

# Contact

**ISIAC2025 Local Organizing Committee**
Quantum Science and Engineering Center, Kyoto University

**Address:** Gokasho, Uji, Kyoto 611-0011, JAPAN
**Email:** isiac2025@ion-beam.jp

# Sponsors

Inoue Foundation for Science

The Kyoto University Foundation


This program is supported by a subsidy from Kyoto Prefecture and Kyoto Convention & Visitors Bureau.




# Supported by

The Atomic Collision Society of Japan

The Physical Society of Japan

The Japan Society of Applied Physics

# International Advisory Committee

- Toshiyuki Azuma (RIKEN, Japan)
- Manolis Benis (University of Ioannina, Greece)
- Amine Cassimi (Centre de Recherche sur les Ions, les Matériaux et la Photonique, France)
- Alain Dubois (Sorbonne University, France)
- Daniel Fischer (Missouri University of Science and Technology, USA)
- Omar Fojon (Instituto de Física Rosario, Argentina)
- Pedro Luis Grande (Universidade Federal do Rio Grande do Sul, Brazil)
- Laszlo Gulyas (Institute of Nuclear Research of the Hungarian Academy of Sciences, Hungary)
- Clara Illescas (Universidad Autonoma de Madrid, Spain)
- Alisher Kadyrov (Curtin University, Australia)
- Xinwen Ma (Chinese Academy of Sciences, China)
- Ladislau Nagy (Babeş-Bolyai University, Romania)
- Rita Prosmiti (Instituto de Fisica Fundamental, Spain)
- Markus Schoeffler (Johann Wolfgang Goethe-Universität, Germany)
- Michael Schulz (Missouri University of Science and Technology, USA)
- Lokesh Tribedi (Tata Institute of Fundamental Research, India)
- Alexander Voitkiv (Heinrich-Heine-University of Düsseldorf, Germany)
- Wania Wolff (Universidade Federal do Rio de Janeiro, Brazil)
- Yong Wu (Institute of Applied Physics and Computational Mathematics, China)

# Local Organizing Committee

- Manabu Saito (Kyoto University, Co-Chair)
- Takuya Majima (Kyoto University, Co-Chair)
- Toshiyuki Azuma (RIKEN)
- Makoto Alex Imai (Kyoto University)
- Kunikazu Ishii (Nara Women's University)
- Yoshiaki Kumagai (Nara Women's University)
- Yoichi Nakai (RIKEN)
- Kaoru Nakajima (Kyoto University)
- Shigeo Tomita (Tsukuba University)
- Hidetsugu Tsuchida (Kyoto University)

# Conference Venue

The symposium will take place at Kihada Hall (Uji Obaku Plaza), located on the Uji Campus of Kyoto University. The Uji Campus is the second campus of Kyoto University, located in Uji City, Kyoto Prefecture.

- Address: Gokasho, Uji, Kyoto 611-0011, Japan

**Access from Central Kyoto to the Conference Venue**

The conference venue, Kyoto University Uji Campus, can be conveniently reached by train from Kyoto City. The nearest stations are JR Nara Line's “Obaku Station” and Keihan Uji Line's “Obaku Station”, both within walking distance of the campus.

**Wi-Fi**

eduroam is available at the conference venue. If you do not have a valid eduroam account, a guest account can be issued upon request at the registration desk.

# Conference Dinner

The Conference Dinner will be held on the evening of July 26 (Saturday) at Kyoryori Ujigawa, a traditional Japanese restaurant located near the UNESCO World Heritage Site Byodoin Temple. Participants can travel by a chartered shuttle bus departing from the conference venue, or alternatively by train (Keihan Obaku Station → Uji Station). Detailed information will be provided during the meeting. We hope you will enjoy the seasonal Japanese cuisine and relaxed atmosphere by the Uji River.

For those arriving by train, the restaurant is about a 4-minute walk from Keihan Uji Station and about an 8-minute walk from JR Uji Station.

Google Maps

JR Obaku Station — Conference Venue (Kihada Hall)

Walk 450 m, 6 min


via unnamed roads — 6 min, 450 m

Mostly flat

Google Maps

## Keihan Obaku Station — Conference Venue (Kihada Hall)

Walk 500 m, 6 min

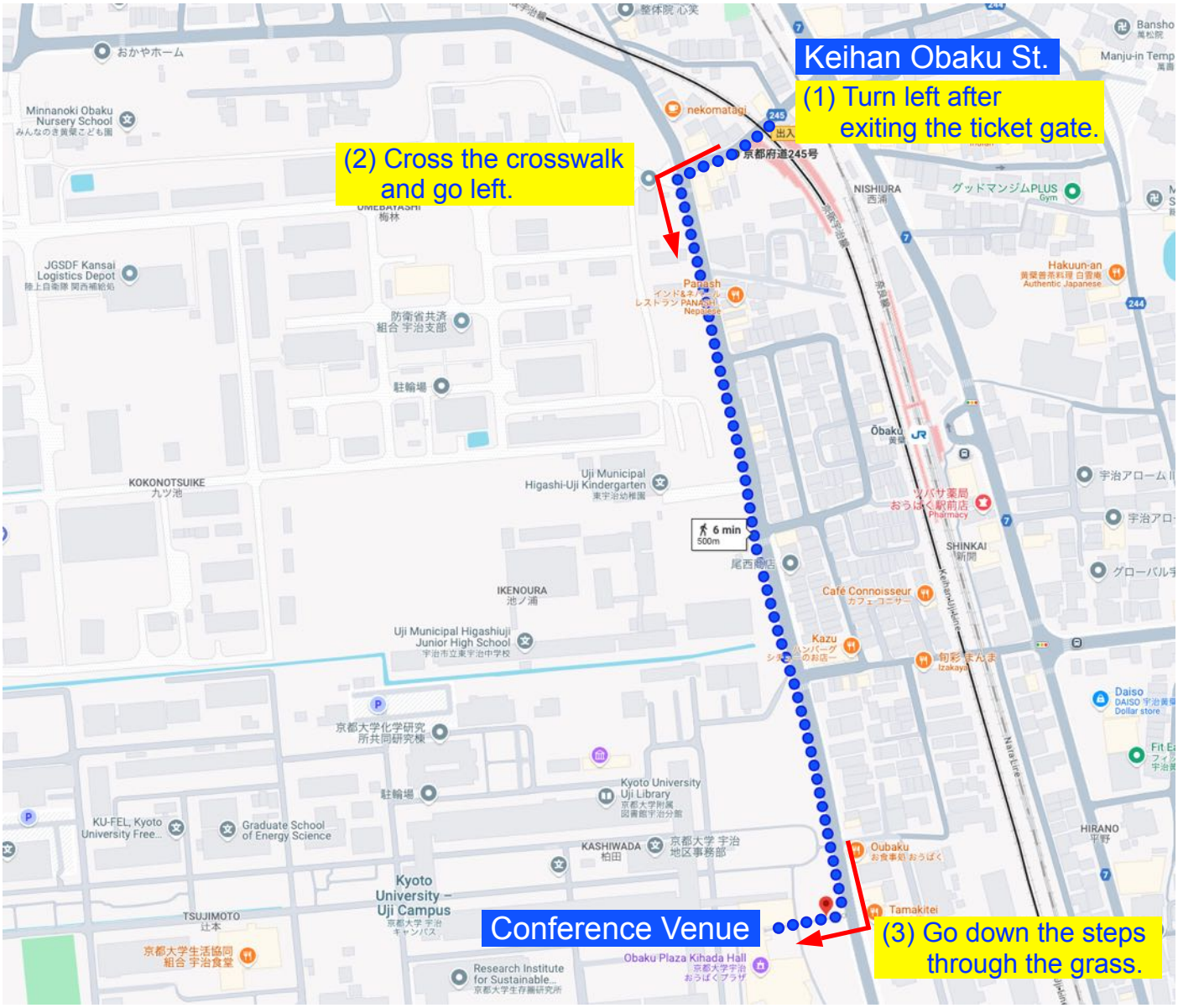


| | | |
|---|---|---|
| via unnamed roads | 6 min | 500 m |

Mostly flat

# Access to the Conference Dinner Venue (Kyoryori Ujigawa) from Uji Stations (Keihan & JR)

Google Maps

Keihan Uji Station — Kyoryori Ujigawa
Walk 300 m, 4 min

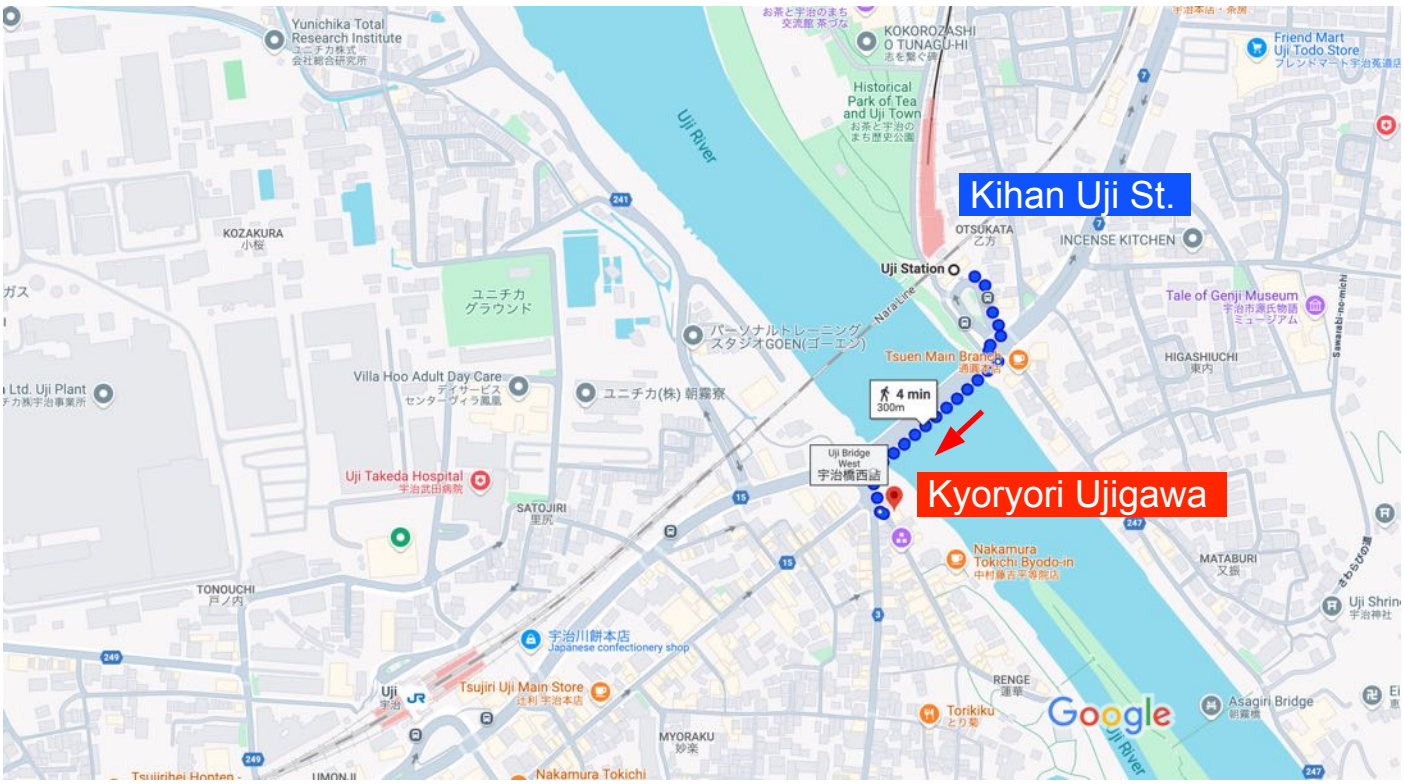


Map data ©2025 100 m

Google Maps

JR Uji Station — Kyoryori Ujigawa
Walk 600 m, 8 min

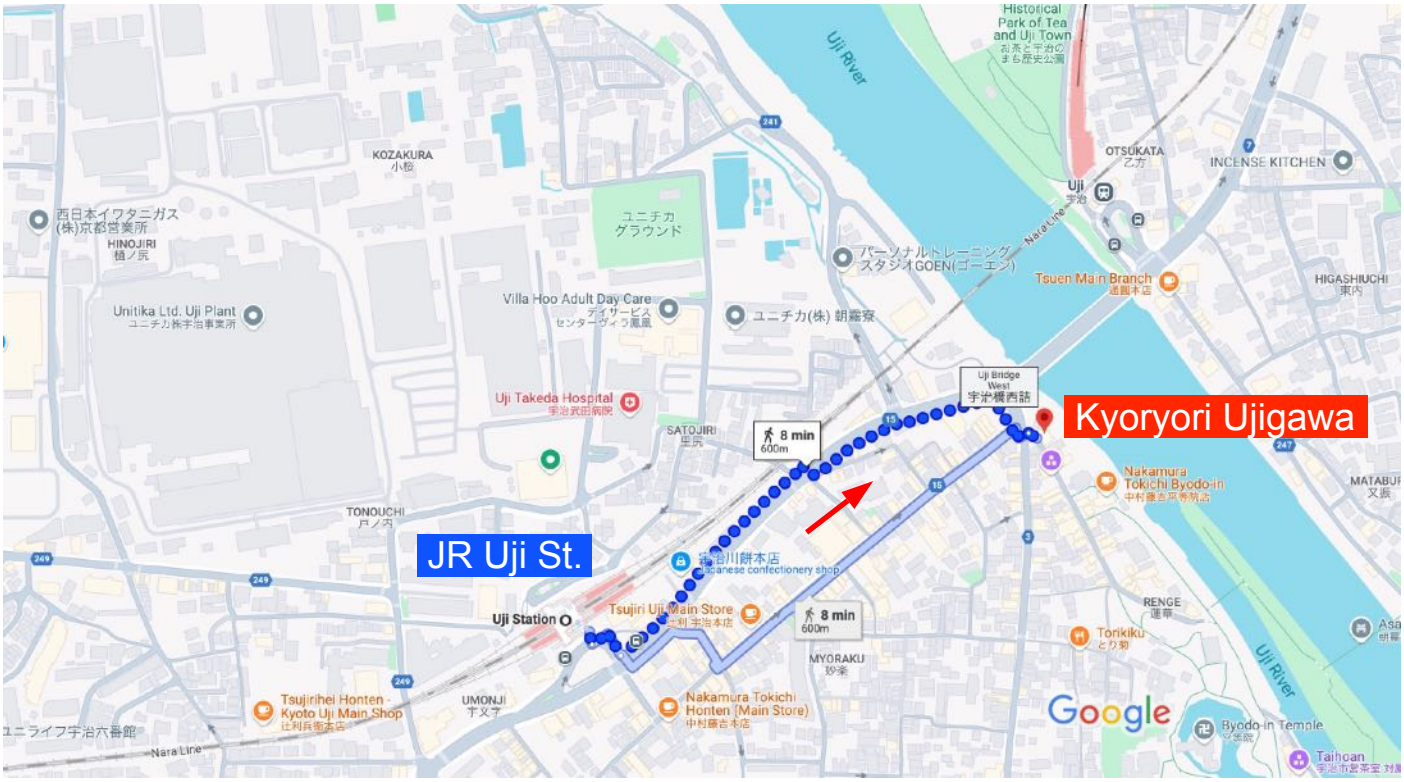

**29th International Symposium on Ion-Atom Collisions (ISIAC 2025)**

July 25-27, 2025 / Uji, Kyoto, Japan

ver.2

## July 25 (Fri.)

| | | |
|---|---|---|
| 12:00 – 13:30 | | Registration |
| 13:40 | | Opening |
| 13:50 | Session 1 * Chair: *Nagy* | *Xiaolong Zhu (I-01)* |
| 14:20 | | *Nicolas Sisourat (I-03)* |
| 14:50 | | *Corey T Plowman (O-01)* |
| 15:10 | | Coffee Break |
| 15:30 | Session 2 Chair: *Ma* | *Christophe Prigent (I-04)* |
| 16:00 | | *Md Abul Kalam Azad Siddiki (I-05)* |
| 16:30 | | *Karoly Tokesi (O-02)* |
| 16:50 | | Short Break |
| 17:00 | | Business Meeting |
| 17:30 – 20:00 | | Welcome Cocktail & Poster Session 1 |

* I-02 has been cancelled.

## July 26 (Sat.)

| | | |
|---|---|---|
| 9:15 | | Annoucements |
| 9:20 | Session 3 Chair: *Montanari* | *Shruti Majumdar (I-06)* |
| 9:50 | | *Ana Beatriz Monteiro-Carvalho (I-07)* |
| 10:20 | | *Zoltán Juhász (O-03)* |
| 10:40 | | Coffee Break |
| 11:00 | Session 4 Chair: *Kadyrov* | *Alexander Voitkiv (I-08)* |
| 11:30 | | *Xiaoqing Hu (I-09)* |
| 12:00 | | *Ann E Orel (O-04)* |
| 12:20 | | Group Photo |
| 12:40 – 14:20 | | Lunch & Poster Session 2 |
| 14:20 | Session 5 Chair: *Voitkiv* | *Shenyue Xu (I-10)* |
| 14:50 | | *Tom Kirchner (I-11)* |
| 15:20 | | *Sankar De (O-05)* |
| 15:40 | | *Tomohiko Nakao (O-06)* |
| 16:00 | | Coffee Break |
| 16:20 | Session 6 Chair: *Orel* | *Baoren Wei (I-12)* |
| 16:50 | | *Nicholas W Antonio (I-13)* |
| 17:20 | | *Junwen Gao (O-07)* |
| 17:40 | | Transportation<br>by Shuttle bus<br>by Train (Keihan Uji Line: Obaku --> Uji) |
| 19:00 – 21:00 | | Conference Dinner<br>Kyoryori Ujigawa<br>(near Byodoin Temple) |

## July 27 (Sun.)

| | | |
|---|---|---|
| 9:15 | | Annoucements |
| 9:20 | Session7 Chair: *Cassimi* | *Teruaki Konishi (I-14)* |
| 9:50 | | *Yusuke Matsuya (I-15)* |
| 10:20 | | *Sergio Diaz-Tendero (O-08)* |
| 10:40 | | Coffee Break |
| 11:00 | Session 8 Chair: *Dubois* | *Henrique Fonteles (I-16)* |
| 11:30 | | *Hiroshi Amekura (I-17)* |
| 12:00 | | *Silvina Segui (O-09)* |
| 12:20 | | Closing |

## **Day 1** (Friday 25 July 2025)

12:00 Registration

13:40 Opening

### **Session 1** Chair: Ladislau Nagy (Babeş-Bolyai University, Romania)

13:50 ***Direct evidence of breakdown of spin statistics in ion-atom charge-exchange collisions*** (I-01)

Xiaolong Zhu (Chinese Academy of Sciences, China)

14:20 ***Antiproton collisions from a fully-correlated time-dependent approach*** (I-03)

Nicolas Sisourat (Sorbonne Université, France)

14:50 ***Excitation of ground-state helium by proton impact*** (O-01)

Corey T. Plowman (Curtin University, Australia)

15:10 Coffee Break

### **Session 2** Chair: Xinwen Ma (Chinese Academy of Sciences, China)

15:30 ***Ion–atom collisions: a benchmark for reliable ion–ion studies*** (I-04)

Christophe Prigent (CNRS, Sorbonne University, France)

16:00 ***CSR-ReMi—an in-ring cryogenic microscope for electron-ion-projectile coincidence spectroscopy*** (I-05)

Md Abul K. A. Siddiki (Max-Planck Institute for Nuclear Physics, Germany)

16:30 ***Impact-parameter and kinematic-information differential ionisation of argon by positron and electron impact*** (O-02)

Karoly Tökési (HUN-REN Institute for Nuclear Research, Hungary)

16:50 Short Break

17:00 Business Meeting

17:30 Welcome Cocktail & Poster Session 1

20:00 End of Day

## **Dav 2** (Saturdav 26 Julv 2025)

09:15 Announcements

### **Session 3** Chair: Claudia C. Montanari (Univ. de Buenos Aires, Argentina)

09:20 ***Multiply-differential study of vibrational dissociative capture in p + $D_2$ collisions*** (I-06)

Shruti Majumdar (Missouri Univ. of Science & Technology, USA)

09:50 ***$O_2^+$ production coming from $CO_2$ single-event electron impact*** (I-07)

Ana B. Monteiro-Carvalho (Universidade Federal Fluminense, Brazil)

10:20 ***Molecular two-centre interference in $O^+$ + CO collisions and its dependence on target coherence*** (O-03)

Zoltán Juhász (HUN-REN Institute for Nuclear Research, Hungary)

10:40 Coffee Break

### **Session 4** Chair: Alisher Kadyrov (Curtin University, Australia)

11:00 ***Break-up mechanism change in ionisation occurring in non-relativistic atomic collisions*** (I-08)

Alexander Voitkiv (Heinrich-Heine University, Germany)

11:30 ***Impact of dimer environments on non-adiabatic dynamics in transient molecules formed via ion-atom collisions*** (I-09)

Xiaoqing Hu
(Institute of Applied Physics & Computational Mathematics, China)

12:00 ***Low-energy collisions of $H^-$ with $B^+$ or $H^+$*** (O-04)

Ann E. Orel (University of California, Davis, USA)

12:20 Group Photo

12:40 Lunch & Poster Session 2

## **Session 5** Chair: Alexander Voitkiv (Heinrich-Heine University, Germany)

14:20 ***Imaging molecular structures and revealing fragmentation dynamics using highly-charged ions*** (I-10)

Shenyue Xu (Chinese Academy of Sciences, China)

14:50 ***Interatomic Coulombic decay in ion-impact collisions – a theoretical perspective*** (I-11)

Tom Kirchner (York University, Canada)

15:20 ***Intra-molecular scattering within di-iodo-acetylene*** (O-05)

Sankar De (Saha Institute of Nuclear Physics, India)

15:40 ***Delayed fragmentation of polyatomic molecules induced by MeV-ion collisions*** (O-06)

Tomohiko Nakao (Kyoto University, Japan)

16:00 Coffee Break

## **Session 6** Chair: Ann E. Orel (University of California, Davis, USA)

16:20 ***Charge-exchange cross-sections for highly-charged ions colliding with atoms and molecules*** (I-12)

Baoren Wei (Fudan University, China)

16:50 ***Charge exchange & ionisation in impurity-ion collisions with atomic hydrogen*** (I-13)

Nicholas Antonio (Curtin University, Australia)

17:20 ***Double-electron capture into auto-ionising states in $N^{7+}$ + He*** (O-07)

Junwen Gao (Hangzhou Normal University, China)

17:40 Transportation to Conference Dinner

19:00 Conference Dinner – Kyoryori Ujigawa (near Byōdō-in)

## **Day 3** (Sunday 27 July 2025)

09:15 Announcements

### **Session 7** Chair: Amine Cassimi (CIMAP CEA/CNRS, France)

09:20 ***Single-hit microbeam technology for single-cell "rad" biology*** (I-14)

Teruaki Konishi (Nat. Inst. for Quantum Science & Technology, Japan)

09:50 ***Track-structure mode and DNA-damage estimation in PHITS v3.35*** (I-15)

Yusuke Matsuya (Hokkaido University, Japan)

10:20 ***Reactivity in amino-acid clusters induced by ion collisions in the gas phase*** (O-08)

Sergio Díaz-Tendero (Universidad Autónoma de Madrid, Spain)

10:40 Coffee Break

### **Session 8** Chair: Alain Dubois (Sorbonne University, France)

11:00 ***Micro-PIXE for iron mapping in ferroptosis*** (I-16)

Henrique Fonteles (Universidade Federal do Rio Grande do Sul, Brazil)

11:30 ***A mystery of ion tracks in silicon – why monatomic ions (hundreds MeV) do not form tracks but $C_{60}$ ions (60 keV) do*** (I-17)

Hiroshi Amekura (National Institute for Materials Science, Japan)

12:00 ***Stopping of charged particles interacting with a phosphorene monolayer – an ab initio approach*** (O-09)

Silvina Segui (Instituto de Física Enrique Gaviola, CONICET-UNC, Argentina)

12:20 Closing Remarks

## Poster Sessions 1

P-01 ***Relevance of electronic excited states in the ionization and fragmentation dynamics of ferrocene induced in collisions with highly charged ions***

F. Aguilar-Galindo, S. Srivastav, A. Domaracka, M. Jbayli, S. Díaz-Tendero, P. Rousseau, S. Maclot

P-02 ***Theoretical Investigation of $NO^+$ Ion Mobility in Helium Based on the Monchick–Mason Approximation***

L. Aissaoui and I. Ghodbane

P-03 ***Benchmark target excitation and ionisation cross sections for $^-p$ + He($1\,^1S$, $2\,^3S$) collisions***

N. W. Antonio and A. S. Kadyrov

P-04 ***Convergent close-coupling approach to ion collisions with multi-electron targets: Application to $^-p$ + C collisions***

N. W. Antonio and A. S. Kadyrov

P-05 ***K-shell lines of neutral Iron atoms in the central region of the Milky Way resolved by the X-ray astronomy satellite XRISM***

Y. Aoki, K. K. Nobukawa, M. Nobukawa, H. Uchiyama, S. Yamauchi, A. Yoshimoto, T. G. Tsuru, H. Uchida, T. Narita, H. Matsumoto, Y. Kanemaru, Y. Maeda, H. Murakami, M. Sawada, Q. D. Wang

P-06 ***Ab initio high energy interactions for N-$H^+$ and $N^+$-H collisions. Integrated and transport cross sections and stopping power.***

M. Buchowiecki

P-07 ***M-shell X-ray emission for Ho target induced by $Li^{1,2,3+}$ ions***

W. L. He, C. R. Zhang, L. Y. Xie, C. Z. Dong

P-08 ***Theoretical and experimental investigations of projectile excitation to autoionizing states in swift carbon and oxygen ions collisions with helium***

A. Dubois, S. Passalidis, A. Laoutaris S. Nanos, A. Biniskos, E. P. Benis, T. J. M. Zouros

P-09 ***Measurement of ion-induced secondary electron emission from metal surfaces***

T. Fujita, J. Kim, A. Suzuki, M. Matsukuma, M. Hoshino

P-10 ***State-resolved autoionizing double-electron capture in intermediate-energy collisions of $C^{4+}$ (1s2s $^3S$) with He***

D. L. Guo, X. B. Zhu, Y. Gao, K. Z. Lin, X. L. Zhu, D. M. Zhao, R. T. Zhang, H. F. Yu, S. F. Zhang, X. Ma

P-11 ***Quantitative evaluation of argon in vanadium nitride films by non-Rutherford backscattering spectrometry and particle induced x-ray emission***

R. Hasebe, T. Osumi, Y. Gotoh

P-12 ***Contributions of Atomic, Molecular and Sputtering Data Workshop Group for the NIFS database***

H. Tsuchida, M. Goto, T. Hirayama, M. Hoshino, Y. Hoshino, A. Igarashi, A. M. Imai, K. Ishii, D. Kato, M. Kato, N. Kimura, M. Kitajima, T. Kusakabe, T. Kawate, K. Moribayashi, T. Morishita, I. Murakami, B. Peterson, H. A. Sakaue, N. Shimakura, K. Soejima

P-13 ***Cluster effects in collisions of hydrogen cluster ions with $H_2$ molecules***

Y. Bai , T. Wang, J. Zhao, S. T. S. Kovács, P. Herczku, R. Rácz, B. Sulik, S. Biri, G. Lakatos, Z. Juhász

P-14 ***Temperature Dependence of the Electron-Induced Radiolysis of Solid $N_2O$: Applications to Astrochemistry in the Outer Solar System***

Z. Juhász, D. V. Mifsud, S. Góbi, P. Herczku, B. Sulik, S. Ioppolo, N. J. Mason, Gy Tarczay

P-15 ***Connection between atomic excitation and ionisation***

N. W. Antonio, I. Bray, A. S. Kadyrov

P-16 ***Electron capture in collisions of highly charged argon ions with hydrogen atoms***

A. M. Kotian, N. W. Antonio, O. Marchuk, A. S. Kadyrov

P-17 ***Development of a Method for Measuring the Energy Loss of MeV Projectile Ions in a Thin Liquid Water Sheet***

H. Imamura, K. Asano, K. Ishii, Y. Kumagai

P-18 ***Excitation of helium by proton and antiproton impact***

L. Nagy, Zs. Bálint, S. Borbély

P-19 ***Molecular formation through reactions of low-energy molecular ions with an ice surface under low temperature conditions***

Y. Nakai, W.M.C. Sameera, K. Furuya, H. Hidaka, A. Ishibashi, N. Watanabe

## Poster Sessions 2

P-20 ***Stopping power in transition metals, the importance of d-electron contribution***

J. P. Peralta, A. M. P. Mendez, D. M. Mitnik, C. C. Montanari

P-21 ***Machine learning model for K-shell ionisation***

D. M. Mitnik, C. C. Montanari, S. Segui, S. Limandri, J. A. Guzmán, A. Carreras, J. C. Trincavelli

P-22 ***An embedding-based neural network approach for stopping power prediction on multi-elemental targets***

F. Bivort Haiek, D. M. Mitnik, A. M. P. Mendez, J. P. Peralta, C. C. Montanari

P-23 ***The effect of irradiated ion on the swelling phenomenon of 4H-SiC***

T. Okawa, S. Momota, M. Watanabe

P-24 ***Positive and negative secondary ion emission from propanol droplets induced by fast heavy-ion collisions***

S. Otsuka, T. Takemura, H. Tsuchida, M. Saito, T. Majima

P-25 ***Hydrogen mediated heavy atom roaming in negative ion***

DG Piekarski, S. Pataraprasitpon, TFM Luxford, Roman Curík, J. Kocisek

P-26 ***Electronically resolved excitation in proton collisions with $H_2$***

C. T. Plowman, L. H. Scarlett, M. C. Zammit, I. Bray, D. V. Fursa

P-27 ***Evidence for the formation of excited fragments in the three body dissociation of methane***

C. P. Safvan, D. Garg, A. Cassimi, X. Fléchard, J. Rangama, J. Rajput

P-28 ***Charge State Distributions of Ions Transmitted Through a Single-Layer Graphene Sheet under Fast $Li^+$ and $Li_2^+$ Ion Irradiation***

K. Saito, Y. Kumagai, K. Ishii

P-29 ***Experimental K-shell ionization cross sections by electron impact: a comprehensive database for $1 \leq Z \leq 92$***

S. Segui, S. P. Limandri, A. C. Carreras, J. C. Trincavelli, J. A. Guzmán, C. C. Montanari, D. M. Mitnik

P-30 ***Coupled-channel calculations of FDCS for ionisation in 75 keV p + He collisions: Emission of low-energy electrons***

K. H. Spicer, N. W. Antonio, M. S. Schöffler, A. S. Kadyrov

P-31 ***State selective charge-exchange cross sections in collisions between $C^{q+}$ ions with sodium atoms***

K. Tőkési, B. G. Csillag, G. Anda, D. Dunai, D. Nagy, D. I. Réfy, M. Vécsei, S. Zoletnik

P-32 ***Energy loss function of samarium determined from the reflection electron energy loss spectroscopy spectra***

T.F. Yang, R.G. Zeng, L.H. Yang, A. Sulyok, M. Menyhárd, K. Tőkési, Z.J. Ding

P-33 ***Electron capture cross sections in $Ne^{8+}$ ions collision with $H_2$ and He***

K. Tőkési, and Y. WU

P-34 ***Ionization of Noble Gases by Collisions with Fast Molecular Ions Depending on the Molecular Axis Orientation***

M. Umemura, Y. Kumagai, K. Ishii

P-35 ***Collision-induced atomic alignment and magnetic-substate ionization of medium- and high-$Z_t$ elements***

X. Wang, Y. Liu, J. Ren, X. Ren, Y. Zhao, Z. Xu, R. Cheng, G. Xiao

P-36 ***Vicinage effect on convoy electrons from carbon foils under heteronuclear diatomic ion bombardment***

Y. Yano, U. Ozeki, T. Takahashi, S. Ishii, K. Sasa, S. Tomita

P-37 ***Influence of plasma ion state and epitaxial atoms in sputtering system***

Gui-Sheng Zeng and Sheng-Hui Chen

## List of Oral Presentations (Invited and Contributed Talks

Ver.4

| Session # | Session Chair | Slot | Speaker | Title |
|---|---|---|---|---|
| Session 1 | Ladislau Nagy | I-01 | Xiaolong Zhu | Direct evidence of breakdown of spin statistics in ion-atom charge exchange collisions |
| | | I-02* | Malay Purkait [Cancelled] | Electron capture and excitation between hydrogen-like projectile and helium atom [Cancelled] |
| | | I-03 | Nicolas Sisourat | Antiproton collisions from a fully-correlated time-dependent approach |
| | | O-01** | Corey T Plowman | Excitation of ground-state helium by proton impact |
| Session 2 | Xinwen Ma | I-04 | Christophe Prigent | Ion – Atom collisions : a benchmark for reliable Ion – Ion Studies |
| | | I-05 | Md Abul Kalam Azad Siddiki | CSR-ReMi: an in-ring cryogenic reaction microscope for electron-ion-projectile coincidence spectroscopy |
| | | O-02 | Karoly Tokesi | Impact parameter and kinematic information for differential ionization of argon by positron and electron impacts |
| Session 3 | Claudia C Montanari | I-06 | Shruti Majumdar | Multiply differential study of vibrational dissociative capture in p + D2 collisions |
| | | I-07 | Ana Beatriz Monteiro-Carvalho | O2+ Production Coming from CO2 single-event electron impact |
| | | O-03 | Zoltán Juhász | Molecular two-center interference in H+ emission from H2 molecule by O+ ion impact and its dependence on the target coherence |
| Session 4 | Alisher Kadyrov | I-08 | Alexander Voitkiv | Breit interaction vs Coulomb force in ionization occurring in nonrelativistic atomic collisions |
| | | I-09 | Xiaoqing Hu | Impact of Dimer Environments on Nonadiabatic Dynamics in Transient Molecules Formed via Ion-Atom Collisions |
| | | O-04 | Ann E Orel | Low Energy Collisions of H- with B+ or H+ |
| Session 5 | Alexander Voitkiv | I-10 | Shenyue Xu | Imaging molecular structures and revealing fragmentation dynamics using highly charged ions |
| | | I-11 | Tom Kirchner | Interatomic Coulombic decay in ion-impact collisions: a theoretical perspective |
| | | O-05 | Sankar De | Intra-molecular scattering within diiodoacetylene |
| | | O-06 | Tomohiko Nakao | Delayed fragmentation of polyatomic molecules induced by MeV ion collisions |
| Session 6 | Ann E Orel | I-12 | Baoren Wei | Charge exchange cross section for highly charged ions collision with atom and molecule |
| | | I-13 | Nicholas W Antonio | Charge exchange and ionisation in impurity ion collisions with atomic hydrogen |
| | | O-07 | Junwen Gao | Double electron capture into autoionizing states in N7+ and He collisions |
| Session 7 | Amine Cassimi | I-14 | Teruaki Konishi | Single Hit Microbeam Technology for Single Cell “Rad” Biology |
| | | I-15 | Yusuke Matsuya | Track-structure mode and DNA damage estimation in PHITS ver. 3.35 |
| | | O-08 | Sergio Diaz-Tendero | Reactivity in clusters of amino acids induced by ion-collisions in the gas phase |
| Session 8 | Alain Dubois | I-16 | Henrique Fonteles | Micro-PIXE for Iron Mapping in Ferroptosis |
| | | I-17 | Hiroshi Amekura | A mystery of ion tracks in silicon:– Monatomic ions of hundreds MeV do not form but C60 ions of 60 keV do – |
| | | O-09 | Silvina Segui | Stopping of charged particles interacting with a phosphorene monolayer: an ab initio approach |

* I-O2 has been canceled.

** A concern has been raised regarding the originality of certain aspects of this contribution, specifically the use and authorship of the method and software code. The matter is currently under review by the appropriate institutional channels. No determination has been made at this stage, and the presentation will proceed pending further clarification.

## List of Poster Presentations

ver.4

| Session # | ID | Presentor | Title |
|---|---|---|---|
| Poster 1<br>25-Jul<br>17:30 - 20:00 | P-01 | Fernando Aguilar-Galindo | Relevance of electronic excited states in the ionization and fragmentation dynamics of ferrocene induced in collisions with highly charged ions |
| | P-02 | Lamia Aissaoui [Withdrawn] | Theoretical Investigation of NO+ Ion Mobility in Helium Based on the Monchick–Mason Approximation [Withdrawn] |
| | P-03 | Nicholas Wayne Antonio | Benchmark target excitation and ionisation cross sections for p-bar +He(1^1S, 2^3S) collisions |
| | P-04 | Nicholas Wayne Antonio | Convergent close-coupling approach to ion collisions with multi-electron targets: Application to p-bar + C collisions |
| | P-05 | Yuma Aoki | K-shell lines of neutral Iron atoms in the central region of the Milky Way resolved by the X-ray astronomy satellite XRISM |
| | P-06 | Marcin Buchowiecki | Ab initio high energy interactions for N-H+ and N+ -H collisions. Integrated and transport cross sections and stopping power. |
| | P-07 | Chenzhong Dong | M-shell X-ray emission for Ho target induced by Li1,2,3+ ions |
| | P-08 | Alain Dubois | Theoretical and experimental investigations of projectile excitation to autoionizing states in swift carbon and oxygen ions collisions with helium |
| | P-09 | Taiki Fujita | Measurement of ion-induced secondary electron emission from metal surfaces |
| | P-10 | Dalong Guo | State-resolved autoionizing double-electron capture in intermediate-energy collisions of C4+ (1s2s 3S) with He |
| | P-11 | Ryo Hasebe | Quantitative evaluation of argon in vanadium nitride films by non-Rutherford backscattering spectrometry and particle induced x-ray emission |
| | P-12 | Masamitsu Hoshino | Contributions of Atomic, Molecular and Sputtering Data Workshop Group for the NIFS database |
| | P-13 | Zoltán Juhász | Cluster effects in collisions of hydrogen cluster ions with H2 molecules |
| | P-14 | Zoltán Juhász | Temperature Dependence of the Electron-Induced Radiolysis of Solid N2O: Applications to Astrochemistry in the Outer Solar System |
| | P-15 | Alisher Kadyrov | Connection between atomic excitation and ionisation |
| | P-16 | Akshit Mahesh Kotian | Electron capture in collisions of highly charged argon ions with hydrogen atoms |
| | P-17 | Yoshiaki Kumagai | Development of a Method for Measuring the Energy Loss of MeV Projectile Ions in a Thin Liquid Water Sheet |
| | P-18 | Ladislau Nagy | Excitation of helium by proton and antiproton impact |
| | P-19 | Yoichi Nakai | Molecular formation through reactions of low-energy molecular ions with an ice surface under low temperature conditions |
| Poster 2<br>26-Jul<br>12:40 - 14:20 | P-20 | Claudia Carmen Montanari | Stopping power in transition metals, the importance of d-electron contribution |
| | P-21 | Claudia Carmen Montanari | Machine learning model for K-shell ionisation |
| | P-22 | Claudia Carmen Montanari | An Embedding-based Neural Network Approach for Allowing Stopping Power Prediction on Multi-elemental targets |
| | P-23 | Taiki Okawa | The effect of irradiated ion on the swelling phenomenon of 4H-SiC |
| | P-24 | Sota Otsuka | Positive and negative secondary ion emission from propanol droplets induced by fast heavy-ion collisions |
| | P-25 | Dariusz Grzegorz Piekarski | Induced Chemistry of triazole derivatives |
| | P-26 | Corey T Plowman | Electronically resolved excitation in proton collisions with H2 |
| | P-27 | Cholakka Parambath safvan | Evidence for the formation of excited fragments in the three body dissociation of methane |
| | P-28 | Kanae Saito | Charge State Distributions of Ions Transmitted Through a Single-Layer Graphene Sheet under Fast Li+ and Li2+ Ion Irradiation |
| | P-29 | Silvina Segui | Experimental K-shell ionization cross sections by electron impact: a comprehensive database for 1 ≤Z ≤92 |
| | P-30 | Kade Spicer | Coupled-channel calculations of FDCS for ionisation in 75 keV p + He collisions: Emission of low-energy electrons |
| | P-31 | Karoly Tokesi | State selective charge-exchange cross sections in collisions between Cq+ ions with sodium atoms |
| | P-32 | Karoly Tokesi | Energy loss function of samarium determined from the reflection electron energy loss spectroscopy spectra |
| | P-33 | Karoly Tokesi | Electron capture cross sections in Ne8+ ions collision with H2 and He |
| | P-34 | Mayumi Umemura | Ionization of Noble Gases by Collisions with Fast Molecular Ions Depending on the Molecular Axis Orientation |
| | P-35 | Xing Wang | Collision-induced atomic alignment and magnetic-substate ionization of medium- and high-Zt elements |
| | P-36 | Yuichiro Yano | Vicinage effect on convoy electrons from carbon foils under heteronuclear diatomic ion bombardment |
| | P-37 | Gui-Sheng Zeng | Influence of plasma ion state and epitaxial atoms in sputtering system |

# Abstracts
## (Invited Talks)

I-01

# Direct evidence of breakdown of spin statistics in ion-atom charge exchange collisions

**XiaoLong Zhu[1,2], Shaofeng Zhang[1,2], Yong Gao[1,2], Dalong Guo[1,2], Jiawei Xu[3], Ruitian Zhang[1,2], Dongmei Zhao[1], Kaizhao Lin[1], Xubin Zhu[1,2], Dadi Xing[1,4], Shucheng Cui[1,4], Stylianos Passalidis[5], Alain Dubois[5,*], and X.Ma[1,2,*]**

[1]Institute of Modern Physics, Chinese Academy of Sciences, Lanzhou 730000, China
[2]University of Chinese Academy of Sciences, Beijing, 100049, China
[3]Advanced Energy Science and Technology, Guangdong Laboratory, Huizhou 516000, China
[4] College of Physics and Electronic Engineering, Northwest Normal University, Lanzhou, 730070, China
[5]Sorbonne Université, CNRS, Laboratoire de Chimie Physique-Matière et Rayonnement, F-75005 Paris, France

**Synopsis** Recent experimental studies have questioned the validity of spin statistics assumptions, particularly in charge exchange processes occurring in atomic MeV collisions. Here, we study spin-resolved single electron capture processes in collisions between $C^{3+}$ ions and helium within an energy range of 1.25–400 keV/u. Using high resolution reaction microscope and multielectronic theoretical approaches, we directly measure and calculate the true population information of the $C^{2+}(1s^2 2s2p\ ^{1,3}P)$ states at the time of electron capture, overcoming the previous experimental and theoretical difficulties. At the level of integral and scattering angle differential cross sections, our results demonstrate the breakdown of pure spin statistics arguments.

The coupling between the charge and spin degrees of freedom of electrons plays a pivotal role in the understanding of the dynamics of atomic and molecular interactions. They are of fundamental importance to interpret the experimental results across various domains. To model these systems and the atomic processes that take place within them, electronic structures and dynamics are often treated approximatel. Spin statistics approximation may then be involved, i.e., the cross sections for the production of states corresponding to a given electronic configuration are weighted on their respective spin degeneracy.

Recent experimental investigations have increasingly challenged the validity of such statistical population assumptions, particularly in charge exchange (electron capture) processes occurring during atomic/molecular collisions [1,2]. In this context, the Reaction Microscope (ReMi) methodology has emerged as a crucial experimental technique capable of directly probing initial electron capture state populations across broad energy ranges. This capability positions ReMi as a pivotal tool for resolving the longstanding spin statistics puzzle in collision-induced charge transfer phenomena.

The investigation is performed both experimentally, employing ReMi technique, and theoretically, within a semiclassical three-electron close-coupling approach. The originality of our investigation is to allow for the direct measurement and comparison of the true population information of the $C^{2+}(1s^2 2l2l'\ ^{1,3}L)$ states at the time of electron capture, without any further data processing to take into account post-collisional effects, as radiative cascade. The cross-section ratio R, between the triplet 2s2p $^3$P and the singlet 2s2p $^1$P capture states, reveals a pronounced energy dependence of the ratio in both approaches, demonstrating a breakdown of pure spin statistics arguments in single electron capture process. Theoretical calculations using a restricted two-electron approach fail to reproduce the energy dependence of the R ratio, highlighting the importance of multielectronic spin-resolved approaches and close-coupling schemes to describe such detailed collisional information. For a detailed discussion of the measurements and calculations, see the published paper [3].

This work was supported by the National Key R&D Program of China under Grant No. 2022YFA1602500, the Strategic Priority Research Program of Chinese Academy of Sciences (Grant No. XDB34020000), and the NSFC of China under Grants No. 11974358 and No. 11934004.

## References

[1] I. Madesis *et al.,* 2020 *PRL* **124** 113401
[2] J. A. Tanis *et al.,*2004 *PRL* **92**, 133201
[3] X L Zhu *et al* 2024 *PRL.* **133** 224

* E-mail: alain.dubois@sorbonne-universite.fr; x.ma@impcas.ac.cn

I-02

# Electron capture and excitation between hydrogen-like projectile and helium atom

**M Purkait**

[1]Department of Physics, Ramakrishna Mission Residential College, Narendrapur, Kolkata-700103, India

**Synopsis** The post and prior version of the four-body boundary corrected continuum intermediate state approximation is applied to calculate the cross sections for electron capture and excitation at intermediate and high impact energies. The initial state of the target active electron is described by a Roothan-Hartree-Fock (RHF) wavefunction. The dynamic correlations explicitly taken into account through the prior form of the complete perturbation potential. The state-selective total projectile angular differential cross sections are calculated and compared with available experimental results. We find a mixed agreement with the experimental data.

For many decades, single-electron-capture (SEC) from one and multi-electron atoms colliding with hydrogen-like projectiles has been investigated theoretically and experimentally because of its fundamental nature. The development of the innovative experimental technique of reaction microscopic renewed this field of ion-atom collision. Many experimental studies of this reaction in the past decade provided valuable data for the applied area and the most significant test for the theoretical models. State-selective electron transfer and excitation in $He^+ - He$ collisions were studied theoretically using a three-electron semi-classical atomic-orbital close-coupling method (SCAOCC) [1] in the energy range varying from 1 to 225 keV/amu. Their calculations show a prominent oscillatory structure in the energy dependence of the integral cross sections, which was explored due to the strong competition between the target-excitation and projectile excitation processes. Later, they have extended the same work by calculating the spin dependent cross sections for PE and TE [2]. Recently, Igarashi and Kato [3] have applied the atomic-orbital close-coupling calculation based on three active electrons, so called AOCC3e for the same collision. Their results were generally in good agreement with the experimental results. So, our work is focused on this collision process by using boundary corrected continuum intermediate state (BCCIS) method. Here one set of results are displayed in Fig.1.

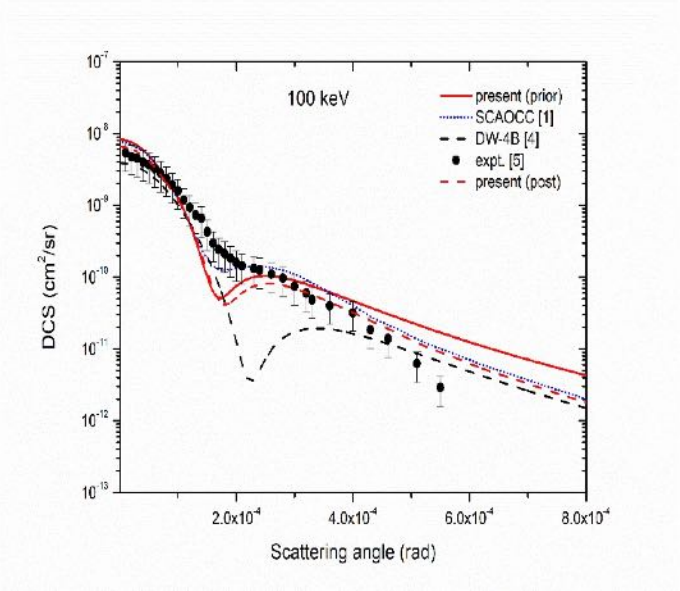


**Figure 1**. Projectile angular differential cross section in $cm^2$/sr for $He^+$-He collision as a function of scattering angle.

Acknowledgement: This work was supported by Anusandhan National Research Foundation (ANRF), New Delhi, India, Under grant no: CRG/2022/001668.

**References**

[1] Gao *et al* 2018 *Phys. Rev. A* **97** 052709

[2] Gao *et al* 2021 *Matter. Radiat. Extremes*. **6** 014404

[3] Igarashi A and Kato D 2024 *Eur. Phys. J. D* **78** 79

[4] Samaddar S *et al* 2020 *J. Phys. B: At. Mol. Opt. Phys*. **53** 245202

[5] Guo D L *et al* 2017 *Phys. Rev. A* **97** 052709

*E-mail: mpurkait_2007@rediffmail.com

I-03

# Antiproton collisions from a fully-correlated time-dependent approach

**N. Sisourat**[1] *

[1]Sorbonne Université, CNRS, Laboratoire de Chimie Physique-Matière et Rayonnement, 75005, Paris, France
[2]Affiliation with laboratory and/or university name, city, zip code, country

**Synopsis** We have investigated antiproton collisions with atoms and molecules in the keV energy range. Using a correlated approach in which all electrons are active, we have computed the single and double ionization cross-sections for various complex systems.

Collisions between antiprotons and atoms and molecules have recently attracted a renewed attention. From a fundamental point of view, these collisions are central to understand the physics of antimatter. For applications, processes occurring in a single antiproton collision are responsible for the slowing down and thus energy deposition of the ions into solids, which is relevant in material science and radiation therapy (see [3,4] and references therein for more on antiproton collision physics and its applications).

In these context, we have recently developed an ab initio model to describe single and double ionization processes in antiproton collisions with atoms and molecules (see [1,2]). Our model is based on a fully correlated close-coupling approach and a Dyson orbital analysis. Furthermore, we introduce the concept of correlation integral in order to quantify and gain insights into the effects of electronic correlation on the ionization processes. Our model has been applied to various collision systems. During the talk, I will present our ab initio model, and report on we have learned so far using it.

## References

[1] C. Jia *et al.* 2023 *Phys. Rev. A* **107** 012808
[2] C. Jia *et al.* 2024 *Phys. Rev. A* **110** 012803
[3] T. Kirchner and H. Knudsen,2011 *J. Phys. B: At., Mol. Opt. Phys.* **44** 122001.
[4] T. Kirchner, in Ion-Atom Collisions: The Few-Body Problem in Dynamic Systems, edited by M. Schulz (De Gruyter, Berlin, Boston, 2019).

*E-mail: Nicolas.Sisourat@sorbonne-universite.fr

I-04

# Ion – Atom collision: a benchmark for reliable Ion – Ion Studies

**C Prigent[1] *, J-Y Chesnel[2], A Gumberidze[3], M. Lestinsky[3], M Jolly[1], A Méry[2], A. de Montbel[1], J-M Ramillon[2], J Rangama[2], S Steydli[1], T Stöhlker[3,4], M Trassinelli[1], D Vernhet[1], and E Lamour[1]**

[1]Institut des NanoSciences de Paris, CNRS, Sorbonne Université, Paris 75005 France
[2]CIMAP, CEA/CNRS/ENSICAEN/Université de Caen Normandie, Caen, 14050, France
[3]GSI Helmholtzzentrum für Schwerionenforschung, Darmstadt, 64291, Germany
[4]Helmholtz Institute Jena and Friedrich Schiller University of Jena, Jena, 07743, Germany

**Synopsis** The importance of electronic processes such as ionization, excitation and capture in many research domains such as fusion, plasma and accelerator physics or even hadrontherapy is widely recognized. Despite the availability of charge exchange cross section data in ion-atom interaction, there is a lack of experimental data in the field of ion – ion collisions, which very often occur in plasma environment. We are developing an experimental program combined with theoretical developments to investigate these collisions from the low (keV/u-keV/u) to the intermediate (MeV/u-keV/u) energy domain.

Ion-ion collisions are among the fundamental processes in all types of plasma in astrophysical objects as well as in the laboratory (e.g. thermonuclear fusion). Their modeling requires details of all relevant atomic processes and knowledge of ion-ion cross sections is therefore essential [1]. Compared to the ion-atom collisions studied since the early 30's, ion-ion collisions correspond to a relatively young field of physics, started in the 80's and mainly dedicated in the keV/u–keV/u domain and/or for low charged systems [2]. In recent years, we have proposed a new program called the FISIC project (Fast Ion Slow Ion Collision [3]) in which a keV/u ion beam platform including an electron cyclotron ion source (Supernanogan type) and its transport beamline is to be connected to the CRYRING storage ring at GSI with MeV/u ion beams to perform crossed-beam experiments in the intermediate velocity regime.

The study of ion-ion collisions is still in its infancy due to the fact that the preparation and detection of a single event always represents a challenging experiment. Inherent difficulties are due to the low density of the target provided by the ion beam. Even under ultra-high vacuum conditions ($10^{-10}$ mbar) in the interaction region, the residual gas density exceeds the ion beam densities (~$10^5$ - $10^6$ particles.cm$^{-3}$). These conditions not only result in low signal count rates (typically between 1 and 100 s$^{-1}$), but also in poor signal-to-background ratios (typically $10^{-2}$ - $10^{-4}$). A high degree of ion beam purity, with well defined shape and optics, combined with coincidence measurements, is therefore mandatory.

In this perspective, we have built a new fully electrostatic purification system (with an omega shape) to get rid of electron capture occurring along the low-energy beam line. This purification system will be installed upstream of the collision chamber to control the "pure" charged state of the incoming beam. In addition, a new electrostatic analyzer has been developed to simultaneously monitor the current of the main beam (in the µAe range) and measure the charge state distribution of ions downstream the collision point (in the fAe range). All these devices have been tested at the ARIBE/GANIL facility over the past few years. Using well-known data of ion-atom cross sections with residual gas, we have been able to obtain quantitative measurements of their performance and limitations [4-5].

Finally, the FISIC plateform is now connected to the SIMPA facility (acronym for Source d'Ions Mulitchargés de PAris) to perform ion-ion collisions in the keV/u-keV/u energy range using x-ray spectroscopy in coincidence with ion spectroscopy [6]. This enables all the devices of the low energy branch of the FISIC project to be tested at the same time. In the future, new cross sections will be measured with highly charged ions, using ion-atom collisions as a benchmark.

**References**

[1] Brouillard F (Ed) 1986 Atomic Processes in Electron-Ion and Ion-Ion Collisions
[2] Bräuning H *et al* 2005 *AIP Conf Proc.* **77** 219
[3] Aumayr F *et al* 2018 *J. Phys. B: At. Mol. Opt. Phys.* **52** 171003
[4] Schury D *et al* 2019 *Rev. Sci. Instrum.* **90** 083306
[5] Jolly M *et al* 2022 *Atoms* **10**(4) 146
[6] M. Joly 2024 PhD Thesis Sorbonne Université

* E-mail: prigent@insp.jussieu.fr

I-05

# CSR-ReMi: an in-ring cryogenic reaction microscope for electron-ion-projectile coincidence spectroscopy

**MAKA Siddiki[1]*, F Herrmann[1], M Schulz[1], W Zhang[1], A Dorn[1], M Grieser[1], O Novotny[1], H Kreckel[1], F Grussie[1], C Medina[1], DV Chicharro[1], F Trost[1], A Wolf[1], T Pfeifer[1], CD Schröter[1], and R Moshammer[1]**

[1]Max Planck Institute for Nuclear Physics, Saupfercheckweg 1, 69117 Heidelberg, Germany

**Synopsis** Recently, a reaction microscope has been successfully commissioned in the cryogenic storage ring (CSR) at the Max Planck Institute for Nuclear Physics (MPIK) in Heidelberg. We present the initial measurements and results of electron capture and electron detachment processes in slow ion-atom/molecule collisions.

Fragmentation of small quantum systems (e.g., atoms, molecules, and clusters) in the presence of external perturbations is a fundamental aspect to understand few-body quantum dynamics [1]. Very often, the dynamical features of collisions (e.g., many-body correlations, impact parameter dependencies) are not directly accessible from absolute cross-section measurements, which are unfolded by the single- or multiple-differential cross-sections. Therefore, fully differential cross-sections with $4\pi$ sr solid angle coverage are essential for probing the underlying collision processes (e.g., ionization, capture, loss, etc.) and provide a stringent test of the theory. A Reaction Microscope (ReMi) [2] enables the study of kinematically complete measurements by reconstructing the three-dimensional momentum components of all fragment products (i.e., recoil ions, electrons) in coincidence with high resolution. On the other hand, a cryogenic storage ring enables quantum-state-selective (electronic, vibrational, and rotational) experiments with stored and cooled molecular ions (both cations and anions) [3]. Hence, the recent addition of the reaction microscope in the cryogenic storage ring (CSR) [4] (the so-called CSR-ReMi [5,6]) allows state-selective differential cross-section measurements, providing insight into the ongoing collision dynamics. Additionally, the prolonged storage time in the cryogenic environment opens up the possibility of observing specific relaxation mechanisms (e.g., vibrational autodetachment) through electron spectroscopy.

The CSR-ReMi offers the opportunity to study collision as well as light-induced breakup processes of small quantum systems with stored and cooled ion beams. The construction of the spectrometer, featuring individual controllable electrodes, enables the operation of the spectrometer in various modes (e.g., single-field, three-dimensional space and time focusing, and velocity map imaging [7]) as required for measuring physical processes. As an example, we studied the state-selective electron capture process in slow ion-atom/molecule collisions (e.g., $Ar^+$-Ar collision system). The manifold, differentially pumped, and well-collimated internal gas jet target allows high-resolution Q-value measurements. For anion-atom/molecule collisions, projectile electron detachment with simultaneous target ionization has been studied systematically to probe the threshold behavior. The signature of the correlated (i.e., electron-electron interaction) process indicates the role of the anions' Compton profile below the threshold [6]. This talk will present the first few atomic collision measurements studied at CSR-ReMi and also provide a future perspective on storage-ring-based experiments.

*E-mail: md.siddiki@mpi-hd.mpg.de

## References

[1] Ullrich *et al.*, 2003 *Springer Berlin, Heidelberg* 978-3-662-08492-2
[2] Ullrich *et al.* 2003 *Rep. Prog. Phys.* **66** 1463
[3] Oldřich Novotný *et al.* 2019 *Science* **365** 676-679
[4] von Hahn R *et al.* 2016 *Rev. Sci. Instrum.* **87** 063115
[5] Schulz M *et al.* 2024 *Phys. Rev. A* **110** 022818
[6] Herrmann F *et al.* 2025 *Phys. Rev. Research* **7** L012082
[7] Ben-Shabo Y, *et al.* 2023 *Phys. Chem. Chem. Phys* **25** 25122-25129

I-06

# Multiply differential study of vibrational dissociative capture in $p + D_2$ collisions

**S. Majumdar[1]*, A. Hasan[2], S. Bastola[3], B. R. Lamichhane[4], R. Lomsadze[5] and M. Schulz [1,6]**

[1]Physics Department and LAMOR, Missouri University of Science & Technology, Rolla, MO 65409, USA
[2]Department of Physics, UAE University, P.O. Box 15551, Al Ain, Abu Dhabi, United Arab Emirates
[3]Embry-Riddle Aeronautical University, Daytona Beach, FL 32114, USA
[4]Eckerd College, St. Petersburg, FL 33711, USA
[5]Tbilisi State University, 1 Ilia Chavchavadze Avenue, Tbilisi 0179, Georgia
[6]Max Planck Institute for Nuclear Physics, 69117 Heidelberg, Germany

**Synopsis** Fully differential cross sections (FDCS) have been measured for vibrational dissociative capture in 75 KeV proton and Deuterium collision.

We have measured fully momentum analyzed projectiles and $D^+$ fragments produced in $p+D_2$ collisions in coincidence. From the data, we extracted fully differential cross sections (FDCS) for vibrational dissociative capture as a function of projectile scattering angle $\theta_p$. A pronounced molecular two-center interference pattern was observed. It is due to indistinguishable projectile diffraction from the two atomic centers of the molecule.

Earlier, we found a similar interference pattern for $p + H_2$ collisions [1]. A surprising result was that the interference pattern was afflicted with a phase shift relative to theoretical expectations. In the case of dissociation through electronic excitation to the $2p\sigma_u$ state, such a phase shift was also observed and could be related to the change of the molecular symmetry during the transition, which has to be compensated by a corresponding switch in symmetry of the projectile [2]. However, in the case of vibrational dissociation, which is characterized by a small KER, the molecular transition does not involve any switch of symmetry. Therefore, the explanation for the phase shift in vibrational dissociative capture must be different.

One important difference between our results for the $H_2$ and $D_2$ targets is that in the former case the phase shift was found to be scattering angle ($\theta_p$) dependent [3], while in the latter case the phase shift was constant at $\pi$. So far, we could only offer a hypothetical explanation for the phase shift observed in vibrational dissociation for an $H_2$ target and the difference to the $D_2$ target. In the vibrational fragmentation process, the nuclei can follow two paths: (i) they can immediately move apart (direct path), (ii) they can initially move closer to each other and then get reflected from the molecular potential barrier at small internuclear distance $D$ (reflected path). In analogy to the classical reflection of a mechanical wave from a fixed end, the second case can cause a $\pi$ phase leap.

The $\theta_p$ dependent phase shift in the case of $H_2$ suggests that there the reflected path is dominant at small $\theta_p$, but the direct path is more important at large $\theta_p$. In contrast, in the case of a $D_2$ target the reflected path dominates at all $\theta_p$. This is also consistent with the FDCS we analyzed as a function of KER for fixed $\theta_p$. For $H_2$ we found an oscillating pattern, which we interpret as interference between the reflected and direct paths. In contrast for the $D_2$ target this structure is completely absent because the reflected path has nothing to interfere with since the direct channel appears to be negligible.

This work was supported by the National Science Foundatiom.

## References

[1] Lamichhane B *et al.* 2017 *Phys. Rev. L:* **119**, 083402
[2] Schmidt L *et al.* 2008 *Phys. Rev. L:* **100**, 057208
[3] Bastola S *et al.* 2024 *Phys. Rev. A:* **109**, 012821

*E-mail: smdrn@umsystem.edu

I-07

# $O_2^+$ production coming from $CO_2$ single-event electron impact

**A B Monteiro-Carvalho[1 *], L Sigaud[1 †] and E C Montenegro[2]**

[1]Instituto de Física, Universidade Federal Fluminense, Niterói, 24210-346, Brazil
[2] Instituto de Física, Universidade Federal do Rio de Janeiro, Rio de Janeiro, 21941-909, Brazil

**Synopsis** This work reports for the first time the absolute cross sections for the production of $O_2^+$ following the ionization of $CO_2$ by electron impact unambiguously. Through the DETOF technique it was possible to measure the kinect energy distribution of the $O_2^+$ fragment, centered at 1.4 eV.

The inventory of molecules in $CO_2$-rich atmospheres, such as our planetary neighbors Venus and Mars, can be significantly impacted, since they are constantly exposed to ionizing radiation, by the fragmentation processes of this particular species. However, the production of $O_2^+$ as a direct result otf $CO_2$ fragmentation had never been quantified before. Since molecular oxygen is considered a potential biosignature, understanding the non-biotic pathways for its production is essential to rule out false positives in the search for extraterrestrial life.

In this work, we identified and measured $O_2^+$ ions in absolute terms and ensured that their production results from the fragmentation of $CO_2$ by electron impact [1]. The break-up processes of $CO_2$ after ionization was studied by means of a pulsed electron gun in the 30 to 800 eV energy range, a gas cell with monitored pressure and a time-of-flight mass spectrometer. The DETOF technique [2] was used to determine the kinetic energy distributions for each produced fragment, via the collection of the recoil ion of interest for different delay times between the projectile-target interaction and the extraction of the ions from the interaction region. This methodology unequivocally ensures that the detected molecular oxygen originates from the fragmentation of the $CO_2$ molecule, with an average kinetic energy of 1.4 eV, and not from a possible residual air contamination inside the vacuum chamber.

This non-biotic pathway for oxygen production opens new perspectives for the artificial generation of $O_2$. Furthermore, it may provide the answer to the high concentration of $O_2^+$ in the upper layers of Mars' atmosphere [3], which remains unexplained by current physico-chemical models and their computational simulations. Finally, as mentioned earlier, this pathway could be of great importance in the investigation of the possibility of extraterrestrial life [4], as it shows that the mere detection of $O_2^+$ does not necessarily imply the presence of biological organisms.

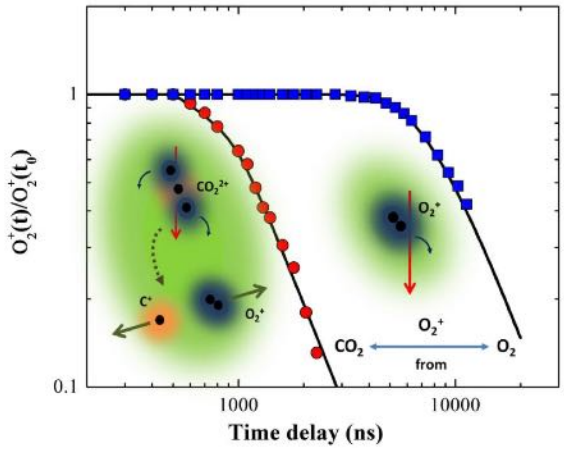


**Figure 1.** Ratio between the collected $O_2^+$ for a delay time *t* and for the minimum time $t_0$ for all delay times. Blue squares - $O_2^+$ produced by $O_2$ ionization, which does not acquire kinetic energy in a fragmentation process; red circles - $O_2^+$ produced by $CO_2$ fragmentation; black lines – theoretical curve for Maxwell-Boltzmann and Gaussian Kinetic energy distributions centered at 1.4 eV, for ionization of $O_2$ and $CO_2$, respectively, as illustrated in the plot.

## References

[1] Monteiro-Carvalho A B, Sigaud L and Montenegro E C, 2024 *Phys. Rev. Lett.* **132** 153002
[2] Sigaud L, de Jesus V L B, Ferreira Natalia and Montenegro E C 2016 *Rev. Sci. Instrum.* **87** 083112
[3] Leblanc F, 2018 *Geophys. Res. Lett.* **45** 468
[4] Krissansen-Totton J, Fortney J J , Nimmo F, and Wogan N, 2021 *AGU Adv, 2,* e2020AV000294

* E-mail: anabeatrizcarvalho@id.uff.br
† E-mail: lsigaud@id.uff.br

I-08

# Breit interaction vs Coulomb force in ionization occurring in nonrelativistic atomic collisions

A.B. Voitkiv

Institute for Theoretical Physics I, Heinrich-Heine-University Duesseldorf,
Universitätsstr. 1, 40225 Duesseldorf (Germany)

It is generally assumed that ionization in collisions of atomic particles,where their constituents (electrons and nuclei) move with velocities much less than the speed of light, is driven solely by the Coulomb force. Here we show, however, that the **Breit interaction** – a *relativistic correction* to the **Coulomb interaction** between electrons – can become a significant (or even the main) actor when the colliding system couples resonantly to the quantum radiation field. In such a case the Breit interaction proceeds via radiative energy "transport" between the colliding particles that has an extremely long range.

I-09

# Impact of Dimer Environments on Nonadiabatic Dynamics in Transient Molecules Formed via Ion-Atom Collisions

Hu Xiaoqing[1]*, Zhu Xiaolong[2], Wei Baoren[3], Wu Yong[1] and Wang Jianguo[1]

*1 Key Laboratory of Computational Physics, Institute of Applied Physics and Computational Mathematics, Beijing 100088, China*

*2 Institute of Modern Physics, Chinese Academy of Sciences, 730000 Lanzhou, China*

*3 Institute of Modern Physics, Key Laboratory of Nuclear Physics and Ion-Beam Application (MOE), Fudan University, Shanghai 200433, China*

Email Address:xiaoqing-hu@foxmail.com

Collisions between keV-energy ion and atom can produce transient molecule, the dynamics of which is entirely governed by a specific non-adiabatic avoided crossing directly associated with the incident channel. Placing such a target within a dimer allows for high-precision measurements of the non-adiabatic dynamics at the avoided crossing under the effects of the dimer environment. Using $He^{2+}$-NeAr collisions as a paradigm, we demonstrate that the collision process is dictated by the avoided crossing between $He^{2+}$-Ne and $He^{+}$-$Ne^{+}$ ($2s^{-1}$) potential energy curves. The neighboring Ar atom induces structural distortions in this crossing, thereby modifying the non-adiabatic transition probability in a manner critically dependent on the Ar atom's spatial configuration relative to the transient He-Ne molecular framework. Through orientation-resolved counting of $Ne^{+}$-$Ar^{+}$ pairs generated via the $Ne^{+}$ ($2s^{-1}$) -Ar interatomic Coulombic decay reaction post-collision, we quantitatively reveal how Ar regulates non-adiabatic dynamics across distinct configurations. These measurements, fully validated by comprehensive quantum calculations, establish a new scheme for detecting and regulating non-adiabatic dynamics in the environment.

Keywords: [Resonant charge transfer, Avoided crossing, Interatomic coulombic decay]

**Ref:**

[1] Jiang. et al, Phys. Rev. A 100, 022705 (2019).

I-10

# Imaging molecular structures and revealing fragmentation dynamics using highly charged ions

**Shenyue Xu[1,2,*], Hang Yuan[1,2], Yue Gao[1,2], Shaofei Gu[1,2], Bo Yang[1,2], Mei Wang[1,2], Dalong Guo[1,2], Xiaolong Zhu[1,2], Yong Gao[1,2], Dongmei Zhao[1,2], Shaofeng Zhang[1,2] and Xinwen Ma[1,2]**

[1]Institute of Modern Physics, Chinese Academy of Sciences, Lanzhou 730000, China
[2]School of Nuclear Science and Technology, University of Chinese Academy of Sciences, Beijing 100049, China

**Synopsis** The highly charged ion, inherent to the strong electric field around it, can stripple off many electrons from a target of molecule or cluster within an ultrafast timescale. Such advantages make highly charged ion beam a unique tool to image structute of a molecule or clusters, and study fragmentation dyanmics of them. We present two recent progresses in the study of highly charged ion in collision with molecules and clusters achieved at the Heavy Ion Research Facility in Lanzhou.

In our study, the reaction microscople setup (also called COLd Target Recoil Ion Momentum Spectroscopy, COLTRIMS) is employed to measure the electrons and ionic fragments in the final state of the collsion processes between molecule or cluster targets and the highly charged ion beams. Figure 1 presents the schematic view of the reaction miecrscope inserted into the Heavy Ion Research Facility in Lanzhou (HIRFL). This reaction microscope can provide the gas jet of not only molecules in gaseous phase, but also molecules that are liquids or powders at room tempature. In addition, various species of highly charged ion beams can be provided by HIRFL, covering the energy range from ~10 keV/u to ~100 MeV/u.

A high resolution Coulomb explosion imaging of three isomers of $C_4H_4N_2$ (pyridazine, pyrimidine, and pyrazine) has been achieved using the 112.5-keV/u $C^{5+}$ beam. The configuration of the three isomers was obtained by detecting ionic fragments $H^+$, $C^{2+}$, $C^+$, and $N^+$ in coincidence. Taking the advantage of fast colliding interaction that creates high charge states of $C_4H_4N_2$ on a subfemtosecond timescale, our approach effectively suppresses the distortion of molecular configuration during explosion, ensuring the high accuracy in structural imaging. This is confirmed by the quantitative agreement of momentum magnitudes between the point-charge model and the measured momenta for all fragments including hydrogen. Our work demonstrates that highly charged ion induced Coulomb explosion is a powerful tool for precisely imaging the initial structures of complex molecules.

In addition, we investigated the relaxiation mechanisms of the hydrated pyrimidine clusters after heavy-ion irradiation. The measurements were performed with the 25-MeV/u bare $Fe^{26+}$ beam and the 112.5-keV/u $C^{5+}$ beam. The carbon beam has been successfully applied in radiotherapy. It was found that inner-valence ionization of the clusters can initiate ICD and trigger proton transfer between water molecules, producing destructive low-energy electrons, HO· radicals, and hydrated protons. The efficiency of ICD was found to increase dramatically with the number of water molecules, making ICD the dominant decay mechanism after inner-valence ionization. Such processes can significantly contribute to the high biological effectiveness of heavy-ion irradiation.

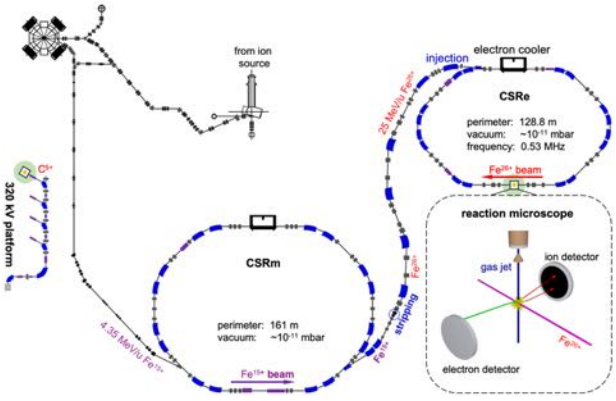


Figure 1. Schematic of the Heavy Ion Research Facility in Lanzhou and the reaction microscope. The two yellow spots denote the locations of the reaction microscopes employed in this study.

## References

[1] Yuan H *et al* 2024 *Phys. Rev. Lett.* **133,** 193002
[2] Gao Y *et al* 2025 *Phys. Rev. X* **15** 011053

* E-mail: s.xu@impcas.ac.cn

I-TT

# Interatomic Coulombic decay in ion-impact collisions: a theoretical perspective

**T Kirchner*** **and D Starko**

Department of Physics and Astronomy, York University, Toronto, Ontario M3J 1P3, Canada

Interatomic Coulombic decay (ICD) is a non-local, radiationless de-excitation process that has garnered widespread interest owing to its ubiquity, its intriguing nature, and its relevance for applications. Predicted in 1997 [1], it was first observed in photoexcited neon clusters and has, over the course of the years, been demonstrated in a large number of systems, including atomic and molecular clusters, liquids, and quantum dots, and in different variants [2]. In its simplest form, ICD is initiated by the removal of an electron from an inner valence shell, provided the excited state created has insufficient energy for a fast Auger-Meitner decay process. In an isolated atom, such a state decays by photon emission, but in a cluster the excitation energy can be transferred to a neighbour where it is used to remove an electron. The latter is the reason for the applied interest in ICD, since (low-energy) electrons are able molecular bond breakers, i.e., adept at inflicting damage to surrounding matter.

In this talk, I will focus on ion-impact-induced ICD in ostensibly simple systems such as neon and argon dimers. I will provide an overview of the experimental evidence for ICD in theses systems and discuss our recent theoretical work [3, 4] aimed at shedding light on the existing data and providing clues for worthwhile future studies.

## References

[1] Cederbaum L S *et al* 1997 *Phys. Rev. Lett.* **79** 4778
[2] Jahnke T *et al* 2020 *Chem. Rev.* **120** 11295
[3] Kirchner T 2021 *J. Phys. B: At. Mol. Opt. Phys.* **54** 205201
[4] Starko D and Kirchner T 2025 *J. Phys. B: At. Mol. Opt. Phys.* **58** 075204

*E-mail: tomk@yorku.ca

I-12

# Charge Exchange Cross Section for Highly Charged Ions Collision with Atom and Molecule

**T Meng, H Yin, Y Wu, M X Ma, P Ma, B Tu, Y Zou and B Wei** *

Institute of Modern Physics, Key Laboratory of Nuclear Physics and Ion-Beam Application (MOE), Fudan University, Shanghai, 200433, China

**Synopsis** The collision of highly charged ions with neutral atoms or molecules is a fundamental process of quantum transition among multi-centers, which is characterized by unique features of a strong Coulomb field condition at the atomic scale, multi-channel involvement, and highly excited state population. Such collision processes are prevalent in various extreme matter environments, such as hot astrophysical plasmas, fusion, and fission processes, and serve as crucial diagnostic tools.

The charge exchange (CX) process between ions and the neutral target is of great significance in explaining the X-ray emission spectrum of the solar system, which has been established as being responsible for the X-ray emissions from comets and the diffuse soft X-ray background. To investigate the CX process in the lab, an experimental instrument setup based on the 150 kV high-voltage platform with an electron cyclotron resonance (ECR) ion source at Fudan University was built. Recently, the absolute single- and double-electron capture cross sections and *nl*-resolved state-selective charge exchange cross sections between low-energy highly charged ions and neutral targets has been measured[1-6].

The *nl* state-selective charge exchange cross-section of $Ar^{8+}$ colliding with He, were performed in the collision energy range from 1.4 to 20 keV/u. It was found electrons were mainly captured in the $n$ = 4 state of $Ar^{7+}$ ions compared to the $n$ = 3, 5, and 6 captures, which was in agreement with the scaling law prediction for dominant capture. And the relative cross sections were also reported for 4*s*-, 4*p*-, 4*d*-, and 4*f*-resolved state-selective capture [1].

To further extend the research, the investigation of the charge exchange process of $O^{6+}$ and He was performed both experimentally and theoretically. The total cross sections and the branch ratios of different state-selective channels ($n$ = 3, 4, 5 and partially 3*s*) for the singlet and double electron capture have been measured in the energy range of 2.63-37.5 keV/u. The state-selective cross section of $n$ = 5 above 4.5 keV/u was reported experimentally for the first time. Total and state-selective cross sections were also calculated by the two-active-electron semi-classical asymptotic-state close-coupling method in the energy range of 0.3-100 keV/u, performing a good agreement with the experiment results. And the importance of electronic correlation was found compared with the previous methods [2, 3].

Furthermore, the total electron capture cross section between $O^{6+}$ and $Ne^{8+}$ with different target have been measured [4, 5].

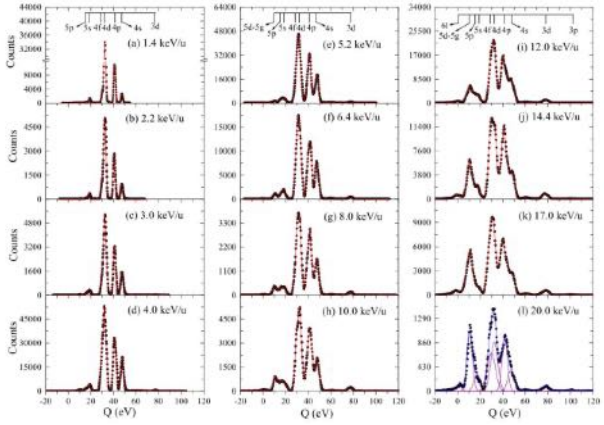


**Figure 1.** The measured Q spectra of CX between $Ar^{8+}$ and He. The black spheres are the experimental measurements and the red lines are used to guide the eyes. The purple and blue lines in the bottom right panel represent the Gaussian curve fitting and the sum of the Gaussian fitting results, respectively.

## References

[1] Xia Z H *et al* 2022 *ApJ* **933** 207
[2] Meng T, *et al* 2023 *New J. Phys.* **25** 093026
[3] Ma M X *et al* 2024 *Phys. Rev. A* **110** 032806
[4] Han J, *et al* 2021 *Astrophys.l J. Suppl. Ser.* **933** 207
[5] Ma P *et al* 2023 *Nucl. Sci. Tech.* **34** 156
[6] Yin H *et al* 2025 *Phys. Lett. A* 546 130527

* E-mail: brwei@fudan.edu.cn

I-13

# Charge exchange and ionisation in impurity ion collisions with atomic hydrogen

**N. W. Antonio[1]*, A. M. Kotian[1] and A. S. Kadyrov[1,2]**

[1]Curtin University, GPO Box U1987, Perth, WA 6845, Australia
[2]Institute of Nuclear Physics, Ulugbek, 100214 Tashkent, Uzbekistan

**Synopsis** Recently the wave-packet convergent close-coupling (WP-CCC) approach to ion-atom collisions has been applied to a number of impurity ion collisions with atomic hydrogen which are relevant for fusion plasma diagnostics, cooling and heating. Here we report on the results obtained for the total and state-selective charge exchange cross sections as well as the total ionisation cross sections for these collisions. The ions considered include $C^{q+}$, $N^{q+}$, $O^{q+}$ and $Ar^{q+}$, where $q$ is the charge state of the impurity ion.

Several ions have been selected as the primary seeding impurities for future fusion reactors. Impurity seeding will be required for reactors such as ITER and DEMO for radiative cooling, plasma control and diagnostics. Fusion plasmas are expected to contain impurities such as carbon, nitrogen, oxygen, argon, and tungsten ions. Some of these impurities are formed through ion seeding, while others by erosion of the first wall materials. The future DEMO reactor will require higher heating power than ITER, which necessitates the use of highly charged impurities to maintain the required temperatures in the divertor region. Charge exchange recombination spectroscopy (CXRS) is a diagnostic technique for measuring the impurity ion density, ion temperature, and plasma rotation within fusion plasmas [1]. The CXRS technique relies on accurate state-resolved charge-exchange cross sections for collisions between seeded impurity ions and the neutral hydrogen beam injected during diagnostics and heating [2].

The wave-packet convergent close-coupling (WP-CCC) approach accompanied with the associated GPU-accelerated computer codes can provide benchmark data on the total and state-selective cross sections for various processes taking place when fully and partially stripped ions collide with hydrogen atoms [3]. The approach is based on the expansion of the total scattering wavefunction using a two-centre pseudostate basis and solving a set of coupled-channel equations resulting from substituting the scattering wavefunction expansion into the full Schrödinger equation. Simulating collisions involving partially stripped ions has been made possible by introducing a model potential to account for the interaction between the projectile ion and the atomic target [4].

In this invited talk, we will present the recent progress made on obtaining an accurate set of cross section data for a number of the previously mentioned ions colliding with atomic hydrogen. More specifically, we will present the results we have obtained from applying the WP-CCC approach to study $C^{q+}$ [4], $N^{q+}$, $O^{q+}$ [5] and $Ar^{q+}$ [6] ions colliding with atomic hydrogen. Generally speaking, there is limited reliable data available for these systems despite their importance not only for fusion plasma diagnostics but also for other applications such as hadron therapy for cancer treatment and astrophysics.

We will finish off by briefly touching on the progress we have made to extend our approach to handle systems with multi-electron ions accounting for electron correlation effects in full.

*E-mail: nicholas.antonio@postgrad.curtin.edu.au

## References

[1] McDermott, R., *et al.*, 2020, *Nucl Fusion* **61**, 016019
[2] Hill, C., *et al.*, 2023, *Nucl Fusion* **63**, 125001
[3] Abdurakhmanov, I. B., Antonio, N. W., Cytowski, M., & Kadyrov, A. S., 2025, *In Proc. International Conference on High Performance Computing* pp 102-114
[4] Antonio, N. W., Plowman, C. T., Abdurakhmanov, I. B., & Kadyrov A. S., 2025, *Phys. Rev. A* **109**, 012817
[5] Kotian, A. M., Antonio, N. W., Marchuk, O., & Kadyrov A. S., 2025, *submitted for publication*
[6] Kotian, A. M., Antonio, N. W., Marchuk, O., & Kadyrov A. S., 2025, *Plasma Phys. Control. Fusion* **66**, 095014

I-14

*Single hit microbeam technology for single cell "RAD" biology"*

Teruaki Konishi, Ph.D
National Institutes for Quantum Science and Technology (QST), Japan

SPICE-QST microbeam is a focused vertical microbeam system designed for sub-cellular target irradiation of adherent mammalian cells. The microbeam delivers 2-$\mu$m diameter beams to target individual cells with a defined number of 3.4 MeV protons at a high-throughput irradiation rate of 300-400 positions per minute [1,2]. It must be noted that SPICE enables irradiation to deliver from a "single" proton to a desired position within the cell. Furthermore, single proton traversal in cell is estimated to result in a low dose, equivalent to several mGy, which make our system unique combined with the other advantageous specification of SPICE compared to other facilities.

Our objective is to utilize microbeam technology to identify these non-DNA/secondary targets and to investigate their involvement in cellular responses. Specifically, we have studied the intracellular response induced by cytoplasmic damage, focusing on the activation of the oxidative stress response pathway, which appeared as a protective response [3,4]. Regarding studies on intercellular responses, we have investigated the bi-directional response between targeted cancer cells and non-targeted normal cells, resulting in the "rescue" of targeted cells, a phenomenon described as a facet of the radiation-induced bystander effect [5]. This presentation will summarize the findings and address further development in microbeam technology for radiation biology.

Acknowledgements: SPICE take in part of IAEA-CRP F11024, "Sub-cellular Imaging and Irradiation using Accelerator-based Techniques." and PIANOFORTE2024,"BOOST", and supported by JSPS-KAKENHI (proposal # 20K20636, #23K21428)

References:

[1] T. Konishi, et al., J Radiat Res, 54 (2013) 736-747.
[2] T. Kusumoto et al., (2025) Eur. Phys. J. Plus, in press.
[3] J. Wang, et al., Radiat Res, 194 (2020) 288-297.
[4] T. Konishi, T., Wang, J., et al., (2025) Eur. Phys. J. Plus 140, 334
[5] N. Autsavapromporn, et al., Biology (Basel), 12 (2023) 1485.

I-15

# Track-structure mode and DNA damage estimation in PHITS ver. 3.35

**Yusuke Matsuya**[1,2]

[1]Faculty of Health Sciences, Hokkaido University, Sapporo, 060-0812, Japan
[2]Nuclear Science and Engineering Center, Japan Atomic Energy Agency, Tokai, 319-1195, Japan

**Synopsis** Particle and Heavy Ion Transport code System (PHITS) is a general-purpose Monte Carlo simulation code that allows the transport of various types of ionizing radiation using physical models that include atomic and nuclear interactions. Over the past decade, track-structure (TS) modes have been developed to simulate atom-radiation collisions, including elastic scattering, ionizations, electronic excitations, dissociative electron attachment, molecular excitations, and charge exchange. Focusing on liquid water, specialized TS modes—specifically, PHITS-ETS for simulating electrons and PHITS-KURBUC for proton and carbon ions—are currently available. Additionally, we have developed a DNA damage estimation model that enables the calculation of DNA damage (i.e., single-strand breaks (SSBs), double-strand breaks (DSBs), and clustered DSBs) based on the spatial patterns of ionizations and electronic excitations. In this presentation, we introduce the track-structure mode dedicated to liquid water and the DNA damage estimation model in the PHITS code, which will contribute to presenting the intrinsic relationship between atomic-ion collisions and radiation-induced biological effects.

Initial DNA damage induced along the radiation track plays a crucial role in determining subsequent biological effects, such as cell death and chromosome aberrations. When investigating the mechanisms of DNA damage induction following exposure, track structure, and the atom-radiation collision are of great importance. In the 1900s, a Monte Carlo method for simulating radiation kinetics at a DNA scale was a powerful tool for clarifying DNA damage induction mechanisms.

Among various Monte Carlo codes, the PHITS code [1] is a general-purpose Monte Carlo simulation code that allows for the transport of diverse ionizing radiations. Particularly, in the recent decade, the track-structure (TS) mode [2] has been developed to simulate individual atom-radiation collisions, including elastic scattering, ionizations, electronic excitations, dissociative electron attachment, molecular excitations (i.e., rotation, vibration, and phonon), and charge exchanges [2]. The TS mode enables the simulation of radiation tracks at a micrometer or smaller scale and can be applied to mechanistic studies of radiation-induced biological effects and detector responses. Figure 1 shows a 1 MeV proton track with secondary electrons at the DNA scale, where the proton and secondary electrons are represented by blue and yellow, respectively. The trajectories were depicted using [t-4dtrack] and PHIG-3D software.

We developed a simple DNA damage estimation model that enables the calculations of single-strand break (SSB), double-strand break (DSB), and its complex forms, such as DSB coupled with a strand break (SB) (DSB+) and that coupled with two SBs (DSB++), using the spatial patterns of ionization and electronic excitations [2]. In this model, we assumed that the numbers of the collisions and the two pairs are proportional to SSB and DSB induction. The model has been verified in comparison with the DNA damage data measured in our studies and reported in the literature, to date.

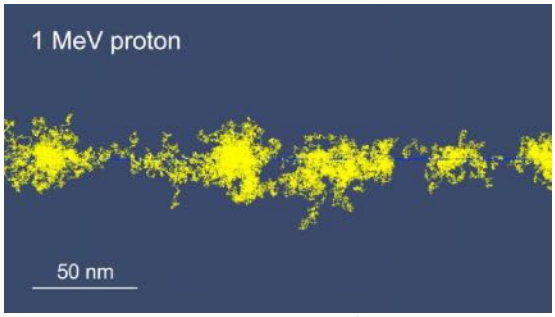


**Figure 1.** Trajectory of a 1 MeV $^{1}$H with secondary e$^{-}$

In the latest version 3.35 of PHITS, the TS mode and the analytical code for DNA damage estimation were included in the PHITS packages. These codes would contribute to a precise understanding of radiation-induced biological effects in future studies.

## References

[1] Sato T *et al.* 2024 *J. Nucl. Sci. Technol.* 61, 127–135, https://phits.jaea.go.jp/index.html
[2] Matsuya Y *et al.* 2022 *Int. J. Radiat. Biol.* 98 (2), 148–157

* E-mail: matsuya.yusuke@hs.hokudai.ac.jp

I-16

2025-06-01

# Micro-PIXE for Iron Mapping in Ferroptosis

**Henrique Fonteles[1]*, Theylor Klippel [1], Daphne Tórgo[2], Guido Lenz[2], Johnny Ferraz Dias[1], and Pedro Luis Grande[1]**

[1] Ion Implantation Laboratory, UFRGS, Porto Alegre, Brazil
[2] Cell Signalling Laboratory, UFRGS, Porto Alegre, Brazil

**Synopsis** Ferroptosis is a promising target for glioblastoma treatment, but its imaging remains challenging. This study explores micro-PIXE as a complementary tool to visualize and quantify ferroptosis in U87 cells treated with inducers like RSL3 and cisplatin. Micro-PIXE revealed iron accumulation and morphological changes in ferroptotic cells, showing potential as a high-resolution, element-specific method for ferroptosis analysis in single cells.

Ferroptosis, a non-apoptotic iron-dependent cell death, holds great potential in several biomedical applications, such as cancer therapy and neurological disease research. Particularly, the growing recognition of the role of ferroptosis in the treatment of glioblastomas is capturing the attention of the scientific community. It is seen as a promising approach to address one of the most prevalent malignant craniocerebral tumors. However, sensitive and specific tools for ferroptosis imaging and quantification at the cellular level remain a challenge. The most used method for imaging involves the use of fluorescent markers, such as Bodipy 581/591 C11, which detects lipid peroxidation, one of the hallmarks of ferroptosis. This work explores the potential of micro-PIXE as a complementary technique for visualizing and quantifying ferroptosis in single cells. To evaluate morphological and elemental changes associated with ferroptosis, we treated the U87 glioblastoma cell line with several ferroptosis inducers, including RSL3 and cisplatin. We then measured the fixed cells on Mylar films in the microbeam line. Micro-PIXE successfully detected and localized iron accumulation within ferroptotic cells, in contrast to non-treated cells, demonstrating its potential for ferroptosis visualization. It was also possible to correlate the 2D micro-PIXE elemental maps with optical images to assess morphological changes due to ferroptosis inducers. This study demonstrates how micro-PIXE can be used as a powerful tool for ferroptosis analysis. Its high spatial resolution and elemental specificity offer unique advantages for studying ferroptosis in various biological contexts. Further research is needed to explore its applications in different cell lines and tissues.

## References

[1] Fonteles H *et al.* 2024 *J. Anal. At. Spectrom.* **39** 2087

*E-mail: fonteleshenrique@gmail.com

I-17

# A mystery of ion tracks in silicon:
## – Monatomic ions of hundreds MeV do not form but $C_{60}$ ions of 60 keV do –

**H Amekura** [1 *]

[1]National Institute for Mateirals Science (NIMS), Tsukuba, 305-0003, Japanon

**Synopsis** While ion tracks in Si has been extensively explored utilizing various monatomic ions up to 3.6 GeV U ions, which provide the highest electronic energy deposition $S_e$ of 24 keV/nm in Si, no tracks have ever been observed under monatomic ion irradiations. Up to now, we have confirmed ion tracks in Si under $C_{60}$ ion irradiation at 6 MeV ($S_e$ = 18.0 keV/nm) and even at 1 MeV (7.5 keV/nm). Here we report further lower energy exploration of the tracks under $C_{60}$ ion irradiation. Something like tracks or craters have been observed under 60-keV irradiation, but not under 30-keV irradiation [1].

While ion tracks are formed in solids under irradiations with swift heavy ions (SHIs), i.e., high-energy heavy ions in the electronic stopping regime [2], this paper reports that ion tracks, or something similar, formed under $C_{60}$ fullerene ion irradiation down to low energy of 60 keV[1].

Crystalline silicon (c-Si) is known as a radiation-hard material against SHI irradiation: In fact, no tracks were observed even irradiated with high-energy heavy ions of 3.6 GeV uranium (electronic stopping power $S_e$ = 23.7 keV/nm [3]). Since sixty carbon atoms are injected at the same time into the same nanoscopic area, $C_{60}$ ions provide higher $S_e$ than GeV U ions. Utilizing $C_{60}$ ions of 30–40 MeV ($S_e$ = 42.7–50.0 keV/nm), the track formation was attained in c-Si in 1998 [4,5], which was simply believed due to the overcoming of the high threshold of ~30 keV/nm under $C_{60}$ ion irradiation.

Recently, we have, however, observed the track formation in c-Si under $C_{60}$ ion irradiation at 6 MeV ($S_e$ = 18.0 keV/nm) and even at 1 MeV (7.5 keV/nm ) [6,7]. The $S_e$ values of the 1-MeV and 6-MeV $C_{60}$ ions were much lower than the threshold value of ~30 keV/nm, which was proposed in past to explain the insensitivity of c-Si against the GeV monoatomic U irradiation.

Here we present the track formation under $C_{60}$ ion irradiation with lower energies than 1 MeV, i.e., between 30 keV and 750 keV [1], since we have confirmed the track formation at 1 MeV $C_{60}$ ion irradiation in a previous paper [6]. With decreasing the ion energy, both the diameter and the length of the tracks decrease. Finally, the length of the ion tracks becomes so short that it is almost difficult to distinguish the tracks from deepened craters connected to the surface. Even though, something like the tracks or the craters were observed down to 60 keV irradiation. They were not observed under 30 keV irradiation. Therefore, the track formation threshold energy exists between 30 and 60 keV, i.e., in very low energies.

* E-mail: amekura.hiroshi@nims.go.jp

### References

[1] Amekura H *et al* 2024 *Nature Commun.* **15** 1786
[2] Amekura H *et al* 2025 *Materialia* **39** 102317
[3] Mary P *et al* 1992 *Nucl. Instr. Meth. In Phys. Res.* **62** 391
[4] Canut B *et al* 1998 *Nucl. Instr. Meth. In Phys. Res.* **146** 296
[5] Dunlop A *et al* 1998 *Nucl. Instr. Meth. In Phys. Res.* **146** 302
[6] Amekura H *et al* 2021 *Scientific Reports* **11** 185
[7] Amekura H *et al* 2023 *Physica Scripta* **98** 045701

# Abstracts
## (Oral Presentations)

O-01*

# Excitation of ground-state helium by proton impact

**C T Plowman[1]*, L H Scarlett[1], M C Zammit[2], I Bray[1] and D V Fursa[1]**

[1]Department of Physics, Curtin University, Perth, Western Australia 6102, Australia
[2]Theoretical Division, Los Alamos National Laboratory, Los Alamos, New Mexico 87545, USA

**Synopsis** We have developed a semi-classical version of the Laguerre-based convergent close-coupling (CCC) approach to study proton collisions with helium. Our excitation cross sections provide a comprehensive dataset from 2 to 2000 keV that are in very good agreement with available measurements for transitions from the ground state into all $n \leq 5$ states. The single-centre approach is found to reproduce the Rosenthal oscillations seen in experiment, indicating accurate modelling of the underlying physics.

Calculation of excitation cross sections in proton-helium collisions has remained a challenge for many decades [1]. Despite a significant amount of experimental work for some transitions, theory has only been available across limited energy ranges and with inconsistent accuracy. Furthermore, most measurements cover intermediate and high energies, but the data that is available for low energy collisions suggests that the cross sections can be significant in this region [2]. This data [2] is normalised to high-energy measurements that are known on an absolute scale [1]. However, the region of overlap between datasets can be small, leading to ambiguity about the magnitude of the cross sections at smaller energies.

We have applied a semi-classical Laguerre-based convergent close-coupling (CCC) approach to calculate a comprehensive dataset for excitation cross sections from proton collisions with ground-state helium. The scattering wave function is expanded in a basis of target states that are constructed using a configuration interaction expansion in terms of both frozen-core and correlation configurations. Diagonalising the target Hamiltonian in this basis yields negative-energy pseudostates that accurately represent the ground state and excited states of interest as well as positive-energy pseudostates that discretise the target continuum. Although this method is based on a single-centre expansion of the scattering wave function, we are able to obtain convergence in the cross sections from 2 to 2000 keV, including the electron loss cross section. To achieve this we use a large number (up to 2568) of target pseudostates in expansion of the scattering wave function to implicitly account for coupling to the electron capture channels with the positive-energy pseudostates.

We find very good agreement with the experimental data where available and significant improvement over previously available calculations. A sample of the present results is shown in Fig. 1 for the excitation of the ground state of helium into the $4^1$P state.

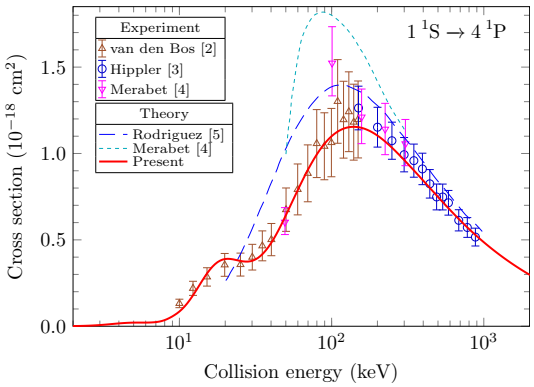


**Figure 1**. Excitation of the $4^1$P state from the $1^1$S ground state of He by proton impact.

Many of the presently considered excitation cross sections feature two peaks. These are caused by coherent mixing of amplitudes in the molecular interpretation of ion-atom scattering [6]. Our results agree well with these features in the experimental data giving us confidence in the accuracy of our approach.

## References

[1] Fritsch W 1991 *Phys. Lett. A* **160** 64
[2] van den Bos J *et al.* 1968 *Physica* **40** 357
[3] Hippler R *et al.* 1974 *J. Phys. B* **7** 618
[4] Merabet H *et al.* 2001 *Phys. Rev. A* **64** 012712
[5] Rodriguez V D *et al.* 1997 *Phys. Rev. A* **55** 4201
[6] Rosenthal H *et al.* 1969 *Phys. Rev. Lett.* **23** 1480

*E-mail: corey.plowman@curtin.edu.au

* *A concern has been raised regarding the originality of certain aspects of this contribution, specifically the use and authorship of the method and software code. The matter is currently under review by the appropriate institutional channels. No determination has been made at this stage, and the presentation will proceed pending further clarification.*

O-02

# Impact parameter and kinematic information for differential ionization of argon by positron and electron impacts

**R. D. DuBois[1†], and K. Tőkési[2*]**

[1]*Missouri University of Science and Technology, Rolla MO 65409 USA*
[2]*HUN-REN Institute for Nuclear Research (ATOMKI), Hungary, EU*

**Synopsis** We present ionization cross sections in collisions between electron and positron impact with Ar(3p) target. The calculations were performed classically using the three body CTMC approximation. We found that the ionization probabilities as a function of impact parameter show different distributions for electron and positron impact. For the case of positron impact the distribution is symmetric, for the case of electron impact the distribution is asymmetric. Furthere more we found that the dominant part of ionization occurs for impact parameters smaller than the 3p radius.

It is well known that the reversal of directions of the Coulomb field for positron and electron impact ionization produces trajectory changes for the projectile. Pre-collision field effects result in a larger impact parameter for positron impact with respect to that for electron impact. In addition, post-collision effects between the post-collision particles introduce additional trajectory effects. In order to test various theoretical models for ionization, comparisons on the differential level are used. For electron impact, a large amount of experimental information, ranging from singly to fully differential, is available whereas for positron impact, relatively few differential studies have been performed. Also, unlike the case for heavy ion impact where impact parameter information can be obtained, post-collision effects effectively prohibit such studies for lepton impact.

However, the Classical Trajectory Monte Carlo method allows us to investigate such kinematic effects and also to obtain information as a function of impact parameter. As an initial study, such information for ionization of argon 3p electrons by 1 keV positrons and electrons is presented. Similar to that used by Sparrow and Olson [1], the argon atom was modeled as a single 3p electron and a central core potential and interactions between all particle pairs are taken into account. Unlike previous studies, the present study also provides information about the impact parameter and the scattering and ejection directions, not just the angles but also whether the directions are "positive" or "negative", i.e., toward, or away from the central core.

We found that our present CTMC model, where the target atoms were described within the single active electron approximation, is in good agreement with existing experimental total, single, and double differential data. The energy distributions for electron and positron impact have the same shape and structure. At the same time, the angular distributions behave completely different which we suggest is associated with a projectile-target core interaction. The ionization probabilities as a function of impact parameter show different impact parameter probability distributions both in shape and, on the fully differential level, are centered at different values depending on the direction of scattering.

**Acknowledgments**
The work was support by the Bilateral relationships between Qatar and Hungary in science and technology (S&T) under the project number 2021-1.2.4-TÉT-2021-00037.

**References**

[1] DuBois R D and Tőkési K 2023 Differential Studies of Argon Particle and Antiparticle Interactions: Present Status and Future Possibilities, Atoms 11 151

† E-mail: dubois@mst.edu
* E-mail: tokesi@atomki.hu

O-03

# Molecular two-center interference in $H^+$ emission from $H_2$ molecule by $O^+$ ion impact and its dependence on the target coherence

**Z Juhász[1*], S T S Kovács[1], V Vizcaïno[2], P Herczku[1], S Demes[1], R Rácz[1], B Sulik[1], S Biri[1], N Sens[2], D V Mifsud[3,1], G Lakatos[1,4], K. K. Rahul [1] and J-Y Chesnel[2]**

[1] Institute for Nuclear Research (Atomki), Debrecen, H-4026, Hungary
[2] CIMAP, UMR 6252 CEA-CNRS-ENSICAEN-UNICAEN, Normandie Université, 14000 Caen, France
[3] University of Kent, Canterbury CT2 7NH, United Kingdom
[4] Doctoral School of Chemistry, University of Debrecen, H-4032, Hungary

**Synopsis** Oscillations were found in the angular distribution of binary-knocked-out $H^+$ ions from $H_2$ molecule by 10-keV $O^+$ ions. These oscillations can be attributed to two-center interference effects. The amplitude of oscillations is enhanced when the nozzle is moved farther from the collision center, *i.e.* when the coherence length in the gas jet is increased. The results show that target coherence has an impact on the molecular fragmentation processes similarly to the case projectile coherence demonstrated earlier.

Effects of projectile coherence on ionization and fragmentation processes have been shown in several studies [1, 2]. The coherence length of ionic projectiles can easily be manipulated by slits. Interference pattern may or may not be apparent depending on the slit settings. Hence, the coherence length has to be considered in quantum calculations when compared to experiments.

In the present study we found that target coherence effects also need to be considered, which can be manipulated by the position of the nozzle in crossed gas jet – ion beam experiments.

We have measured the emission of $H^+$ fragment from $H_2$ molecules induced by oxygen ions of 10-keV projectile energy at HUN-REN ATOMKI using a field-free time of flight (FFTOF) setup described in ref [3]. The fragments due to binary collisions are distributed along a ridge in the velocity map. This ridge is split due to molecular rotation as it was shown in Ref. [3].

There is a finer structure along the ridge as well. This can be seen when the emission cross section is plotted as function of the observation angle (Fig. 1). There are visible oscillatory deviations in the cross section with respect to the two-body elastic scattering calculations. These can be attributed to the two-center effects of the $H_2$ molecule.

The amplitude of the oscillations decreases when the nozzle is moved closer to the ion beam. According to van Cittert–Zernike theorem, the coherence length of the ejected molecules is proportional to the distance from exit of the nozzle *l*. The interference pattern was pronounced when the coherence length was at least as long as the internuclear distance $r$=1.4 a.u.

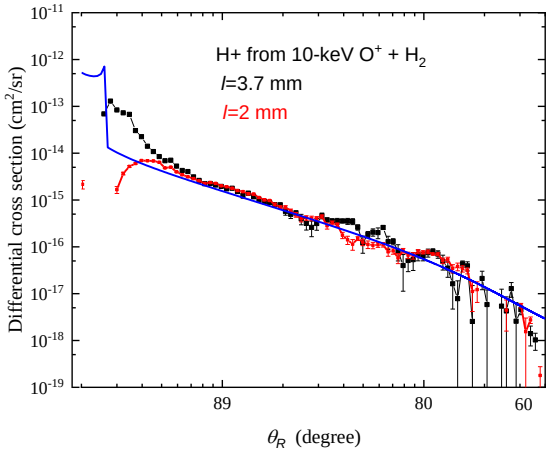


**Figure 1.** Differential emission cross section as function of the observation angle with two different nozzle position *l* indicated in the figure, in comparison with two-body elastic scattering calculations (blue curve).

This work is supported by the CNRS International Research Project (IRP) RAD-ASTRO and by NKFIH ADVANCED grant (No. 151196).

## References

[1] Alexander J S *et al* 2008 *Phys. Rev. A* **78** 060701
[2] Egodapitiya K N *et al* 2011 *Phys. Rev. Lett.* **106** 153202
[3] Juhász Z *et al* 2023 *Phys. Rew. A* **107** L010801

* E-mail: zjuhasz@atomki.hu

O-04

# Low energy collisions of $H^-$ with $B^+$ or $H^+$

**Å Larson[1]*, J Hörnquist [1], B Arslanoglu [1]. M Begau [1] and A E Orel[2]**

[1]Department of Physics, Stockholm University, SE-106 91 Stockholm, Sweden
[2]Department of Chemical Engineering, University of California, Davis, 95616, California, USA

**Synopsis** Results from *ab initio* calculations on mutual neutralization in collisions of $H^-$ with $B^+$, as well as double charge transfer in $H^-$ + $H^+$ collisions are presented.

In mutual neutralization (MN), an electron transfer between oppositely charged ions results in formation of neutral fragments. In double charge transfer (DCT), two electrons are transferred.

The study of MN in collisions of $B^+$ with $H^-$ is motivated by the need for plasma modeling at ITER [1]. Boronisation of the plasma wall is planned to reduce the amount of impurities and contamination, and to protect the wall from corrosion. Boron atoms will enter the plasma, where boron cations can be formed. Hydrogen anions are believed to be formed in detached plasmas of the divertor, by dissociative attachment of vibrationally excited $H_2$ molecules [1].

The potential energy curves and non-adiabatic coupling elements of the seven lowest electronic states of BH in $^1\Sigma^+$ symmetry have been calculated using the Multi Reference Configuration Interaction method with an extended basis set that allows for accurate computations of both Rydberg states and the ion-pair state. The coupled Schrödinger equation for the nuclear motion is then solved numerically in a strict diabatic representation. Calculated MN cross section is displayed in the upper panel of the Figure. At low collision energies, the MN process is dominated by formation of H + B($^2S$ ($2s^2 4s$)) with a ratio of 54 % at a collision energy of 1 meV.

In collisions of $H^+$ with $H^-$, several processes are possible such as MN, associative ionization and DCT. We have recently developed a "unified model" [2] of the $H_2$ reaction complex that allows to describe various reactive scattering process involving the same set of coupled states [2–4]. Here, we present cross section for DCT, a process that has been studied both experimentally and theoretically before. The cross section shows interesting structures and our model demonstrate the importance of including highly excited Rydberg states as well as rotational couplings between states of $^1\Sigma^+_{g/u}$ and $^1\Pi_{g/u}$ symmetries. These couplings have been neglected in previous studies.

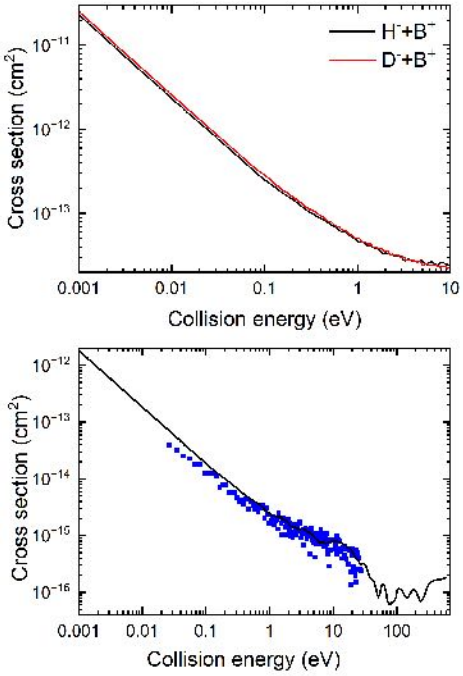


**Figure 1**. Upper panel: Calculated cross sections for MN in collisions between $H^-$/$D^-$+$B^+$. Lower panel: Calculated and measured [6] DCT cross sections for $H^-$+$D^+$.

## References

[1] Hill C, 2023 *"The Formation and Properties of Molecules in Edge Plasmas, Summary Report of the First Research Coordination Meeting"*, IAEA, INDC(NDS)- 0896 Distr. LP,NE,SK.
[2] Hörnquist J *et al.* 2022 *Phys. Rev. A.* **106**, 062821
[3] Hörnquist J *et al.* 2023 *Phys. Rev. A* **108**, 052811
[4] Hörnquist J *et al.* 2024 *Phys. Rev. A* **109**, 052808
[5] Zong W. *et al.*, 1999 *Phys. Rev. Lett.* **83**, 951
[6] Urbain X., Private communications.

*E-mail: aasal@fysik.su.se

O-05

# Intra-molecular scattering within diiodoacetylene

**Manisha Samal[1]*, P. Bhatt[2], H. Tezuka[3], G. Vesapidze[4], J. Matsumoto[3], C. P. Safvan[2], H. Shiromaru[3] and Sankar De[1]†**

[1]Saha Institute of Nuclear Physics, A CI of Homi Bhabha National Institute, Kolkata 700064, India.
[2]Inter-University Accelerator Centre, Aruna Asaf Ali Marg, New Delhi, India.
[3]Department of Chemistry, Tokyo Metropolitan University, Hachioji, Tokyo, Japan.
[4]School of Technology, Ilia State University, Tbilisi, Georgia.

**Synopsis** The fragmentation of multiply charged diiodoacetylene (DIA) by low-energy $Ar^{8+}$ collisions reveals a perpendicular emission of carbon and iodine ions, deviating from expected collinear breakup. Classical Coulomb explosion simulations reproduce this behavior, highlighting strong Coulombic interactions in the dissociation dynamics. The kinetic energy releases of four-body fragmentation channels of $C_2I_2{}^{q+}$ are investigated for $q$ up to 10, in which generation of high $q$ ions requires conversion of the projectile collision energy to the electronic energy alongside electron capture. During analysis of two- and three-body breakup channels, we observed that although C-I bond cleavage dominates, notable C-C bond breakage is also possible. Detection of $C_2I_2^{4+}$ in TOF spectrum suggests the persistence of a highly charged molecular frame.

The fragmentation dynamics of DIA is studied using multi-hit coincidence time-of-flight (TOF) measurements [1]. The experiment was carried out using 3 keV/u $Ar^{8+}$ projectiles, produced by an ECR ion source at the Tokyo Metropolitan University (TMU), Japan. The multi-hit position-sensitive TOF measurements of recoil ions were initiated by the detection of charge-exchanged $Ar^{6+}$ projectiles.

We first focus on four-body coincidence events as shown in Fig. 1, involving highly charged states of DIA, reaching up to a total charge of 10. The momentum correlations among fragment ions in the four-body fragmentation process reveal two key aspects. First, all dissociation channels proceed via the instantaneous breakup of all bonds. Second, the emission directions of carbon and iodine ions are predominantly perpendicular to each other, deviating from the intuitive expectation that fragments from a linear molecule would align [2]. Simulated fragment trajectories, based on a classical Coulomb explosion model, effectively reproduce this fragmentation pattern, highlighting the significant role of Coulombic interactions between the dissociating carbon and iodine ions.

Newton diagram and Dalitz plot analysis reveal two distinct fragmentation pathways in the three-body breakup; concerted fragmentation, where both C-I bonds break simultaneously, and sequential fragmentation, characterized by stepwise bond cleavage. Although the expected bond breakage predominantly involves C-I bonds, our findings unexpectedly indicate significant C-C bond breakage as well.

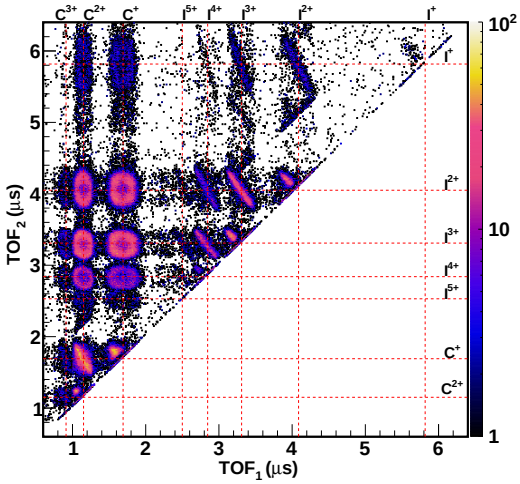


**Figure 1**. Four-fold coincidence map of DIA breakup triggered by $Ar^{6+}$.

*S. D. acknowledges the Japan Society for the Promotion of Science (JSPS) for Invitation Fellowship (short term).*

## References

[1] M. Samal *et al.* 2025 *Phys. Rev. A* **111** 032819
[2] S. De *et al.* 2008 *Phys. Rev. A* **77(2)** 022708

*E-mail: manishasamal0602@gmail.com
†E-mail: sankar.de@saha.ac.in

O-06

# Delayed fragmentation of polyatomic molecules induced by MeV ion collisions

**T Nakao[1 *], T Yanagawaya[1], H Tsuchida[1,2], M Saito[1,2] and T Majima[1,2 †]**

[1]Department of Nuclear Engineering, Kyoto University, 615-8540 Kyoto, Japan
[2]Quantum Science and Engineering Center, Kyoto University, 611-0011 Uji, Japan

**Synopsis** Delayed fragmentation provides valuable insights into the stability and the dissociation mechanism of intermediate ions. In this study, we employed fast ion collisions to investigate delayed fragmentation in nucleobases, hydrocarbons, and alcohols. Delayed fragmentation from singly charged intermediate ions was observed only in the nucleobases and the specific alcohols, indicating that sufficient degrees of freedom in the molecule are required for the delayed fragmentation.

Intermediate ions generated by excitation and ionization of polyatomic molecules can dissociate with long lifetimes of several hundred nanoseconds or more. Delayed fragmentation has been studied because it provides information on the internal energy of intermediate ions and on sequential dissociation processes. Two mechanisms have been proposed so far: one involving metastable electronically excited states and another originating from vibrationally excited states. The former has been reported for $C_2H_n$ ($n$ = 2, 4, 6) [1], while the latter has been observed in adenine [2] and cyclodipeptides [3]. However, the factors governing this difference remain unclear. To gain new insights into the underlying processes, in this study, we measured the delayed fragmentation of isolated molecules using MeV-energy fast ions, which have not been employed as excitation sources in previous studies.

Experiments were conducted using a 1.7 MV Cockcroft–Walton-type tandem accelerator at Quantum Science and Engineering Center, Kyoto University. Pulsed carbon or proton beams were employed as projectiles. The fragments were extracted by an electrostatic field, detected with a microchannel plate detector, and recorded in list mode using a fast multi-channel scaler. The mass-to-charge ratios ($m/q$) of the fragments were determined by time-of-flight (TOF) mass spectrometry. The target molecules employed were as follows: nucleobases (adenine $C_5H_5N_5$, guanine $C_5H_5N_5O$, cytosine $C_4H_5N_3O$, thymine $C_5H_6N_2O_2$, uracil $C_4H_4N_2O_2$), hydrocarbons (acetylene $C_2H_2$, ethylene $C_2H_4$, ethane $C_2H_6$), and alcohols (methanol $CH_3OH$, ethanol $CH_3CH_2OH$, 1-propanol $CH_3(CH_2)_2OH$, 2-propanol $CH_3CH(OH)CH_3$).

Delayed fragmentation was identified by the coincidence measurements of fragments. Figure 1 shows the TOF correlation map obtained from adenine. The long diagonal tails correspond to the delayed fragmentation. In adenine, many delayed fragmentation pathways were observed. For some of these, the fragmentation lifetimes $\tau$ were also determined after correcting the detection efficiency of neutral fragments. For example, the following pathways were obtained: $C_5H_5N_5^+ \rightarrow C_4H_4N_4^+ + HCN$ ($\tau$ = 0.67 ± 0.09 μs in 0.5-MeV $H^+$ collisions), $C_5H_5N_5^{2+} \rightarrow C_4H_3N_4^+ + CH_2N^+$ [4]. Delayed fragmentation pathways from both singly and doubly charged intermediate ions were observed in guanine, whereas only those from singly charged intermediate ions were detected in cytosine, thymine, and uracil. In hydrocarbons, delayed fragmentation occurred only in pathways where $H^+$ or $H_2^+$ detach from doubly charged intermediate ions. In alcohol molecules, delayed fragmentation from singly charged intermediate ions was not observed in methanol. The results indicate that sufficient degrees of freedom in the molecule are required for the delayed fragmentation.

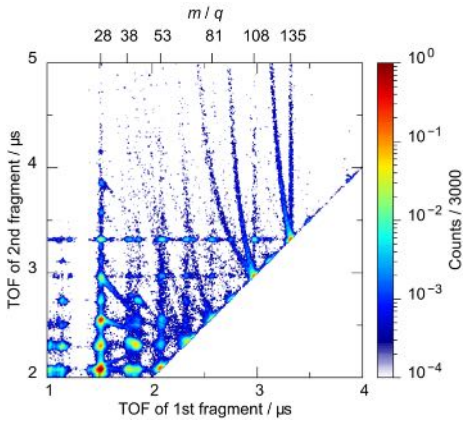


**Figure 1.** TOF correlation map obtained from adenine.

## References

[1] Field and Eland 1993 *Chem. Phys. Lett.* **211** 436–442
[2] Martin *et al* 2008 *Phys. Rev. A* **77** 062513
[3] Chiarinelli *et al* 2022 *Phys. Chem. Chem. Phys.* **24** 5855–5867
[4] Nakao *et al* 2024 *J. Chem. Phys.* **161** 054302

* E-mail: nakao.tomohiko.65w@st.kyoto-u.ac.jp
† E-mail: majima@nucleng.kyoto-u.ac.jp

O-07

# Double electron capture into autoionizing states in $N^{7+}$ and He collisions

**J J Niu[1], W W Zhang[1], Y Y Qi[2] and J W Gao[1]***

[1]School of Physics, Hangzhou Normal University, 311121, Hangzhou, China
[2]College of Mechanical Engineering, Jiaxing University, Jiaxing 314001, China

**Synopsis** We investigate single- and double-electron capture (SEC and DEC) in $N^{7+}$–He collisions using a two-active-electron semiclassical asymptotic-state close-coupling (SCASCC) approach. The calculated total and partial cross sections show good agreement with available experimental data. Our analysis indicates that the measured true DEC cross sections may occurs through radiative stabilization of asymmetric $N^{5+}$ $(2\ell n\ell')$ states.

Electron capture processes in collisions of $N^{7+}$ ions with He have been extensively investigated, owing to their importance in fusion and astrophysical plasmas. Despite that, significant discrepancies remain between experimental and theoretical results, particularly for two-electron processes, which are still insufficiently understood. In this work, we employ a two-active-electron SCASCC approach [1] to calculate total and partial cross sections for SEC and DEC, with particular attention to DEC into autoionizing states (ADC). Fig. 1 presents our calculated total ADC cross sections as a function of the impact energy, compared with the previous theoretical and experimental investigations. As noted by Wu et al. [2], ADC can proceed via two decay pathways: autoionization, resulting in transfer ionization (TI), or radiative stabilization, yielding true DEC. Consequently, the experimental ADC cross sections are inferred as the sum of DEC and TI contributions.

Our results exhibit excellent agreement with the ADC measurements of Wu et al. [2] for energies above 20 keV/u. However, at lower energies, a discrepancy emerges, with our calculations exceeding the experimental data by up to 30% at 4 keV/u, likely due to their normalization procedure. Moreover, earlier experimental data at approximately 5 keV/u [3–5] exceed both our results and those of Wu et al. by more than a factor of two. In contrast, our predictions are in good agreement with the theoretical results of Harel and Jouin [6] in the 0.7–2 keV/u energy range, although deviations of up to 37% are observed at higher energies.

Furthermore, the experimental true DEC cross sections reported by Wu et al. [2], attributed to radiative stabilization of asymmetric $N^{5+}$ $(2\ell n\ell')$ states, are consistent with our ADC cross sections for $N^{5+}$ $(2\ell n\ell'; n > 5)$ above 20 keV/u, lending support to their interpretation. Below this energy, however, our predicted asymmetric $N^{5+}$ $(2\ell n\ell')$ cross sections deviate from the experimental values, increasing with decreasing energy. At the conference, we will also present partial ADC cross sections for the dominant $(2\ell n\ell')$ and $(3\ell n\ell')$ channels to further elucidate the underlying mechanisms.

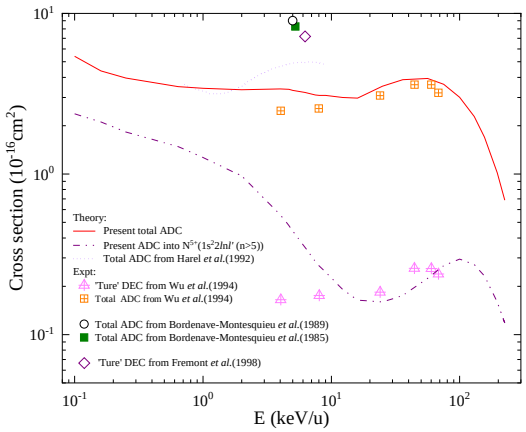


**Figure 1**. Total ADC cross sections as a function of impact energy.

## References

[1] Gao J W *et al.* 2024 *Phys. Rev. A* **109** 012801
[2] Wu W *et al.* 1994 *Phys. Rev. A* **50** 502
[3] Bordenave-Montesquieu A *et al.* 1985 *Nucl. Instrum. Methods Phys. Res. B* **9** 389
[4] Bordenave-Montesquieu A *et al.* 1989 *J. Phys. Colloques* **50** C1
[5] Frémont F*et al.* 1998 *Phys. Rev. A* **57** 4379
[6] Harel C*et al.* 1992 *J. Phys. B* **25** 221

*E-mail: gaojunwen@hznu.edu.cn

O-08

# Reactivity in clusters of amino acids induced by ion-collisions in the gas phase

**Sergio Díaz-Tendero**[1,2,3 *], **Ori Licht**[4], **Mariana Leiferman**[1], **Michal Roth**[4], **Sumit Srivastav**[5], **Fernando Aguilar-Galindo**[1,2], **Patrick Rousseau**[5] **and Yoni Toker**[4]

[1]Departamento de Química, Universidad Autónoma de Madrid, Spain
[2]Institute for Advanced Research in Chemistry (IAdChem), Universidad Autónoma de Madrid, Spain
[3]Condensed Matter Physics Center (IFIMAC), Universidad Autónoma de Madrid, Spain
[4]Physics Department and Institute for Nanotehcnology and Advanced Materials, Bar-Ilan University, Israel.
[5]Normandie University, ENSICAEN, UNICAEN, CEA, CNRS, CIMAP, Caen, France.

**Synopsis** In this communication we present a joint experimental and theoretical investigation showing how ionizing radiation triggers the formation of peptide bonds in clusters of amino acids in the gas phase. Experimentally, the charged fragments resulting in collisions of highly charged ions with clusters of amino acids in the gas phase are analyzed in coincidence with mass spectrometry. Simulations were carried out using molecular dynamics and the density functional theory.

When ionizing radiation interacts with molecules or clusters in the gas phase, it induces ionization and excitation. This phenomenon is observable regardless of the type of ionizing radiation used, including collisions with multiply charged ions, energetic synchrotron radiation, or intense laser fields. The direct consequence of this interaction is the formation of molecular species with high degrees of excitation and ionization, leading to fragmentation into two or more positively charged moieties which repeal each other, the so-called Coulomb explosion. However, alongside this process, a variety of other phenomena occur in competition; these include intramolecular charge transfer [1,2], hydrogen migration [3–5], roaming of a neutral fragment [6,7] or even intermolecular reactivity in a cluster forming larger species [8,9]. These reactions are triggered by ionization and excitation and can only be observed if they occur within the femtosecond timescale, characteristic of the Coulomb explosion.

In this communication we present how ionizing radiation induces the formation of peptide bonds in clusters of amino acids in the gas phase. In the past, simulations and experiments were carried out in parallel to understand the possible mechanisms involved [8,9]. Due to these promising previous results, we have expanded the study, including clusters of other amino acids. The main objective of this study is to evaluate the conditions of peptide bond formation in pure clusters of glycine, threonine, valine, serine and cysteine in the gas phase induced by collisions with alpha particles. We will show that after ionization and excitation, protonated clusters are formed after emission of neutral moieties. In a second step, peptide bonds are then formed from the protonated clusters with the corresponding release of a water molecule (see Figure 1). Different mechanism in the studied clusters will be presented and discussed during the communication.

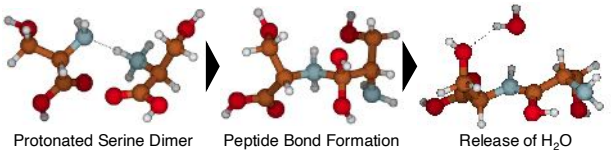


**Figure 1.** Mechanism of peptide bond formation in a protonated serine dimer.

## References

[1] Rousseau P *et al* 2021 *Sci. Adv.* **7** eabg9080
[2] Aguilar-Galindo F *et al* 2024 *Phys. Chem. Chem. Phys.* **26** 7638
[3] Maclot S *et al* 2013 *J. Phys. Chem. Lett.* **5** 3903
[4] Kling NG *et al* 2019 *Nat. Commun.* **10** 2813
[5] McDonnell M *et al* 2020 *J. Phys. Chem. Lett.* **11** 6724
[6] Mishra D *et al* 2022 *Phys. Chem. Chem. Phys.* **24** 433
[7] Mishra D *et al* 2024 *Nat. Commun.* **15** 6656
[8] Rousseau P *et al* 2020 *Nat. Commun.* **11** 3818
[9] Licht O *et al* 2023 *Angew. Chem. Int. Ed.* **62** e202218770

* E-mail: sergio.diaztendero@uam.es

O-09

# Stopping of charged particles interacting with a phosphorene monolayer: an *ab-initio* approach

**S Segui[1], M Moshayedi[2]*, and Z Mišković[2]**

[1]Instituto de Física E. Gaviola, CONICET and Universidad Nacional de Córdoba, Córdoba, 5000, Argentina
[2]Dept. of Applied Mathematics, and Waterloo Institute for Nanotechnology, University of Waterloo, Waterloo, N2L 3G1 Canada

**Synopsis** *Ab initio* data for the conductivity tensor of doped phosphorene, obtained from a DFT code in the optical limit, are used for calculating the stopping and image forces acting on a point charge travelling on a straight trajectory parallel to a 2D monoatomic layer.

Phosphorene is a 2D direct-gap semiconductor with a strongly anisotropic in-plane conductivity and its optical response can be dynamically tuned by changing the doping density $n$. Its crystalline structure gives place to large variations of mechanical, electrical and optical properties along the principal axes, making it of interest for optoelectronic applications. In particular, much effort is devoted to accurately describe phosphorene's characteristic hyperbolic plasmon polariton modes.

In this context, external charged particles constitute ideal probes to explore these features over a broad range of frequencies and wavelengths. The interaction of an incident particle and the 2D material is mediated, under certain conditions, by its optical response and can be modeled within the classical dielectric response framework [1], with a planar conductivity tensor as its main ingredient.

In this work we assess the stopping and image forces acting on the incident particle of charge $Ze$ travelling along a rectilinear trajectory parallel to an anisotropic 2D material representing doped phosphorene. The present formalism yields closed form expressions for the forces in terms of the phosphorene conductivity tensor components $\sigma_{x,y}$. We use *ab initio* data for $\sigma_{x,y}$ obtained from a time-dependent DFT code within the random phase approximation in the optical limit, for given values of the doping density $n$ [2, 3]. This model includes the contributions from intra- and inter-band transitions, and evaluates the tensor components along the main crystal axes.

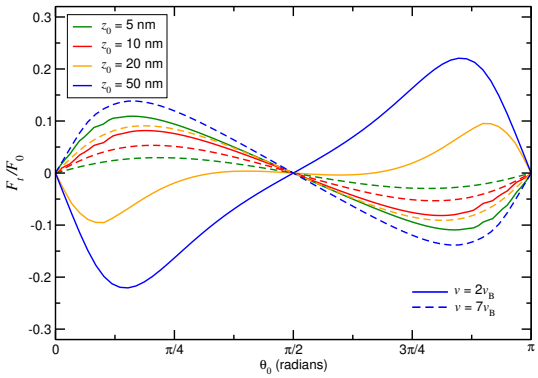


**Figure 1**. Normalized $F_t$ (with $F_0 = (Ze/2z_0)^2$) vs. the angle $\theta_0$ for a particle with $\overline{v} = 2$ and $\overline{v} = 7$ at various distances $z_0$ from the phosphorene plane.

We study the variation of the forces with the different parameters involved: the reduced velocity of the particle $\overline{v} = v/v_B$ (with $v_B = e^2/\hbar$), the distance $z_0$ from the monolayer, and the angle $\theta_0$ between the trajectory and the AC axis. Fig. 1 shows how the distance from the surface can affect the intensity and direction of the transverse component of the stopping force, $F_t$, for a particle traveling with velocities $\overline{v} = 2$ and 7 over a phosphorene layer with doping density $n = 10^{13}$ cm$^{-2}$. Finally, we compare with the results obtained using analytical models for the conductivity tensor [1].

## References

[1] Moshayedi M *et al.* 2022 *Phys. Rev. B* **105** 075429
[2] Novko D *et al.* 2021 *Phys. Rev. B* **104** 115421
[3] Despoja V and Lyon K 2023 *Private comm.*

*E-mail: silvina.segui@mi.unc.edu.ar

# Abstracts

## (Poster Presentations)

P-01

# Relevance of electronic excited states in the ionization and fragmentation dynamics of ferrocene induced in collisions with highly charged ions

**F Aguilar-Galindo[1,2 *], S Srivastav[3], A Domaracka[3], M Jbayli[3], S Díaz-Tendero[1,2,4], P Rousseau[3], and S Maclot[3]**

[1]Chemistry Department, Universidad Autónoma de Madrid, Madrid, Spain
[2]Institute for Advanced Research in Chemical Sciences, Universidad Autónoma de Madrid, Madrid, Spain
[3]Normandie Univ. ENSICAEN, UNICAEN, CEA, CNRS, CIMAP, Caen, France
[4]Condensed Matter Physics Center, Universidad Autónoma de Madrid, Madrid, Spain

**Synopsis** Delayed fragmentation of doubly ionized ferrocene ($Fc^{2+}$) is studied through quantum chemistry simulations, including ab initio approaches such as CASPT2, revealing the role of electronically excited states in the observed dynamics.

Ferrocene (Fc), $Fe(C_5H_5)_2$, is the best-known example of metallocenes, sandwich-like molecules with a metallic cation (iron in this case) and two organic rings (cyclopentadienide for Fc) which interact with the central ion through their π electrons. Fc is important for many different purposes, such as substituent in drugs for several diseases. Also, Fc is very stable under ambient conditions and presents a highly reversible oxidation-reduction process, reason why it is also used as reference in electrochemical measurements in non-aqueous solvents.

Stability of Fc upon double ionization has been measured in the ARIBE facility, the low-energy ion beam facility of GANIL (Caen, France). In these experiments an unexpected delay in the formation of some peaks has been found.

By carrying out Quantum Chemistry calculations based on Density Functional Theory (DFT), we have explored the potential energy surface (PES) of the charged ferrocene, to find the different possible products and intermediates as well as to determine the reaction barriers that could favor kinetically specific channels. We also performed ab initio molecular dynamics (AIMD) simulations, in order to identify other fragmentation channels when the internal energy of the molecule is high.

Finally, and using highly accurate *ab initio* methods, such as Complete Active Space Perturbation Theory at order 2 (CASPT2) we have computed the electronic excited states of the dicationic structure ($Fc^{2+}$), to provide an explanation of the delayed fragmentations that were observed experimentally. Our hypothesis, the generation of the $Fc^{2+}$ in an electronically excited state due to the ionization from bound molecular orbitals (π orbitals, which are more sensitive to the interaction with the $Xe^{20+}$ cation used as projectile) was reinforced by the obtention of a state with a double-excitation character and whose lifetime is long enough to induce chemical reactivity, leading to the fragmentation of the ferrocene.

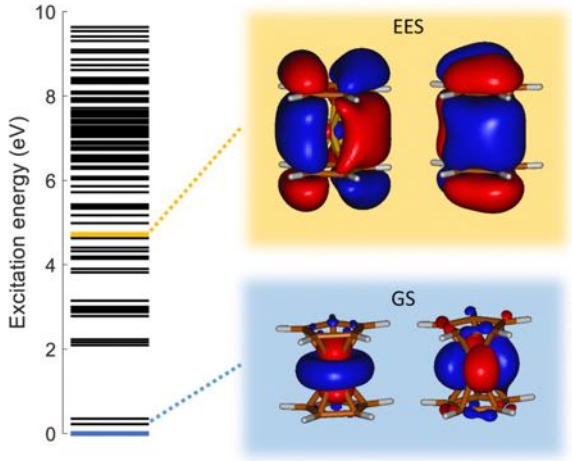


**Figure 1.** Molecular orbitals which are singly occupied in the excited state of interest (yellow box) and in the ground state (blue box).

## References

[1] F. Aguilar-Galindo, V.T.T. Nguyen, R. Singh, A. Domaracka, B.A. Huber, S. Díaz-Tendero, P. Rousseau and S. Maclot. 2024 *Phys. Chem. Chem. Phys.* **28** 7638

* E-mail: fernando.aguilar-galindo@uam.es

P-02

# Theoretical Investigation of $NO^+$ Ion Mobility in Helium Based on the Monchick–Mason Approximation

**L Aissaoui**[1] * **and I Ghodbane**[1] †

[1] Physics of Radiations and their Interactions with Matter Laboratory (PRIMALAB), University of Batna 1, Batna, 05000, Algeria.

**Synopsis** By applying the Monchick–Mason Approximation within both quantum-mechanical and classical frameworks, we developed two distinct methodologies for calculating ion mobility in rare gases across a range of temperatures: one based on average interaction potentials, and the other on average transport cross-sections.

Helium is the most commonly utilized buffer gas in drift-tube experiments focused on measuring ion-neutral reaction rate coefficients. As a result, a precise understanding of energy potential surfaces (EPS) and transport cross-sections is essential for elucidating ion transport properties, including ion mobility and diffusion. This study aims to investigate the quantum-mechanical calculation of ion mobility for $NO^+$ ions in helium under low gas temperature conditions, employing the ab initio potential energy surfaces of Viehland *et al.*, [1]. The study employs the modified version of Monchick–Mason Approximation [2] to calculate the effective potential, which is subsequently used to derive the quantum-mechanical diffusion cross-section through NUMEROV program and the classical cross-sections via Viehland's PC.F95 program. Ion mobility and diffusion coefficients are then computed using Viehland's GC.F95 program [3], with calculations conducted for two distinct gas temperatures: 4.3 K, 77 K, and 300 K.

The ion mobility of $NO^+$ ions in helium was calculated and compared against available experimental data, as well as against values derived using the effective cross-section method through the MMA2 approach. The computed results demonstrate that ion mobility values derived from the effective potential closely align with the experimental data, offering a superior match compared to those obtained via the effective cross-section approach.

Based on the outcomes of this study, we can underscore the reliability of using the MMA2 method for determining the effective potential of its application to the effective cross-section. This approach yields more accurate predictions for ion mobility, highlighting its potential for more precise modeling of ion transport in helium and other similar systems.

## References

[1] Viehland L A *et al.* 1996 *J. Chem. Phys.* **211** 1
[2] Monchick L *et al.* 1961 *J. Chem. Phys.* **35** 1676
[3] Yousef A *et al.* 2007 *J. Chem. Phys.* **127** 154309

*E-mail: aissaouilamia@yahoo.fr
†E-mail: imane.ghodbane@univ-batna.dz

P-03

# Benchmark target excitation and ionisation cross sections for $\bar{p} + \mathrm{He}(1\,^1S, 2\,^3S)$ collisions

**N. W. Antonio**[1]*, **and A. S. Kadyrov**[1,2]

[1]Curtin University, GPO Box U1987, Perth, WA 6845, Australia
[2]Institute of Nuclear Physics, Ulugbek, 100214 Tashkent, Uzbekistan

**Synopsis** Atomic excitation and ionisation in antiproton collisions with helium initially in the singlet and triplet states is considered. This is done by employing an implementation of the convergent close-coupling approach to ion-atom collisions using the Coulomb-Sturmian functions. A comprehensive set of results for the elastic, ionisation, and excitation cross sections in both initial configurations of the target are presented. The cross sections for antiproton collisions with triplet state helium are calculated for the first time.

Obtaining accurate benchmark data for ion-atom collisions is crucial for a wide range of practical applications. The most important data needed for applications is often the cross sections for various scattering processes. With recent advancements in available computing resources [1], we are able to study these systems with much better accuracy and detail than ever before.

Antiproton collisions with helium atoms have attracted significant interest [2]. However, important data is still missing for these collisions or there is no agreement between various theories. Being one of the simplest problems involving two electrons, it is of utmost importance to have a complete set of accurate benchmark results for all scattering processes that can occur. Furthermore, the helium target can be initially configured in two different electronic spin states, the singlet and triplet states. The total spin is conserved throughout the collision which allows us to investigate the dependence of the scattering cross sections on the initial target spin for the first time.

A new version of the convergent close-coupling approach to ion-atom collisions using the Coulomb-Sturmian basis (referred to as CS-CCC) is developed and applied to $\bar{p} + \mathrm{He}(1^1S, 2^3S)$ collisions [3]. We show that a unified treatment of the excitation and ionisation processes [4] can be applied for this system as well. Furthermore, we present the total elastic as well the single-electron ionisation and single-electron excitation cross sections for incident energies between 1 keV and 1 MeV. Fig. 1 shows the cross section for excitation of $3^1S$ state of He. There is significant disagreement between various calculations.

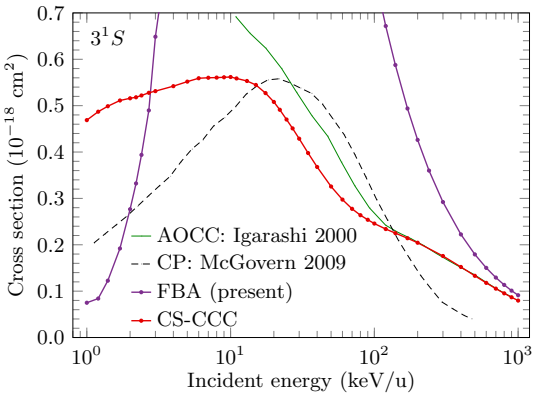


**Figure 1.** Cross sections for $3^1S$ excitation in $\bar{p} + \mathrm{He}(1^1S)$ collisions as functions of the incident energy. The present CS-CCC and FBA calculations are shown alongside previous calculations [5, 6].

## References

[1] Abdurakhmanov, I. B., Antonio, N. W., Cytowski, M., & Kadyrov, A. S. 2025 *In Proc. International Conference on High Performance Computing* pp 102-114
[2] Kirchner, T., & Knudsen H., 2011, *J. Phys. B* **44**, 122001
[3] Antonio N. W., & Kadyrov A. S., 2025, *Phys Rev. A* **111**, 052806
[4] Antonio N. W., Bray I., & Kadyrov A. S. 2024 *Phys. Rev. A* **110** 032810
[5] Igarashi A., Ohsaki A., & Nakazaki S. 2001 *Phys. Rev. A* **64** 042717
[6] McGovern M., *et al.* 2009 *Phys. Rev. A* **79** 042707

*E-mail: nicholas.antonio@postgrad.curtin.edu.au

P-04

# Convergent close-coupling approach to ion collisions with multi-electron targets: Application to $\bar{p}$ + C collisions

**N. W. Antonio***, **and A. S. Kadyrov**

Curtin University, GPO Box U1987, Perth, WA 6845, Australia

**Synopsis** The single-centre semi-classical convergent close-coupling approach to ion-atom collisions has been extended to model collisions with arbitrary multi-electron atoms. This is achieved by generating a set of target pseudostates using the multi-configuration interaction method. This new approach is applied to study antiproton collisions with atomic carbon. We present results for the elastic-scattering, excitation, and single-ionisation cross sections as well as the dominant state-resolved excitation cross sections.

Accurate cross section data for collisions involving multi-electron targets such as carbon, nitrogen, and oxygen atoms are important for various applications. Carbon and other impurities are present in fusion reactors (like tokamaks). Ion collisions with carbon help researchers understand erosion, sputtering, and impurity transport in the plasma. Currently there are no experimental measurements for heavy-ion collisions with carbon atoms. This is due to the difficulty of producing atomic carbon in sufficiently large quantities in a well-defined initial state. Furthermore, there is very little previous theoretical work available for collisions with this target [1] due to the complexity of the scattering problem in hand.

In this work, we report on the extension of the single-centre semi-classical Coulomb-Sturmian convergent close-coupling (CS-CCC) approach [2, 3] to model collisions with multi-electron targets. This extension has been made possible by writing a new general atomic structure code capable of generating a set of pseudostates to describe the entire target spectrum. The code is based on the configuration interaction method to represent the target states in terms of a set of multi-electron configuration state functions.

To demonstrate the capabilities of the new method, we apply it to study $\bar{p}$+C collisions. We calculate the elastic-scattering, excitation, and single-ionisation cross sections. We also calculate state-resolved cross sections for excitations from the $2s$ and $2p$ shells. As an example, in Fig. 1 we show the incident energy dependence of the total cross section for ionisation in $\bar{p}$+C collisions. The CS-CCC results are shown alongside the present first Born approximation (FBA) calculations. To demonstrate the importance of generating pseudostates in a multi-configurational manner, we also present the corresponding calculations using the frozen-core (FC) method. One can see that relaxing the FC approximation results in a significant increase in the total ionisation cross section at all incident energies considered. We compare our results to the ones using the basis-generator method (BGM) by Lüdde *et al.* [1]. The CS-CCC and BGM results merge with the present multiconfiguation FBA ones at high energies.

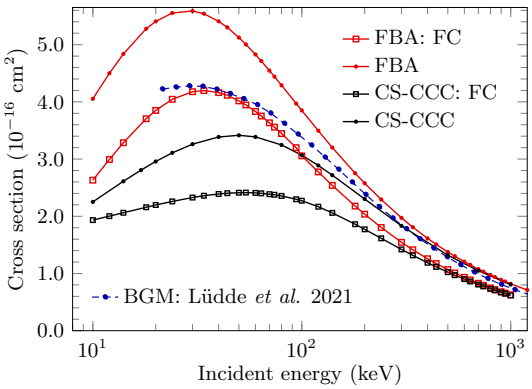


**Figure 1**. Cross section for ionisation in $\bar{p}$+C collisions. The present CS-CCC and FBA calculations are shown alongside the previous BGM results by Lüdde *et al.* [1]

## References

[1] Lüdde, H., *et al.* 2021, *Phys. Rev. A*, **104**, 032813
[2] Antonio, N. W., Bray, I., & Kadyrov, A. S., 2024, *Phys. Rev. A* **110**, 032810
[3] Antonio, N. W., & Kadyrov, A. S., 2025, *Phys Rev. A* **111**, 052806

*E-mail: nicholas.antonio@postgrad.curtin.edu.au

P-05

# K-shell lines of neutral Iron atoms in the central region of the Milky Way resolved by the X-ray astronomy satellite XRISM

**Y Aoki[1 *], K K Nobukawa[1 †], M Nobukawa[2], H Uchiyama[3], S Yamauchi[4], A Yoshimoto[4], T G Tsuru[5], H Uchida[5], T Narita[5], H Matsumoto[6], Y Kanemaru[7], Y Maeda[7], H Murakami[8], M Sawada[9] and Q D Wang[10]**

[1]Faculty of Science and Engineering, Kindai University, Higashi-Osaka 577-8502, Japan
[2]Department of Teacher Training and School Education, Nara University of Education, Nara 630-8528, Japan
[3]Faculty of Education, Shizuoka University, Shizuoka, 422-8529, Japan
[4]Faculty of Science, Nara Women's University, Nara 630-8506, Japan
[5]Department of Physics, Kyoto University, Kyoto 606-8502, Japan
[6]Department of Earth and Space Science, Osaka University, 1-1 Toyonaka 560-0043, Japan
[7]Japan Aerospace Exploration Agency, Institute of Space and Astronautical Science, Sagamihara 252-5210, Japan
[8]Faculty of Informatics, Tohoku Gakuin University, Sendai 984-8588, Japan
[9]Department of Physics, Rikkyo University, Tokyo 171-8501, Japan
[10]Department of Astronomy, University of Massachussets Amherst, MA 01003, USA

**Synopsis** Previous X-ray astronomy studies found K-shell emission lines of neutral iron atoms from the central region of the Milky Way. The emission lines are thought to be emitted by atoms in molecular clouds irradiated by X-rays or cosmic-ray particles. We performed high-resolution spectroscopy of the K-shell lines for the first time in the central region of the Galaxy using the microcalorimeter onboard XRISM. We report a beautiful K-shell line spectrum and associated spectral features, which have not been discovered by previous X-ray CCD observations.

K-shell line emission from neutral iron atoms in the central region of the Milky Way (the Galactic center region) was first discovered in the 1990s by the ASCA satellite (Koyama et al. 1996), which was the first to be equipped with an X-ray CCD with the good enough energy resolution to resolve the iron K-shell lines into the lines from neutral iron, $Fe^{24+}$, and $Fe^{25+}$. Since the intensity distribution of the K-shell lines of neutral iron atoms is correlated with giant molecular clouds, the emission lines are thought to be emitted by neutral iron atoms in dense gas photoionized by external X-rays, or ionized by low-energy cosmic rays (mainly protons and electrons, but also some heavy ions).

The new X-ray astronomy satellite XRISM (Tashiro et al. 2024) was launched on September 6, 2023. It is equipped with the microcalorimeter Resolve (Kelley et al. 2024) with the energy resolution of 4.5 eV (FWHM) at 6 keV, and can provide new information on the neutral iron lines by observing spectral features that could not be resolved by X-ray CCDs. We observed the Galactic center region with XRISM for the purpose of observing the iron K-shell lines. The total effective exposure time was 139 ksec.

In this presentation, we report the following results of the Resolve high-resolution spectroscopy. First, we detected prominent iron $K\alpha_1$ and $K\alpha_2$ lines, and also obtained the $K\beta$ spectrum with a feature attributed to the satellite $K\beta'$ on the low energy side. These features had not previously been resolved by X-ray CCD observations. We then detected a shoulder-shaped structure on the low energy side of the $K\alpha_2$ line, in the 6.28−6.34 keV band. The energy band and the flux ratio to the $K\alpha$ lines suggest that the structure consists of neutral iron K-shell lines that were Compton-scattered in dense gas. This finding provides insights into both the irradiation source and the column density of dense gas. We also detected a line-shaped structure on the high energy side of the $K\alpha_1$ line at $6425 \pm 36$ eV at a significance level of ~2.5σ. The intensity ratio to the $K\alpha_1$ line is ~1%. The line-shaped structure may be a satellite K-shell line with multiple vacancies (e.g., $K\alpha_{3,4}$ satellite). In this scenario, the intensity of the satellite can constrain what the projectiles are. Finally, prospects for future XRISM observations of the Galactic center will be presented.

## References

[1] Koyama K *et al.* 1996 *PASJ* **48** 249
[2] Tashiro M *et al.* 2024 *Proc. SPIE 13173, SPIE Astronomical Telescopes + Instrumentation Plenaries 2024*
[3] Kelley R *et al.* 2024 *Proc. SPIE 13093, SPIE Astronomical Telescopes + Instrumentation Plenaries 2024*

* E-mail: messier.aoki@kindai.ac.jp, † E-mail: kumiko@phys.kindai.ac.jp

P-06

# Ab initio high energy interactions for N-H$^+$ and N$^+$-H collisions. Integrated and transport cross sections and stopping power.

**M Buchowiecki**[1] *

[1]University of Szczecin, Szczecin, 70-453, Poland

**Synopsis** The applicability of the commonly used Molpro software was demonstrated for calculating the short range region of potential energy curves. Cross sections and nuclear stopping power were calculated [1] and compared with the previous results based on extrapolation [2].

The interactions between N($^4$S)-H$^+$ and the N$^+$($^3$P)-H($^2$S) were calculated using the multireference configuration interaction (MRCI) method within the MOLPRO software. This study extends the previous research to short-range distances, reaching $10^{-3}$ bohr.

The results enable an analysis of the extrapolation of the short-range limits of colliding atoms and ions with the $a\exp(-br)/r$ functional form. It was observed that at the shortest distances, atoms and ions interact with a Coulomb type potential. The high energy integrated cross sections (ICS), transport cross sections and nuclear stopping power (NSP) cross sections were calculated and differences from values derived from extrapolated potentials are discussed. The comparison with the SRIM code is performed.

Additionally, the long-range behavior of the N($^4$S)-H$^+$ interaction from the previous study was corrected and the effect of neglecting potential energy curves in calculations of NSP cross sections was examined.

Although nuclear interactions dominate at small interatomic distances, accurately calculating the potential is crucial for a precise description of interactions. Only at high energies (above 10 hartree in case of the present study), all PECs merge and gradually become one straight line on a log-log plot.

The previous calculations of ICS and transport cross sections for N-H$^+$ and N$^+$-H collisions were extended to higher energies (for the N-H$^+$ collisions also the low energy values were significantly corrected). The proper calculation of the short range limits of PECs is important for transport cross sections. It was found that SRIM-2013 code underestimated the NSP cross sections.

It was shown that it is essential to calculate NSP with the exact and complete set of PECs. At higher energies, proper extrapolation, or preferably *ab initio* calculation, of the high energy region of PECs is essential, especially when interactions are based on a single PEC.

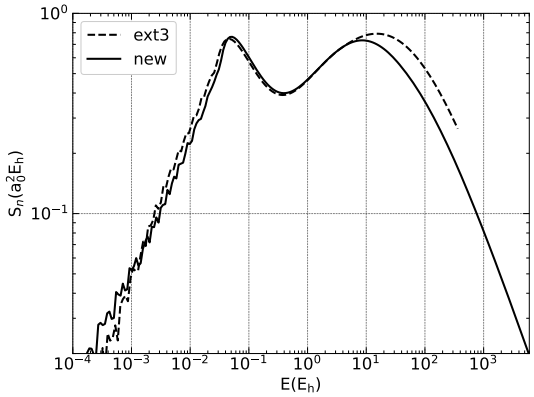


**Figure 1**. The NSP cross section of the N-H$^+$ collisions calculated with the present PEC (new), compared with PEC extrapolated at short distances (ext3).

## References

[1] Buchowiecki M 2025 *Nucl. Instrum. Methods Phys. Res. B* **562** 165645

[2] Buchowiecki M 2023 *At. Data Nucl. Data Tables* **151** 101574

*E-mail: marcin.buchowiecki@usz.edu.pl

P-07

# M-shell X-ray emission for Ho target induced by $Li^{1,2,3+}$ ions

**W L He, C R Zhang, L Y Xie and C Z Dong** †

Key Laboratory of Atomic and Molecular Physics and Functional Materials of Gansu Province, College of Physics and Electronic Engineering, Northwest Normal University, Lanzhou 730070, People's Republic of China

**Synopsis** The total M-shell and $M_\xi$, $M_\alpha$, $M_\beta$ and $M_\gamma$ X-ray production cross sections of Ho induced by 1 - 9 MeV $Li^{q+}$ ($q$ = 1 - 3) ions are calculated using the atomic electron removal cross sections code based on the ECPSSR theory, for direct ionization and non-radiative electron capture. The calculations show excellent agreement with the available experimental values.

The X-ray emission is an important consequential result from the inner-shell ionization during the interaction of highly charged ions with atoms, which provides significant information about atom configuration and the mechanism of such collisions. Reliable data on the atomic inner-shell ionization and subsequent emission of the characteristic X-rays are required for different applications including elemental composition analysis by ion beam analysis (IBA) like particle-induced X-ray emission (PIXE), as well as in basic research involving projectile charge change and energy loss, recoil ion production, or target vacancy rearrangement and X-ray production [1, 2]. In particular, there is pronounced scarcity of experimental and theoretical data for heavy-ion M-shell X-ray production cross sections, when compared to light ions, such as protons and helium induced K- and L-shell ionization cross section data.

In this work, we systematically investigated the direct ionization and non-radiative electron capture processes of Ho bombarded by 1 - 9 MeV $Li^{q+}$ ($q$ = 1 - 3) ions. The detailed direct ionization, non-radiative electron capture, the various M series lines and the total M-shell X-ray production cross sections of Ho are calculated using the ERCS24 code [3] based on the first Born and ECPSSR theories. Fig. 1 (a-c) shows the total M-shell X-ray production cross sections as a function of energy of the incident lithium ions, and compared with the available experimental and theoretical values from Ref. [2]. It is clear that the results from the first Born theory were significantly overestimated, while the inclusion of corrections in the ECPSSR theory gives results are in excellent agreement with the experimental measurements by Yu et al. [2]. Furthermore, the X-ray production cross sections of $M_\xi$, $M_\alpha$, $M_\beta$ and $M_\gamma$ lines from different M-shell series are comprehensively analyzed in relation to the charge states of incident lithium ions.

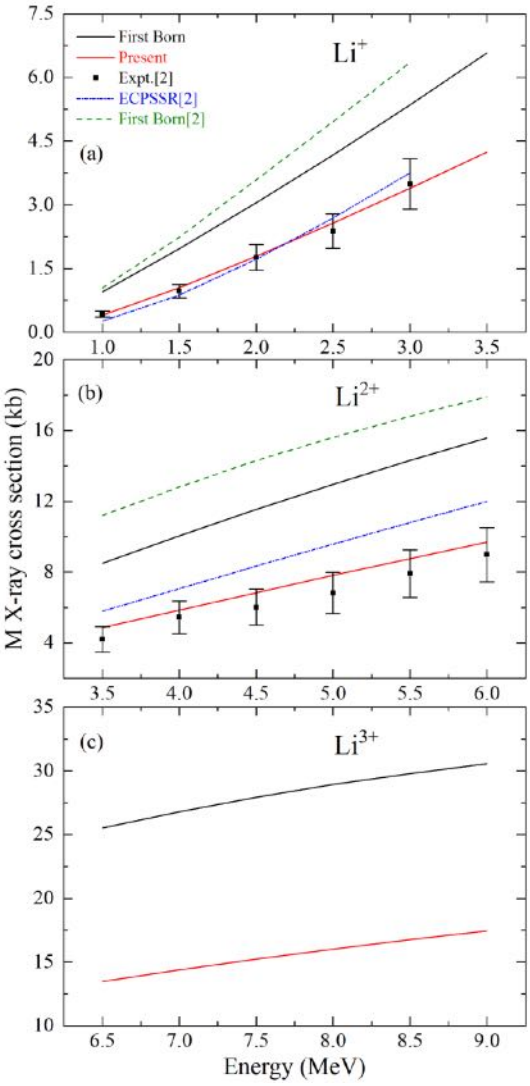


**Fig 1.** The total M-shell X-ray production cross sections in Ho by 1 - 9 MeV $Li^{1,2,3+}$ ions.

## References

[1] Tanis J A 1985 *Phys. Rev. A.* **31** 750
[2] Yu Y C et al 2004 *NPB.* **219** 284–288
[3] Horvat V 2024 *Comput. Phys.* **299** 109147

† E-mail: dongcz@nwnu.edu.cn

P-08

# Theoretical and experimental investigations of projectile excitation to autoionizing states in swift carbon and oxygen ions collisions with helium

**A. Dubois[1 *], S. Passalidis[1], A. Laoutaris[2,3], S. Nanos[3,4], A. Biniskos[4], E.P. Benis[4], and T.J.M. Zouros[2]**

[1]Sorbonne Université, CNRS, Laboratoire de Chimie Physique- Matière et Rayonnement, F-75005 Paris, France
[2]Department of Physics, University of Crete, GR-70013 Heraklion, Greece
[3]Tandem Accelerator Laboratory, Institute of Nuclear and Particle Physics, NCSR "Demokritos", GR-15310 Aghia Paraskevi, Greece
[4]Department of Physics, University of Ioannina, GR-45110 Ioannina, Greece

**Synopsis** The production of the projectile 2s2p $^3$P and 2s2p $^1$P autoionizing states is investigated in 0.5-1.5 MeV/u collisions of He-like carbon and oxygen ($1s^2$, 1s2s $^3$S, 1s2s $^1$S) ions with helium targets. The experimental results are obtained using high-resolution Auger projectile electron spectroscopy at 0° relative to the beam direction. The theoretical cross sections are evaluated using a three-electron asymptotic state close-coupling approach. Comparison and discussion of the results will be presented at the symposium.

We report results on double excitation and single excitation to autoionizing states,

$$Z^{q+}(1s^2, 1s2s\ ^{1,3}S) + He \rightarrow Z^{q+}(2s2p\ ^{1,3}P) + He(All)$$

with $Z^{q+} \equiv C^{4+}, O^{6+}$ and where He(All) indicates that the projectile excitation processes are considered whatever the final state (ground, excited, ionized) of the target after the collision. These latter channels are considered in the calculations since the final state of helium was not experimentally determined.

The experiment was conducted at the National Center for Scientific Research "Demokritos" 5.5 MV Tandem accelerator facility, utilizing Zero-degree Auger projectile spectroscopy (ZAPS) setup, allowing for the detection of projectile Auger electrons with high efficiency and high energy resolution. Due to the stripping process, the two-electron ion beams provided by the accelerator are composed by ions in ground state ($1s^2$) but also in long lifetime metastable states (1s2s $^{1,3}$S), which survive to the target. Their respective fractions are determined using our "two-spectra" measuring technique and three-component model [1].

The theoretical resuts were obtained through a semiclassical close coupling approach, using an asymptotic (atomic) state expansion of the scattering wavefunction, see e.g. [2] for detail. The collision systems are described within a three-electron treatment and a full configuration interaction scheme. so that the helium target carries only one active electron, throught a model potential.

In the symposium, Auger single differential cross sections will be presented for spin-conserved $^{1,3}S \rightarrow {}^{1,3}P$, see Fig. 1 from [3], and spin-exchange ($^{1,3}S \rightarrow {}^{3,1}P$) excitation. A systematic comparison between experimental and theoretical outcomes will be provided, as well tentative interpretations of the differences, the measurements being higher than the predictions.

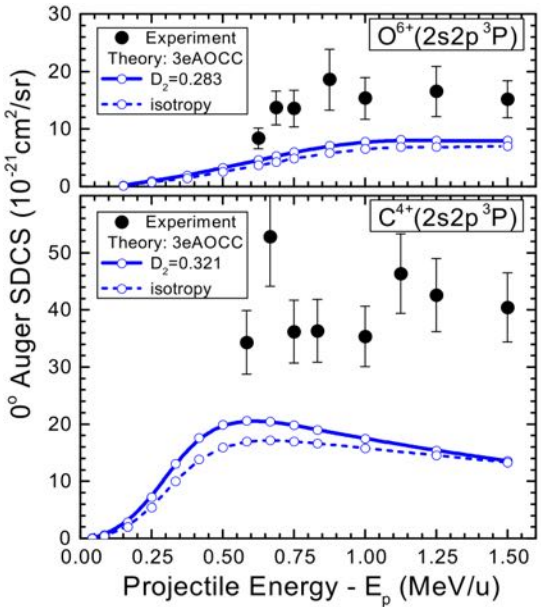


**Figure 1.** Absolute 0◦ Auger single-differential cross sections as function of impact energy for production of the (2s2p $^3$P) in collision between He and (1s2s $^3$S) initial state of $C^{4+}$ and $O^{6+}$ projectiles. See [3] for detail.

## References

[1] Zouros TJM *et al* 2024 *J. Phys. B: At. Mol. Opt. Phys.* **58** 055201
[2] Gao J W *et al* 2018 *Phys.Rev. A.* **97** 052709
[3] Laoutaris A *et al* 2024 *Phys. Rev. A* 109 032825

* E-mail: alain.dubois@sorbonne-universite.fr

P-09

# Measurement of ion-induced secondary electron emission from metal surfaces

**T Fujita[1], J Kim[2], A Suzuki[2], M Matsukuma[2] and M Hoshino[1]***

[1]Department of Physics, Sophia University, Tokyo, 102-8554, Japan
[2]Tokyo Electron Technology Solutions Limited, Yamanashi, 407-0192, Japan

**Synopsis** We developed a new apparatus for measuring the ion-induced secondary electron emission yield from metal surfaces, aiming to improve plasma modeling accuracy for semiconductor manufacturing processes. Using an ion gun, we irradiated copper and molybdenum samples with $Ar^+$ ions at accelerated energies of 0.5, 1.0, and 2.0 keV. The measured secondary electron yields were in good agreement with previous studies on copper and molybdenum. Surface observations using the SEM confirmed an increase in surface roughness due to sputtering.

For modeling the behavior of low-temperature plasmas used in etching and chamber cleaning processes in the manufacturing of large-scale integrated circuits, quantitative atomic and molecular data on various elementary processes in the plasma are essential. In particular, cross-sections data for low-energy electron collisions are of critical importance. Since plasmas are generally generated through electron impact excitation and ionization, we have conducted quantitative measurements of collision cross sections for both elastic and inelastic scattering processes (such as vibrational and electronic excitations) between low-energy electrons and gas-phase atoms or molecules.

Recently, in plasma modeling, secondary electron emission caused by ions generated through electron impact ionization colliding with surrounding metal walls has attracted significant attention as a key process. A detailed understanding of the mechanisms involved in the interactions between emitted electrons and metal walls is expected to lead to more accurate plasma simulations. Therefore, in this study, we newly developed an apparatus for measuring the ion-induced secondary electron emission yield from metal surfaces and conducted corresponding measurements.

The secondary electron emission yield, $\gamma$ is commonly used as an indicator of the number of electrons emitted when a metal surface is irradiated by an ion or an electron. It is defined as the number of secondary electrons emitted per incident particle. In this study, we used an ion gun (USG-3, *ULVAC-Phi, Inc.*) as the ion beam source. This system generates ion beams via electron impact ionization by a hot filament and focuses the ion beam using an electrostatic einzel lens. The acceleration voltage can be adjusted to 0.5, 1.0, and 2.0 keV under appropriate focusing conditions. For the measurement of the yield $\gamma$, a retarding electrode capable of applying a negative voltage was installed in front of the sample holder to return secondary electrons emitted by ion irradiation back to the sample surface. A picoammeter was directly connected to the sample holder, and the reduction in ion current due to secondary electron emission was measured as a function of the retarding voltage.

In this study, we irradiated copper and molybdenum samples with $Ar^+$ ions at 0.5, 1.0, and 2.0 keV, and measured the secondary electron emission yield $\gamma$. The $\gamma$ value obtained from irradiation with a 2.0 keV $Ar^+$ ion beam showed good agreement with previous studies on copper [1] and molybdenum [2–3]. In addition, the surface condition of the copper sample after $Ar^+$ ion irradiation was observed using a scanning electron microscope (SEM), and an increase in surface roughness due to sputtering was also confirmed (Fig. 1).

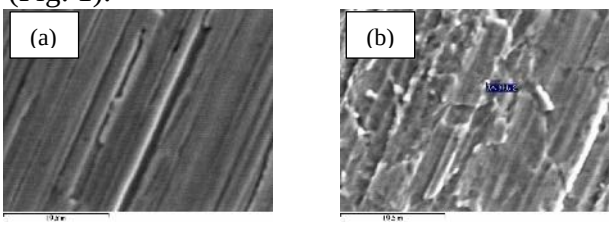


**Figure 1.** SEM images of Cu: (a)before irradiation, (b)after irradiation.

## References

[1] Buschhaus R *et al* 2022 *Plasma Sources Sci. Technol.* **31** 025017
[2] Ferrón J *et al* 1981 *J. Phys. D: Appl. Phys.* **14** 1707
[3] Hagstrum H D 1956 *Phys. Rev.* **104** 672

* E-mail: masami-h@sophia.ac.jp

P-10

# State-resolved autoionizing double-electron capture in intermediate-energy collisions of $C^{4+}$ ($1s2s\ ^3S$) with He

**D L Guo[1,2]*, X B Zhu[1,2], Y Gao[1,2], K Z Lin[1,2], X L Zhu[1,2], D M Zhao[1,2], R T Zhang[1,2], H F Yu[1], S F Zhang[1,2] and X Ma[1,2]**

[1]Institute of Modern Physics, Chinese Academy of Sciences, Lanzhou 730000, China
[2]University of Chinese Academy of Sciences, Beijing 100049, China

**Synopsis** We report on an investigation of the autoionizing double-electron capture process in 10-40 keV/u collisions of $C^{4+}$ ($1s2s\ ^3S$) ions with He. We demonstrate that the low-lying energy levels of the core-excited four-electron system can be precisely determined, providing a benchmark for sophisticated theoretical calculations. Furthermore, our findings suggest a novel mechanism that enhanced the significance of metastable states.

Single and double electron capture are fundamental processes that occur in ion-atom collisions. The knowledge gained from the studies on these processes not only enhances our understanding of atomic and molecular physics but also finds practical applications in diverse fields.

Using a high-resolution COLTRIMS reaction microscope spectrometer [1], we focus on the investigation of autoionizing double-electron capture (ADC) by $C^{4+}$ ($1s2s\ ^3S$), where the projectile is left in double or triply excited states. The relative partial cross sections for electron capture to specific $n\ell$ levels of the projectile can be directly determined from the longitudinal recoil-ion momentum (Figure 1), without the need for corrections related to cascade effects and the lifetimes of projectile Auger states, facilitating comparisons with theoretical calculations. Notably, these measurements allow us to determine the energy levels of the core-excited states of the four-electron system, which are inaccessible by other spectroscopic methods.

Additionally, we demonstrated that although the concentrations of metastable ions are low, the cross sections for transfer ionization of metastable states can be significantly higher than those for the ground state. The tendency of autoionizing states to decay preferentially to lower singly excited states with high efficiency may lead to a notable enhancement of characteristic lines in applications such as plasma equilibrium and diagnostics. This finding introduces a novel scenario that amplifies the role of metastable states in relevant fields.

The present experimental data are of direct relevance for understanding the effects of the metastable ions in the diverse plasma and important in the advancement of theoretical methods.

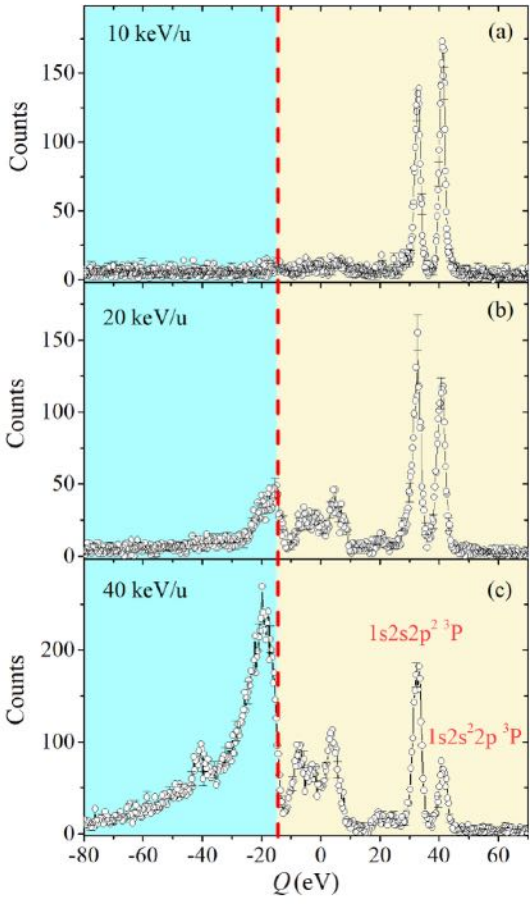


**Figure 1**. The measured $Q$ value distribution.

## References

[1] Gao Y *et al.* 2024 *Rev. Sci. Instrum.* **95** 043302

*E-mail: guodalong@impcas.ac.cn

P-11

# Quantitative evaluation of argon in vanadium nitride films by non-Rutherford backscattering spectrometry and particle induced x-ray emission

**R Hasebe [*], T Osumi and Y Gotoh [†]**

Department of Electronic Science and Engineering, Kyoto University, Kyoto 615-8510, Japan

**Synopsis** The ratio of argon incorporation in thin films of vanadium nitride was assessed using particle induced x-ray emission (PIXE) and non-Rutherford backscattering spectrometry (n-RBS). The results showed that the ratio of argon in the film increased as the partial pressure of argon increased.

Sputtering is widely used as a deposition method for thin film coating. However, in the sputtering process, reflected Ar atoms from the target surface can be incorporated into the growing film, resulting in degrading the physical and chemical properties of the film. In hard coatings such as titanium nitride, vanadium nitride (VN), and Diamond-Like Carbon (DLC), high Ar content may reduce hardness and wear resistance by changing the crystal structure and promoting defect formation [1, 2]. Therefore, the quantitative evaluation of Ar atom incorporation is important. In contrast, quantitative analyses of Ar incorporation in thin films have been conducted in only a few studies.

The purpose of this study is to evaluate the incorporation of Ar in VN films deposited by reactive RF sputtering using a combination of non-destructive analytical techniques, non-Rutherford Backscattering Spectrometry (n-RBS) and Particle Induced X-ray Emission (PIXE). The VN films were deposited at an RF power of 50 W and a substrate temperature of 300°C, under a total pressure of 1 Pa, with a mixture of Ar and $N_2$ as the process gas. In n-RBS, we cannot detect Ar signal because its signal overlaps with vanadium signal. However, PIXE enables us to detect Ar signal. The nitrogen-to-vanadium (N/V) composition ratio was evaluated using n-RBS, and the argon-to-vanadium (Ar/V) ratio was evaluated by PIXE. As a result, we evaluated the ratio of Ar in the films together with the nitrogen composition.

In this work, a tandem accelerator at Kyoto University was used with a 1.63 MeV proton beam. PIXE measurements were performed simultaneously using a silicon drift detector (SDD) with a 125 μm mylar as an absorber.

Figure 1 shows the relationship between the Ar partial pressure and the Ar concentration in the films. At the Ar partial pressure of 0.95 Pa, the incorporation of Ar reached approximately 0.91 at.%.

The results indicate that higher Ar partial pressures lead to increased incorporation of Ar in the film. In this study, it was shown that the combined use of n-RBS and PIXE is effective to quantitatively assess Ar gas incorporation in sputtered thin films. This approach could be useful in process control to prevent unintended Ar incorporation.

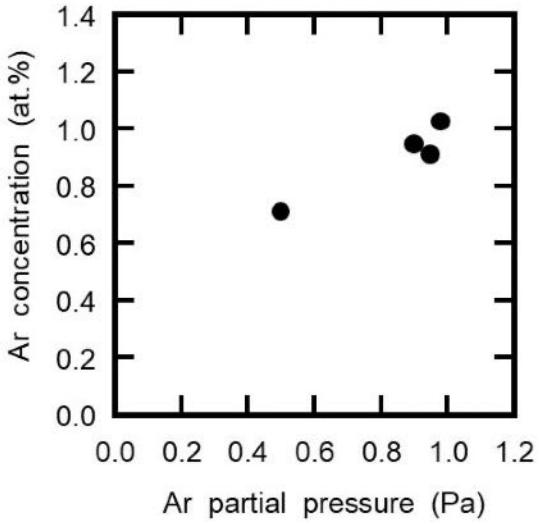


**Figure 1.** Ar concentrations of VN films prepared at some different Ar partial pressures.

## References

[1] Maja P *et al* 2011 *Processing and Application of Ceramics.* **5** (1) 19-23

[2] Linda A *et al* 2019 *Surface & Coatings Technology.* **378** 124948

[*] E-mail: hasebe.ryo.73m@st.kyoto-u.ac.jp

[†] E-mail: gotoh.yasuhito.5w@kyoto-u.ac.jp

P-12

# Contributions of Atomic, Molecular and Sputtering Data Workshop Group for the NIFS database

**H. Tsuchida**[1†], M. Goto[2], T. Hirayama[3], M. Hoshino[4*], Y. Hoshino[5], A. Igarashi[6], A.M. Imai[1], K. Ishii[7], D. Kato[2], M. Kato[2], N. Kimura[2], M. Kitajima[8], T. Kusakabe[9], T. Kawate[10], K. Moribayashi[11], T. Morishita[12], I. Murakami[2], B. Peterson[2], H.A. Sakaue[2], N. Shimakura[13], and K. Soejima[13]

[1] Kyoto University, Kyoto 615-8540, Japan
[2] National Institute for Fusion Science (NIFS), Gifu 509-5292, Japan
[3] Rikkyo University, Tokyo 171-8501, Japan
[4] Sophia University, Tokyo 102-8554, Japan
[5] Kanagawa University, Kanagawa 221-8686, Japan
[6] Miyazaki University, Miyazaki 889-2192, Japan
[7] Nara Women's University, Nara, 630-8506, Japan
[8] Institute of Science Tokyo, Tokyo 152-8551, Japan
[9] Kindai University, Osaka 577-8502, Japan
[10] Naka Fusion Institute, QST, Ibaraki 311-0193, Japan
[11] Kansai Institute for Photon Science, QST, Kyoto 619-0215, Japan
[12] The University of Electro-Communications, Tokyo 182-8585, Japan
[13] Niigata University, Niigata 950-2181, Japan

**Synopsis** Atomic, molecular and sputtering data workshop group in National Institute for Fusion Science (NIFS) has constructed database for cross sections in various processes of electron and ion collisions with atoms and molecules as well as for ion-sputterings from solid surfaces related to various plasma processes, including those in fusion research, and has continued to collect, accumulate, operate, and release data for many years. We will present recent activities of our data worshop group in NIFS.

Fundamental atomic and molecular database for cross sections in electron and ion collisions with atoms and molecules covering a wide range of energy regions as well as for ion-induced supperings from solid surfaces are essential in plasma modellings relevant not only for fusion plasma research but also industrial applications of plasmas and astronomical observations. Present working group in National Institute for Fusion Science (NIFS) has constructed an atomic and molecular database related to various plasma processes, including those in fusion research, and has continued to collect, accumulate, update the data for many years, because NIFS has been promoting collaborative research organizing working groups of domestic experts to update and make more accessible the numerical database of collision cross sections of atoms and molecules in plasmas and ion sputtering yields and reflection coefficients on solid surfaces.

The working group has searched and reviewed literatures relevant to cross section data for various processes of electron and ion collisions with many molecules [1]. New data collected by this working group were added to the NIFS database (https://dbshino.nifs.ac.jp) for molecular target, i.e. AMOL (electron collision) and CMOL (ion collision). Recently, cross section data for electron collisions and heavy particle collision with atoms and ions of high-Z elements have been surveyed and collected [2]. The new data for excitation-, ionization- and total-cross sections for electron collision with atoms and ions of high-Z elements were stored into the NIFS database AMDIS. For the heavy particle impact cross section data, new data were stored into the NIFS database CHART.

Since 2019, we have surveyed new data for ion-sputtering of solid surfaces. In this working group, in addition to literature survey, new measurements of self-sputtering yield were conducted at 300 keV and 1 MeV energies, and empirical formula by Eckstein and Yamamura have been also examined with the data set including the new measurements. Based on these results, a novel neural network taking into account the empirical laws is being constructed to make a reliable prediction possible.

We will present our recent activities of our deta workshop group in NIFS at the conference.

This work has been partly supported by the NIFS Domestic Collaboration Research Programs (Proposal numbers NIFS23KIIF024 and NIFS23KIIF033).

**References**

[1] Kimura M *et al* 2006 NIFS-DATA **98**, 1-38
[2] Kitajima M et al NIFS-DATA in preparation

† E-mail: tsuchida.hidetsugu.4a@kyoto-u.ac.jp
* E-mail: masami-h@sophia.ac.jp

P-13

# Cluster effects in collisions of hydrogen cluster ions with $H_2$ molecules

**Y Bai[1], T Wang[1,2], J Zhao[1,2], S T S Kovács[3], P Herczku[3], R Rácz[3], B Sulik[3], S Biri[3], G Lakatos[3,4], Z Juhász[3*]**

[1] School of Nuclear Science and Technology, Lanzhou University, 730000, China
[2]MOE Frontiers Science Center for Rare Isotopes, Lanzhou University, Lanzhou 730000, China
[3] HUN-REN Institute for Nuclear Research, Debrecen, H-4026, Hungary
[4] Doctoral School of Chemistry, University of Debrecen, H-4032, Hungary

**Synopsis** We measured fragment emission from $H_2$ molecules induced by different hydrogen cluster ions of $H_n^+$. We observed that the emission cross sections do not scale with the number of the projectile centers *n* indicating the synergic effects of the cluster.

In order to understand the basic processes of fusion reactions in extreme dense plasma, e.g. in the core of sun and inertial confinement fusion (ICF) plasma, we need to study multi center collisions. Stopping force of hydrogen cluster ions was studied in solids by W. Brandt *et al.* in the 1970s [1] and it was found to be different than the one expected by additive rules. This effect is called the vicinage effect and later it was studied by many laboratories [2,3]. There is a very limited study of collisions hydrogen cluster ions on gas targets however [4]. Despite, the lack of experimental results for hydrogen cluster ions, such data are much in demand for solar and ICF fusion studies [3].

By using the hydrogen cluster ions and their isotopologues ($H_n^+$, $D_n^+$) as projectile, we can simulate the multi-body collisions at a few keV energy in the relevant plasmas. The *n* value of cluster-ion projectiles may affect the scattered and recoiled centers' kinetic energy and angular distribution, and in turn it may affect fusion reaction rate.

We studied experimentally collisions of equivelocity $H_n^+$ ($D_n^+$) ions ($n$=1−3) on $H_2$($D_2$) target at HUN-REN ATOMKI by a field-free time of flight (FFTOF) setup described in [5]. Cross sections for binary recoiled $H^+$($D^+$) centers as function of the scattering angle were determined, see part of the results in Fig. 1.

It was found that the emission cross sections are higher for the cluster ions than that can be expected by additive rules particularly for the $H_3^+$ ions. For deuteron cluster ions, the effect was smaller. The results demonstrate that cluster effects are present in gas phases and may influence fusion plasma processes.

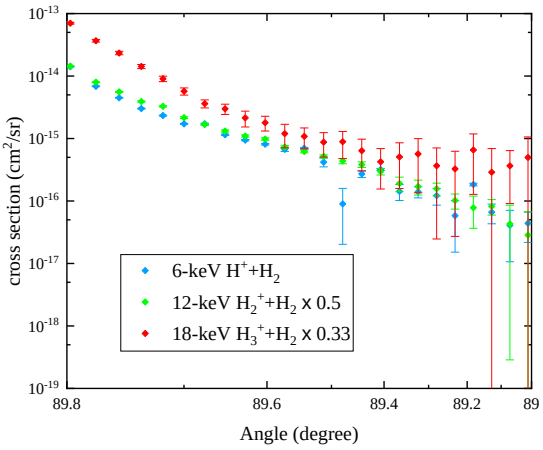


**Figure 1.** Differential emission cross sections of $H^+$ fragment ions form the target $H_2$ molecules induced by different hydrogen cluster ion impact indicated in the figure. Results are normalized to one center of the projectile.

This research was supported by Nature Science Foundation of China (NSFC, No.12275112), and by NKFIH ADVANCED grant (No. 151196).

## References

[1] Brandt W, Ratkowski A, Ritchie R H 1974 *Phys. Rev. Lett.* **33** 1325
[2] L'Hoir A *et al* 2012 *Phys. Rew. A* **85** 042901
[3] Wang G *et al* 2018 *Matt. Rad. Extr.* No. **2** 67
[4] Farizon B *et al* 1999 *Nucl. Inst. Meth. B* **154** 312
[5] Juhász Z *et al* 2023 *Phys. Rew. A* **107** L010801

* E-mail: zjuhasz@atomki.hu

P-14

# Temperature Dependence of the Electron-Induced Radiolysis of Solid $N_2O$: Applications to Astrochemistry in the Outer Solar System

**Z Juhász,[1,*] D V Mifsud,[1] S Góbi,[2,3] P Herczku,[1] B Sulik,[1] S Ioppolo,[4] N J Mason,[1,5] and Gy Tarczay[2,3,6]**

[1]HUN-REN Institute for Nuclear Research (ATOMKI), Debrecen H-4026, Hungary
[2]MTA-ELTE Lendület Laboratory Astrochemistry Research Group, Institute of Chemistry, Eötvös Loránd University, Budapest H-1518, Hungary
[3]Laboratory of Molecular Spectroscopy, Institute of Chemistry, Eötvös Loránd University, Budapest H-1518, Hungary
[4]Centre for Interstellar Catalysis, Department of Physics & Astronomy, Aarhus University, Aarhus DK-8000, Denmark
[5]School of Physics & Astronomy, University of Kent, Canterbury CT2 7NH, United Kingdom
[6]Centre for Astrophysics & Space Science, Eötvös Loránd University, Budapest H-1518, Hungary

**Synopsis** Radiation-induced chemistry in low-temperature molecular ices is a key component of astrochemistry. Recent studies have elucidated the chemistry of $N_2O$ under conditions relevant to pre-stellar nebulae, but comparatively little work has been performed under conditions more relevant to outer Solar System environments that are characterized by higher temperatures. Here, we studied the influence of temperature (20-60 K) on the 2 keV electron-induced radiolysis of crystalline $N_2O$ ices by calculating the relevant *G*-values, and demonstrated that this is indeed a temperature-dependent process.

$N_2O$ is a likely surface constituent of icy outer Solar System bodies whose surfaces are rich in nitrogen. The surfaces of these bodies are continually exposed to ionizing radiation in the form of the solar wind or galactic cosmic rays. However, although the radiolysis of solid $N_2O$ at temperatures relevant to pre-stellar nebulae has been well-defined, little analogous work has been performed at higher temperatures relevant to the outer Solar System [1]. In this study, we used the Ice Chamber for Astrophysics-Astrochemistry [1,2] to prepare neat crystalline $N_2O$ ices at 20, 30, 40, 50, and 60 K; which were then exposed to a 2 keV electron beam that was used to mimic space radiation. The radiolysis of the $N_2O$ ices were monitored *in situ via* Fourier-transform transmission absorption mid-infrared spectroscopy. Spectra acquired during irradiation were used to quantify the abundance of $N_2O$, expressed as molecular column densities (molecules $cm^{-2}$), at various dose levels.

The radiolytic destruction rate of $N_2O$ at the different temperatures that were considered in this study was quantified through the *G*-value; i.e., the number of $N_2O$ molecules destroyer per 100 eV of energy dosed into the ice. Our analysis demonstrated that the destruction *G*-value of crystalline $N_2O$ is indeed temperature-dependent, with higher temperatures being associated with more negative *G*-values (Figure 1). The calculation of these *G*-values has also allowed us to estimate the survivability of $N_2O$ ice in the outer Solar System at these temperatures expressed as the number of years of exposure to ionizing radiation required to destroy the $N_2O$. By considering the cosmic ray dose rates at 40 AU for icy material at the surface (i.e., within the top $10^{-6}$ cm) of a KBO and that buried beneath $10^{-3}$ cm of material, we have estimated the survivability of crystalline $N_2O$ ice as being on the order of a few thousand and a few billion years, respectively [1].

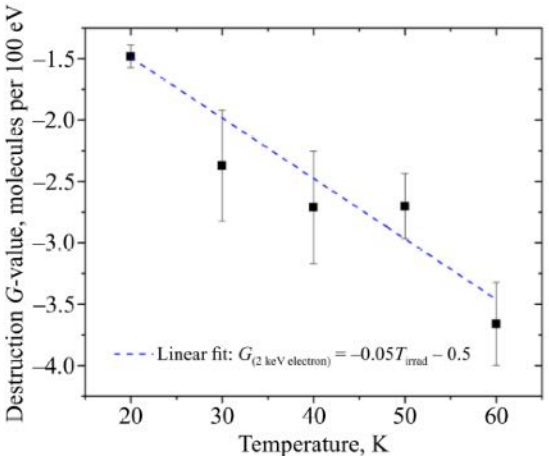


**Figure 1.** $N_2O$ ice *G*-value variation with temperature.

This research was supported by a NKFIH ADVANCED grant (No. 151196).

## References

[1] Mifsud DV *et al* 2025 *Low Temp. Phys.* **51** 459
[2] Herczku P *et al* 2021 *Rev. Sci. Instrum.* **92** 084501

* E-mail: zjuhasz@atomki.hu

P-15

# Connection between atomic excitation and ionisation

**N. W. Antonio, I. Bray and A. S. Kadyrov** *

Curtin University, GPO Box U1987, Perth, WA 6845, Australia

**Synopsis** A common nature of atomic excitation and ionisation in ion-atom collisions is investigated. Using the $\bar{p}+\mathrm{H}(1s)$ collision system as an example, we demonstrate that the state-resolved excitation cross sections multiplied by $n^3$, where $n$ is the principal quantum number of the excited state, and the corresponding partial singly differential ionisation cross section form two parts of a single function. This allows one to obtain the excitation cross section for any state and the energy-differential ionisation cross section at the threshold. This method can be used in theoretical approaches to excitation and ionisation, as well as experiments.

When a projectile collides with an atom it may scatter elastically or lead to excitation of the target. It can also ionise the target if the projectile has sufficient energy. An interesting aspect of the ionisation process in atomic collisions is its relation to excitation. In fact, as early as 1924, Sommerfeld [1] predicted that the oscillator strengths from the discrete states merge with the differential one from the continuum at the ionisation threshold. Furthermore, based on the Oppenheimer scaling rule [2], Rudd and Macek [3] suggested that the average excitation cross section below the ionisation limit merges continuously with the ionisation cross section above the ionisation limit in ion-atom collisions. However, the idea has not been further developed. In this work we quantitatively show a continuity between excitation and ionisation of atomic hydrogen. We introduce a function that unifies these scattering processes. It links the state-selective excitation cross sections, $\sigma_{n\ell}$, and the corresponding partial singly differential ionisation cross section (SDCS), $\mathrm{d}S_\ell/\mathrm{d}E$, where $n$ and $\ell$ are the principal and orbital angular momentum quantum numbers of the excited state, $E$ is the energy of the ejected electron. We then demonstrate how this function can be used to get the state-resolved target-excitation cross sections for any bound state including the Rydberg ones. Furthermore, it gives the energy-differential ionisation cross section at, and arbitrarily close to, the ionisation threshold.

To illustrate this idea, we study $\bar{p}+\mathrm{H}(1s)$ collisions using the Coulomb-Sturmian implementation of the convergent close-coupling approach to ion-atom collisions [4]. As an example, in Fig. 1 we plot $n^3\sigma_{n\ell}$ and $\mathrm{d}S_\ell/\mathrm{d}E$ for $\ell = 0-4$. One can see that $n^3\sigma_{n\ell}$ and $\mathrm{d}S_\ell/\mathrm{d}E$ align and join at the ionisation threshold for each value of $\ell$. Furthermore, it is interesting to note different functional behaviour of $\mathrm{d}S_\ell/\mathrm{d}E$ for different values of $\ell$. For $\ell = 0$ and 1, $n^3\sigma_{n\ell}$ fall as they approach the ionisation threshold. However, for $\ell \geq 2$, the situation is opposite, i.e. they increase towards the threshold. It is remarkable that the connection between excitation and ionisation holds regardless. A similar idea has also been applied to connect excitation and ionisation cross sections in electron-hydrogen atom scattering [5].

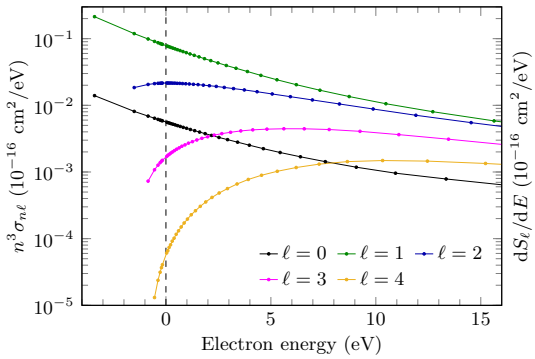


**Figure 1**. The $n\ell$-resolved cross sections for excitation in $\bar{p}+\mathrm{H}(1s)$ collisions, multiplied by $n^3$, and the $\ell$-partial SDCS for ionisation as functions of electron energy for $\ell = 0-4$.

## References

[1] Sommerfeld A. 1924 *Atombau und Spektrallinien.* Vol 1
[2] Oppenheimer J. R. 1928 *Phys. Rev.* **31** 349
[3] Rudd M. E. and Macek J. H. 1974 *Case Studies in Atomic Physics* pp. 47–136
[4] Antonio N. W., Bray I. and Kadyrov A. S. 2024 *Phys. Rev. A* **110** 032810
[5] Antonio N. W., Bray I. and Kadyrov A. S. 2024 *Phys. Rev. A* **110** 062810

*E-mail: a.kadyrov@curtin.edu.au

P-16

# Electron capture in collisions of highly charged argon ions with hydrogen atoms

**A M Kotian[1]*, N W Antonio[1], O Marchuk[2], and A S Kadyrov[1,3]**

[1]*Curtin University, Perth, WA 6845, Australia*
[2]*Forschungszentrum Jülich GmbH, Institut für Energie- und Klimaforschung-Plasmaphysik, 52425 Jülich, Germany*
[3]*Institute of Nuclear Physics, Ulugbek, 100214 Tashkent, Uzbekistan*

**Synopsis** The two-centre wave-packet convergent close-coupling method is used to model collisions of highly charged Ar ions with atomic hydrogen. We have calculated state-selective electron-capture cross sections over the 10 to 1000 keV/u energy range. The limited number of calculations available in the literature are in disagreement with one another. Our results may help resolve this discrepancy.

In fusion reactors such as ITER and DEMO, impurity seeding will be required for radiative cooling, plasma control and diagnostics. Charge-exchange recombination spectroscopy is a diagnostic technique capable of measuring the impurity ion density, ion temperature and plasma rotation within the fusion plasma [1]. This technique requires accurate state-resolved electron-capture cross sections for collisions between the seeded impurity ions and the neutral hydrogen beam injected during plasma discharge.

We use the two-centre wave-packet convergent close-coupling (WP-CCC) method alongside a model potential approach [2] to compute state-selective cross sections for electron capture in $Ar^{16+}$, $Ar^{17+}$, $Ar^{18+}$–H($1s$) collisions [3]. For these systems, capture into states with the final-state principal quantum number $n = 14 - 17$ are found to be the most important to consider. Experimental measurements for these collision systems are not readily available in the literature. The classical trajectory Monte Carlo (CTMC) method was employed by Errea *et al.* [4] and Schultz *et al.* [5] to model state-selective electron capture in these collision systems. However, their results differ by over an order of magnitude at low energies. The cross section for electron capture into the $n = 16$ shell in $Ar^{16+}$–H($1s$) collisions has been plotted in Fig. 1. At energies below 70 keV/u, the present results lie between the two sets of CTMC calculations. McDermott *et al.* [1] have used the CTMC data to calculate the density profiles of the seeded argon impurities in the ASDEX Upgrade. They have reported that the data by Errea *et al.* [4] underestimate the density profile whilst those by Schultz *et al.* [5] are larger by over an order of magnitude, suggesting that the true partial cross section lies between the two sets of CTMC calculations. Our results support this claim. Preliminary results for the other charge states of argon will also be presented.

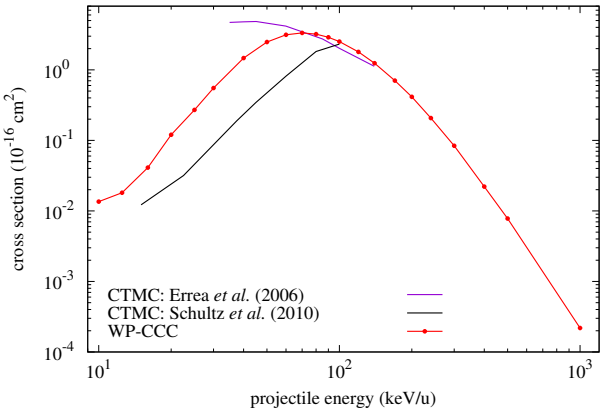


**Figure 1**. The cross section for electron capture into the $n = 16$ shell in $Ar^{16+}$–H($1s$) collisions. The present WP-CCC results are compared with the CTMC [4, 5] calculations.

## References

[1] McDermott R M *et al.* (The ASDEX Upgrade Team) 2021 *Nucl. Fusion* **61**, 016019
[2] Antonio N W *et al.* 2024 *Phys. Rev. A* **109**, 012817
[3] Kotian A M *et al.* 2024 *Plasma Phys. Control. Fusion* **66**, 095014
[4] Errea L F *et al.* 2006 *J. Phys. B: At. Mol. Opt. Phys.* **39**, L91
[5] Schultz D R *et al.* 2010 *J. Phys. B: At. Mol. Opt. Phys.* **43**, 144002

*E-mail: akshit.kotian@postgrad.curtin.edu.au

P-17

# Development of a Method for Measuring the Energy Loss of MeV Projectile Ions in a Thin Liquid Water Sheet

**H Imamura[1], K Asano[1], K Ishii[2] and Y Kumagai[2]***,

[1]Graduate School of Humanities and Sciences, Nara Women's University, Nara, 630-8506, Japan
[2]Department of Physics, Nara Women's University, Nara, 630-8506, Japan

**Synopsis** Understanding the interaction between fast ions and materials is crucial for advancing charged particle cancer therapy. Since liquid water is the primary constituent of the human body, accurate stopping cross sections of water are essential for precise treatment planning in charged particle therapy. We have developed a method to measure the energy loss of MeV projectile ions in liquid water. We irradiated a thin sheet of liquid water with 1 MeV protons and measured the energy spectrum of the transmitted protons.

Interactions between fast ions and matter, and the subsequent chemical reactions, have garnered wide interest in fields from astrophysics to life sciences. Charged particle therapy has made remarkable advances in cancer treatment over the past few decades [1]. In this therapy, carbon projectiles with energies ranging from several hundred MeV to several GeV pass through the human body and are directed toward cancer tumors located at depths of several centimeters to several tens of centimeters. These ions gradually lose energy as they propagate through the body and then deposit most of their remaining energy at a specific depth, once their energy falls to a few MeV. Thus, the depth resolution in charged particle cancer therapy relies on the Bragg peak effect, making accurate stopping cross sections over a wide energy range essential for treatment planning.

Since the human body is composed primarily of water, precise stopping cross sections of liquid water are critical for predicting energy deposition in tissue. Moreover, detailed understanding of ion-liquid interactions is key to maximizing therapeutic effects while minimizing damage to surrounding healthy cells.

In this study, we developed an experimental method to measure the energy loss of MeV projectile ions passing through liquid water, in order to obtain the corresponding stopping cross sections. As a demonstration, 1 MeV protons were transmitted through a thin liquid water sheet, and their energy spectra were measured.

The water sheet was introduced into the vacuum environment by colliding two cylindrical jets using a microfluidic nozzle [2]. The thickness of the sheet was expected to be a few micrometers. The tandem Van de Graaff electrostatic accelerator at Nara Women's University [3] provided the 1 MeV proton beam. A 90-degree analyzing magnet monochromatized the proton beam, achieving an energy resolution of $\Delta E/E = 10^{-3}$. The proton beam passed through two slits with diameters of 0.5 mm and irradiated the water sheet. The vacuum in the upstream beamline was maintained by a differential pumping system incorporating the downstream slit. The energy spectra of protons transmitted through the water sheet were measured using a silicon solid-state detector positioned downstream at a small forward scattering angle.

The measured energy spectra showed that 1 MeV protons lost approximately 60 keV after passing through the water sheet. The experimental energy loss has been reproduced by PHITS [4], a Monte Carlo simulation code, when the water sheet thickness is assumed to be $\sim$2 $\mu$m. The assumed thickness is consistent with that expected from the experimental conditions.

This work was supported by JSPS KAKENHI (No. 24K06977) and the JST-Mirai Program (No. JPMJMI17A1).

## References

[1] Schardt D. *et al.* 2010 *Rev. Mod. Phys.* **82** 383
[2] Koralek J. D. *et al.* 2018 *Nat. Comm.* **9** 1353
[3] Shiomi-Tsuda N. *et al.* 1999 *Nucl. Instrum. Methods.* B **129** 1
[4] Sato T., 2013 in *J. Nucl. Sci. Technol.* **50** 913

*E-mail: yoshiaki@cc.nara-wu.ac.jp

P-18

# Excitation of helium by proton and antiproton impact

**L Nagy***, **Zs Bálint and S Borbély**

Faculty of Physics, Babeş-Bolyai University, Cluj, 400084, Romania

**Synopsis** We calculated excitation cross sections and transition probabilities for the helium atom, analyzing the results for both proton and antiproton impact. In addition, the results are compared with available experimental data and other calculations.

The excitation of helium by proton impact have long been the subject of both experimental and theoretical studies [1]. In contrast, theoretical studies of excitation due to antiproton impact remain scarce. This is unlike the case of ionization, for which several groups have investigated and compared the cross sections for proton and antiproton projectiles, discussing the effect of the projectile's charge sign [2]. In the present work, we have calculated the excitation cross sections in case of both projectiles for different impact energies. These calculations were performed using an *ab initio* method based on the numerical solution of the time-dependent Schrödinger equation for the two-electron system (time-dependent close-coupling, TDCC), as well as with a first-order perturbative approximation that does not account for the projectile's charge sign. Figure 1 presents the excitation cross sections to three excited states across a range of impact energies. It can be observed that the excitation cross sections for the excitation to the 2p state are almost identical for protons and antiprotons. For this excitation, the higher-order effects are still important, but the effects for small and large impact parameters cancel each other out. The perturbational results overestimate the TDCC ones for all energies, especially on the lower side. In the case of the other two excitations studied, the results for protons are comparatively higher than those for antiproton projectiles. The difference increases for lower impact energies, because here higher-order effects, responsible for the dependence on the projectile charge sign, are more important. Additionally, we have compared our results with the recommended experimentally based values of [1], with other theoretical results for protons [3], and with the few theoretical results available for antiprotons [4,5]. Our results show a good agreement with these data in most cases [6].

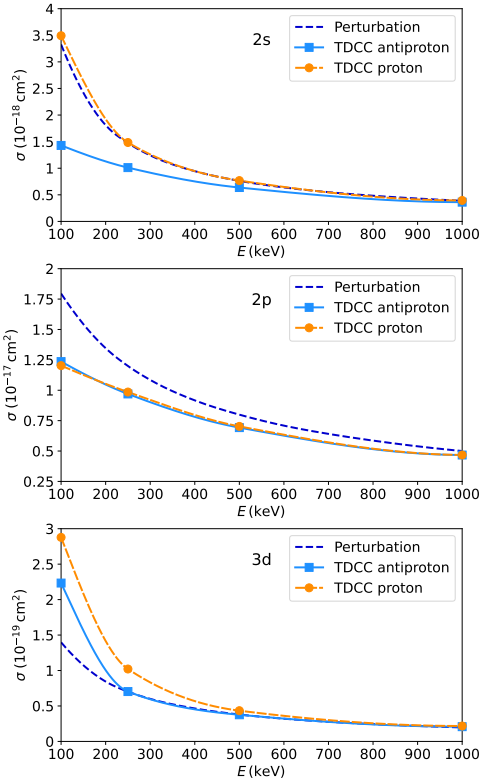


**Figure 1**. Excitation cross sections of helium as a function of the impact energy for proton and antiproton projectiles.

## References

[1] De Heer F *et al.* 1992 *Atomic and Plasma–Material Interaction Data for Fusion* **3** 47-50
[2] Andersen L H *et al.* 1987 *Phys. Rev. A* **36** 3612–3629
[3] Alladustov S U *et al.* 2019 *Phys. Rev. A* **99** 052706
[4] Igarashi A *et al.* 2000 *Phys. Rev. A* **62** 052722
[5] McGovern M *et al.* 2009 *Phys. Rev. A* **79** 042707
[6] Bálint Zs *et al.* 2024 *Atoms* **12** 57

*E-mail: ladislau.nagy@ubbcluj.ro

P-19

# Molecular formation through reactions of low-energy molecular ions with an ice surface under low temperature conditions

**Y. Nakai[1,2 *], W.M.C. Sameera[2,3], K. Furuya[4], H. Hidaka[2], A. Ishibashi[5], N. Watanabe[2]**

[1] RIKEN Nishina Center for Accelerator-based Science, Wako, 351-0198, Japan
[2] Institute of Low Temperature Science, Hokkaido University, Sapporo060-0819, Japan
[3] Department of Space, Earth and Environment, Chalmers University of Technology, SE-412 96, Gothenburg, Sweden
[4] Star and Planet Formation Laboratory, RIKEN, Wako, 351-0198, Japan
[5] Graduate School of Arts and Sciences, The University of Tokyo, Meguro, Japan

**Synopsis** We report the experiments for the molecular formation through impingement of several-electron-volt $CH_3^+$ ions upon an ice surface under low temperature conditions. In the experiment using amorphous solid water (ASW), methanol production was detected after $CH_3^+$ irradiation. We also found that hydroxy groups in the produced methanol originated from water molecules in ASW using isotopic labeling. We will also touch on our recent progress for the experiments using methanol solid.

Despite the very low temperature environment of molecular clouds, a wide variety of chemical species have been observed. Gas-phase ion-molecule reactions are essential for the formation of various molecules in molecular clouds. Experimental studies in the past few decades have also shown that hydrogenation reactions on icy interstellar grains are indispensable even for the formation of simple molecules, such as hydrogen and water [1]. Furthermore, we may suppose that the interactions of gas-phase ions with icy grain surfaces play some role. In fact, theoretical investigations suggested that the reactions of low-energy ions with an ice surface could be new molecular formation pathways [2,3]. However, few experimental trials for such reactions were conducted because the reaction products are trace and their detection is difficult. Thus, we have developed an experimental apparatus capable of detecting trace reaction products and conducted experiments on the reaction of low-energy $CH_3^+$ ions with a water ice surface [4], which was already theoretically investigated [2].

The ions were generated with a conventional electron-impact ionizer, and their masses were selected in the Wien filter. The mass-selected ions were decelerated down to the energy range of several electron volts and irradiated on the surface of ASW. The reaction products were detected using the ion-pickup method [5,6]. Some of the $Cs^+$ ions impinging on the ice surface at 40 eV picked up neutral species on the surface and were scattered as composite ions of $CsM^+$, where M is a picked-up neutral species. The mass of M was determined by analyzing the mass of $CsM^+$ ions. The reaction products were identified by comparing the mass spectra obtained by the ion-pickup method before and after $CH_3^+$ irradiation.

The production of $CH_3OH$ was observed after $CH_3^+$ irradiation on the ASW surface at 11 K. No other products were detected. This methanol formation should require a hydroxy group originating from a water molecule on the ASW surface. Thus, to confirm this, we conducted the experiment at 12 K using the ASW made from $D_2O$. Surely, we detected $CH_3OD$ molecules, not $CH_3OH$. It was also confirmed that hydroxy groups in the produced methanol originated from water in ASW. We also performed control experiments under experimental conditions identical to those of the $CH_3^+$ irradiation experiments, except that the $CH_3^+$ ions were blocked. In the control experiments, no methanol appeared.

To explore reactions on the icy grain surface without theoretical predictions, we are also conducting experiments for the reactions of low-energy $CH_3^+$ ions with a methanol solid surface at low temperatures because not a few amount of methanol exists on icy grain surface. We will also include our recent progress in the experiments using a methanol solid.

## References

[1] Watanabe N and Kouchi A 2008 *Prog. Surf. Sci.* **83** 439
[2] Woon D E 2011 *Astrophys. J.* **728** 44
[3] Woon D E 2021 *Acc. Chem. Res.* **54** 490
[4] Nakai Y *et al* 2023 *Astrophys. J.* **953** 162
[5] Kang H 2011 *Bull. Korean Chem. Soc.* **32** 389
[6] Ishibashi A *et al* 2021 *Astrophys. J. Lett.* 921 L13

* E-mail: nakaiy@riken.jp

P-20

# Stopping power in transition metals, the importance of $d$-electron contribution

**J P Peralta[1], A M P Mendez[1], D M Mitnik[1] and C C Montanari[1]***

[1]Instituto de Astronomía y Física del Espacio, CONICET and Universidad de Buenos Aires, 1428 Buenos Aires, Argentina

**Synopsis** The contribution of the $d$-electrons to the stopping power has been widely discussed in various experimental works as a break of the expected linear dependence of the stopping power on the ion velocity. In this work, we present a non-perturbative model to describe the response of the loosely bound $d$-electrons of the transition metals of groups 8-11. We focus on the cases of H in Fe, Ni, Cu, Pd, Ag, Pt, and Au, because of their technological applications and the large amount of available data. We describe the stopping power in an extended energy region, showing good agreement with experimental values and recent TDDFT results.

The transition metals exhibit complex electronic structures, with the open $d$-orbital partly promoted to the conduction band, and the remaining electrons loosely bound. The contribution of the $d$-electrons to the stopping power has been widely discussed in various experimental works [1, 2]. Theoretical models for the energy loss at low velocities in metals predict a proportional dependence of the stopping power on the ion velocity [3]. However, the experimental values show a broken straight line with a change in slope [4]. In this work, we present a non-perturbative model for the $d$-subshell contribution to electronic energy loss, based on the *inhomogeneous* velocity profile [5] given by

$$f_{nd}(p) = \frac{(2\pi)^3}{2} \, |\Phi_{nd}(\vec{p})|^2, \qquad (1)$$

with $\Phi_{nd}(\vec{p})$ being the Fourier transform of the wave functions $\phi_{nd}(\vec{r})$, normalized to the number of electrons in the $nd$-subshell.

We analyse the cases of $3d$ (Fe, Ni, and Cu), $4d$ (Pd and Ag) and $5d$ (Pt and Au) transition metals. For example, Figure 1 shows the stopping cross-section of protons in Ni as a function of the impact velocity. We display our results for the $d$-subshell, the conduction electrons (FEG), and the total value. These values are compared with the available experimental data in [6]. The description of the experimental data is very good, with the calculated $d$-electron contribution being crucial at very low velocities. We also compare our results with recent time-dependent density functional theory (TDDFT) values [7], showing excellent agreement.

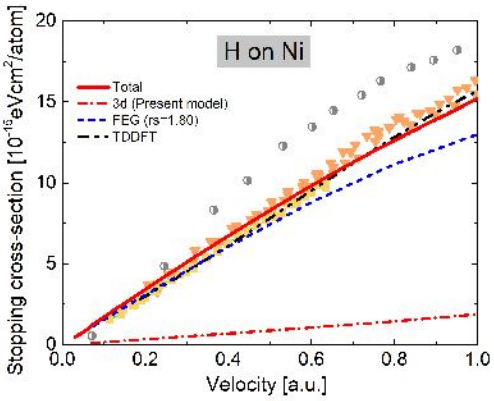


**Figure 1**. Low-energy stopping cross-section of Ni for H as a function of the impact velocity. Curves: total stopping (red-solid line), $d$-electron contribution (red dash-dotted line), FEG stopping (blue-dashed line), and TDDFT results [7] (dark-dash-double-dotted line). Symbols: experimental data, orange-triangles [1], yellow-squares [2], grey-circles, data in [6] previous to 1990.

## References

[1] Möller S P *et al.* 2002 *Phys. Rev. Lett.* **88**, 193201
[2] Bruckner B *et al.* 2018 *Nucl. Instr. Meth. Phys. Res. B* **423**, 82
[3] Fermi E and Teller E 1947 *Phys. Rev.* **72**, 399
[4] Cantero E D *et al.* 2009 *Phys. Rev. A* **80**, 032904
[5] Peralta J P *et al.* 2025 *Phys. Rev. A* **111**, 032808; *Atoms* **13** 22
[6] IAEA Stopping Power Database
[7] Quashie E E and Correa A A 2018 *Phys. Rev. B* **98**, 235122

*E-mail: mclaudia1@iafe.uba.ar

P-21

# Machine learning model for $K$-shell ionisation

**D M Mitnik[1], C C Montanari[1]*, S Segui[2], S Limandri[2], J A Guzmán[2], A Carreras[2], J C Trincavelli[2]**

[1]Instituto de Astronomía y Física del Espacio, CONICET and Universidad de Buenos Aires, 1428 Buenos Aires, Argentina

[2]Instituto de Física Enrique Gaviola, CONICET, Universidad Nacional de Córdoba, 5000 Córdoba, Argentina.

**Synopsis** A deep neural network was implemented to model the experimental $K$-shell ionisation cross sections based on two input features: the atomic number and the incoming electron energy. The machine learning algorithm was applied to elements with atomic numbers ranging from 1 to 92 and incident energies from the threshold to relativistic values.

When dealing with large volumes of data or seeking trends and patterns in complex datasets, machine learning (ML) approaches become a valuable tool [1,2]. In this presentation, we analyse the present state of the art of the $K$-shell ionisation of atoms by electron impact, based on the recent experimental database [3]. We implemented a fully connected feedforward neural network to model the $K$-shell ionisation cross-sections, $\sigma_K$, based on two input features: the target atomic number and the incoming electron energy. A large random portion of the data was used to train a neural network, while the remaining data was set aside, constituting the test set.

The trained neural network demonstrated excellent predictive performance. The coefficient of determination reached $R^2 = 0.998$ in the training set and $R^2 = 0.997$ in the test set, indicating a strong generalisation and minimal overfitting. We display in Figure 1 the residual histograms, where symmetric distributions centred around zero can be observed, which confirms the unbiased behaviour of the model. As can be seen, the distribution of residuals obtained with the test dataset is very similar to that achieved with the training dataset, which supports the model's reliability. The cross sections obtained with the present ML model compare very well with the experimental data in a large energy range, predicting values in energy regions where no measurements have been performed, and also covering a large number of elements for which no experimental values are available.

The developed ML code can be freely used in Google Colab platform using this link

*E-mail: mclaudia@iafe.uba.ar

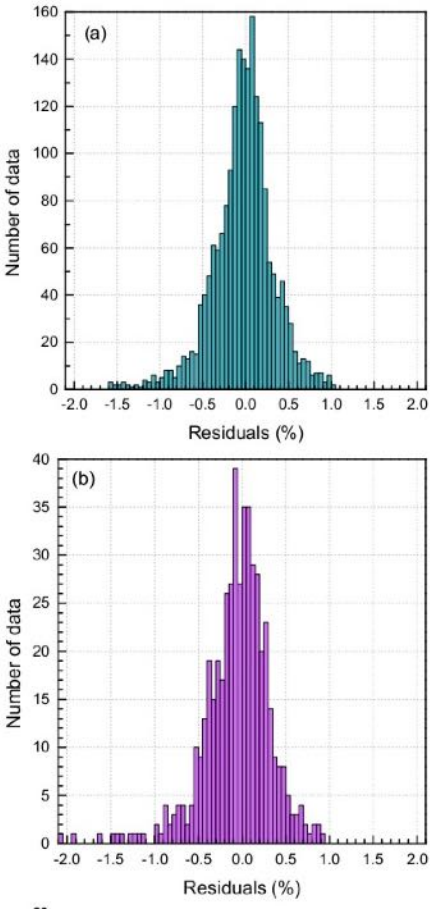


**Figure 1**. Histogram of residuals of $\log \sigma_K$ in the training dataset (a); and in the test dataset (b)

## References

[1] Jaderberg B *et al.* 2024 *Phys. Rev. A* **110** 052423
[2] Bivort Haiek F *et al.* 2022 *J. Appl. Phys.* **132** 245103
[3] Segui S *et al.* 2025 Experimental K-shell ionization cross sections by electron impact: a comprehensive database for $1 \leq Z \leq 92$

P-22

# An embedding-based neural network approach for stopping power prediction on multi-elemental targets

**F Bivort Haiek[1,2] D M Mitnik[1] A M P Mendez[1], J P Peralta[1], and C C Montanari[1]***

[1]Instituto de Astronomía y Física del Espacio, CONICET and Universidad de Buenos Aires, 1428 Buenos Aires, Argentina

[2] Ciencias de Datos, Facultad de Ciencias Exactas y Naturales, Universidad de Buenos Aires, 1428 Buenos Aires, Argentina

**Synopsis** We present a novel neural network architecture for predicting electronic stopping power across diverse target materials. Our approach integrates the strengths of two established frameworks: adopting the data preprocessing methodology and output layer structure from ESPNN, while leveraging the powerful material embeddings generated by SchNet's final layers to represent target compositions. Utilising the Materials Project database to obtain target structures, we explored various heuristics to assign the appropriate crystalline structure for each material. Our model was trained on publications up to 2013 for training and subsequent publications for validation. It demonstrates superior predictive performance compared to the industry-standard SRIM software.

Continuing our work on predicting Stopping Power with Neural Networks, ESPNN [1], which was developed for monoelemental targets, we now propose to tackle multi-elemental targets in different states. Compounds involve larger and more varied chemical compositions, which exist in different phases and structural conformations.

To address this problem, we propose reusing representations already learned by models with physical foundations, which have been trained on very large datasets, and utilising them as input for a new network that we will train on top of. Upon consulting the literature, we find that various neural network models employ molecular structures to predict material quantities. One of the major exponents is SchNet [2], which takes as input the coordinates of atoms $r_i$ and an embedding vector that represents their characteristics $x_i^0$. We can view the network layer as updating (refining and adding contributions from nearby atoms) these embeddings in such a way that the vectors of atom $i$ in layer $l$ will be $x_i^l$. We chose the version of SchNet trained to predict the formation energy for materials in the Materials Project [3], which is a database that stores information about approximately 200,487 distinct materials. In particular, it has the crystal geometry for each material. What makes this database particularly suitable for extrapolating well to stopping power predictions is that it covers materials for almost all elements in the first six rows of the periodic table.

*E-mail: mclaudia@iafe.uba.ar

This work aims to employ machine learning algorithms on the 2024 IAEA database [4] to predict accurate electronic stopping power cross sections for any ion in a solid compound target in a wide range of incident energies. Thus, our new model utilises all the filtering, datapoint selection methods, training parameters and model features we have used in [1], together with the last encoding for atom $i$ in a SchNet model [2], as well as an encoding of the state as extra features. Additionally, it calculates the contribution of each atom to the stopping power separately and then takes an average. Our approach achieves very good performance for all projectile types examined, with a mean absolute percentage error (MAPE) on measurements after 2018, much lower than the usually employed SRIM code [5]. A current limitation of our approach is that it relies on the molecular structures being stored in the Materials Project [3]. In the following works, we will extend the model to utilise geometries extracted from more general databases.

## References

[1] Bivort Haiek F *et al.* 2022 *J. Appl. Phys.* **132** 245103
[2] Schütt K T *et al.* 2019 *J. Chem. Theory Comput.* **15** 448
[3] Jain A *et al.* 2013 *APL Mater.* **1** 011002
[4] IAEA Stopping Power Database Electronic Stopping Power of Matter for Ions
[5] Ziegler J F 2013 Stopping Range of ions in Matter SRIM

P-23

# The effect of irradiated ion on the swelling phenomenon of 4H-SiC

**T. Okawa[1*], S. Momota[1†], M. Watanabe[††]**

[1]Kochi University of Technology, Tosayamada, Kami, Kochi, 782-8502, Japan

**Synopsis** The swelling phenomenon of 4H-SiC was investigated by irradiating C, O, and Ar ions, whose projected ranges are identical. The observed results reveal that the saturation value and the fluence dependence of swelling height change systematically according to the species of ions.

Recently, the application of silicon carbide (SiC) as power semiconductor materials has made progress because of its wide band gap and high thermal conductivity. On the other hand, it is difficult to process SiC due to its high hardness and chemical stability. Applying the swelling phenomenon of SiC induced by ion-beam irradiation [1,2], a new fabrication process of 3-dimensional nanostructures can be established. The fluence dependence of the swelling phenomenon on SiC has been frequently reported [3,4], however, there are few investigations to disclose the effect of ion species on the phenomenon.

In this work, 4H-SiC substrates were irradiated with $C^{2+}$, $O^{3+}$ and $Ar^{4+}$ beams through a stencil mask at room temperature, and the height of step structures induced by the irradiation was measured by an Alpha-step IQ. The energy of each beam was adjusted so that the projected range ($R_p$) would be a constant value 264nm, referring to SRIM 2013 code (Table 1).

**Table 1**. Energy of ions and $R_p$ calculated by SRIM 2013

| Ion | Energy [keV] | $R_p$ [nm] |
|---|---|---|
| $C^{2+}$ | 154 | |
| $O^{3+}$ | 186 | 264 |
| $Ar^{4+}$ | 400 | |

A monotonic increase at low fluence and saturation behavior are observed in swelling height for all ions, as shown in Fig. 1. It is obvious that saturation values of the swelling height increase with atomic number of ion ($Z$). Furthermore, the non-linear behavior at low fluence becomes obvious for C and O ions.

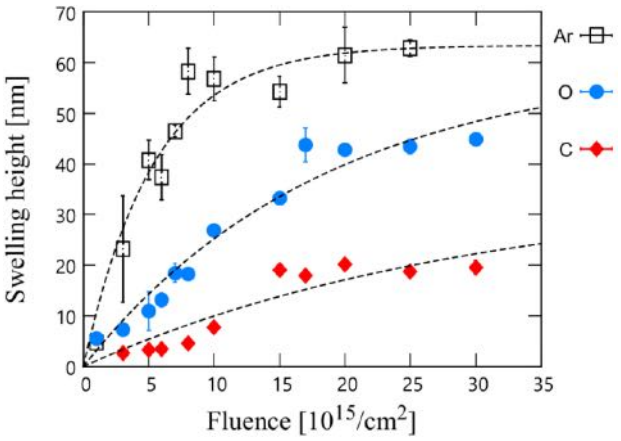


**Figure 1.** Swelling height of 4H-SiC vs fluence. Dashed lines are the fitting results by the DI model.

Referring to the study of Kerbiriou *et al* [4], "Direct Impact" (DI) model, which simply describes the fluence dependence of disorder induced by ion-beam irradiation, was used to analyze the present results. For Ar beam, the fitting results based on the DI model is in agreement with the observed results. In contrast, disagreement between the fitting results and the observed results expands with decreasing $Z$. This result implies that the irradiation effect of C or O ion includes additional factors to promote disorder in 4H-SiC.

## References

[1] W. Jiang *et al.*, 2004 *J. Appl. Phys.* **95** 4687-4690
[2] J.M. Williams *et al.*, 1983 *Nucl. Instr. Meth.* **209/210** 317-323
[3] S. Momota *et al.*, 2019 *Vacuum.* **170** 108963
[4] X. Kerbiriou *et al.*, 2009 *J. Appl. Phys.* **105** 073513

* E-mail: 285058y@gs.kochi-tech.ac.jp
† E-mail: momota.sadao@kochi-tech.ac.jp
†† Present address: Sumitomo Heavy Industries Ion Technology Co., Ltd, Osaki, Shinagawa-ku, Tokyo, 141-6025, Japan

P-24

# Positive and negative secondary ion emission from propanol droplets induced by fast heavy-ion collisions

**S. Otsuka[1], T. Takemura[1], H. Tsuchida[1,2], M. Saito[1,2], and T. Majima[1,2] ***

[1]Department of Nuclear Engineering, Kyoto University, 615-8540 Kyoto, Japan
[2]Quantum Science and Engineering Center, Kyoto University, 611-0011 Uji, Japan

**Synopsis** We performed a mass spectrometric study of positive and negative secondary ions emitted from the surfaces of 1-propanol and 2-propanol microdroplets upon irradiation by fast heavy ions. Our results quantitatively revealed pronounced differences in the secondary ion yields of certain fragment ions, depending on isotopic structure.

Our research aims to elucidate the molecular-level reaction processes induced by high-energy heavy ions in condensed phases. We recently developed an experimental technique using microdroplet targets for MeV-energy heavy ions in high-vacuum conditions [1-3]. In this study, we examined positive and negative secondary ions emitted from the surfaces of 1-propanol (1-PrOH) and 2-propanol (2-PrOH) microdroplets irradiated with MeV-energy heavy ions. These propanol isomers were chosen as a model system to explore how geometrical structure affects reaction pathways in alcohol molecules. By comparing our results with gas-phase data, we discuss mechanisms of fragment ion formation characteristic of condensed-phase environment, such as liquids and solids.

Experiments were performed using a 2 MV tandem Pelletron accelerator at the Quantum Science and Engineering Center, Kyoto University. Projectiles were 4-MeV $C^{3+}$ ions. Liquid droplets of 1-PrOH and 2-PrOH were generated by ultrasonic atomization and introduced into a collision chamber through a differential pumping system. Forward-scattered incident ions were detected by a semiconductor detector, which served as the start trigger for time-of-flight (TOF) mass spectrometric analysis of the emitted secondary ions.

For positive ions, as in methanol [2] and ethanol [1] droplets, protonated cluster ions, reaction product ions, and fragment ions were observed. Figure 1(a) shows an expanded view of the low-mass region of the TOF mass spectra. The vertical axis represents the secondary ion yield, normalized to the number of collisions between the projectile ions and the droplets. The most abundant fragment ion was observed at $m/z$ = 43. This observation differs significantly from previous gas-phase studies, in which 1-PrOH and 2-PrOH primarily yield $CH_3O^+$ ($m/z$ = 31) and $C_2H_5O^+$ ($m/z$ = 45), respectively [4]. Based on the study using ethanol droplets [1], it is known that fragment ions are primarily formed through protonated ions after a rapid proton transfer. Therefore, it is likely that the fragment ion at $m/z$ = 43 is also generated from the dissociation of protonated propanol ions.

For negative ions as well, deprotonated propanol cluster ions, reaction product ions, and fragment ions were observed. As shown in Fig. 1(b), $C_4^-$ and $C_4H^-$, which were also observed from ethanol droplets, were clearly identified. Additionally, although not shown in the figure, weak peaks corresponding to $C_6H^-$ and $C_8H^-$ were observed. The peaks at $m/z$ = 41 and 43 exhibited strong isotope dependence, suggesting that the characteristics of bond dissociation in the negative ion states are influenced by molecular structure.

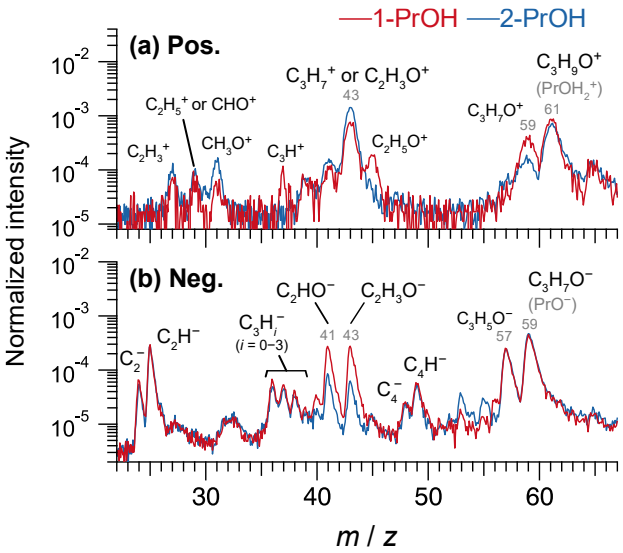


**Figure 1.** Expanded views of TOF mass spectra of (a) positive and (b) negative secondary ions emitted from 1-propanol and 2-propanol droplets.

## References

[1] T. Majima et al., J. Chem. Phys. 153 224201
[2] T. Majima et al., J. Phys. Chem. A 126, 8988
[3] K. Kitajima et al., J. Phys. B: At. Mol. Opt. Phys. 57, 132001
[4] NIST Mass Spectrometry Data Center.

* E-mail: majima@nucleng.kyoto-u.ac.jp

P-25

# Hydrogen mediated heavy atom roaming in negative ion

**DG Piekarski[1]*, S Pataraprasitpon[1], TFM Luxford[2], Roman Čurík[2] and J Kočišek[2]**

[1]Institute of Physical Chemistry, Polish Academy of Sciences, 01-224 Warsaw, Poland
[2]J. Heyrovský Institute of Physical Chemistry v.v.i., The Czech Academy of Sciences, Dolejškova 3, 18223 Prague, Czechia

**Synopsis** Our study of triazole derivatives' reactivity with low-energy electrons reveals how hydrogen position affects reaction dynamics. Energy-dependent ion yields shows significant differences for two molecules. Calculations reveal that bromine atom migration is energetically more favored than hydrogen atom migration when H atom is adjacent to Br. This is enabled by the favorable formation of a non-covalent complex of Br- around the triazole ring. The interplay between Br and H is driven by light atom moderator, while heavy singly negatively charged atom is traveling around 4H-1,2,4-triazole ring.

Triazole derivatives are widely used bioisosteres and chiral organocatalysts that mimic various functional groups while maintaining high resistance to external conditions. [1, 2] In particular cases such as removing azole-based antifungal reagents from wastewater, their extra stability is an unwanted property. Low-energy electrons can be used to change the stability of this special class of organic molecules. [3] We show that two very similar target molecules, 3-bromo-1H-1,2,4-triazole (1HBrT) and 3-bromo-4H-1,2,4-triazole (4HBrT), differ only by the position of one hydrogen atom but exhibit different reactivity after low-energy electron attachment. The origin of such discrepancy is explained as the ability of 4HBrT anion to facilitate straightforward negative bromine roaming. This reaction mechanism is reflected in different intensities and fragments in dissociative electron attachment experiments, mainly Br- vs. HBr releases. Thus, roaming is quantified by quantum chemical calculations. Potential energy surfaces, molecular dynamics, and analytic continuation calculation demonstrate that the position of hydrogen on the ring is crucial and determines the character of the lowest-lying resonant state. Consequently, it affects the exothermic motion of the Br- around the triazole ring. A picosecond long resonance lifetime allows such roaming dynamics, particularly a high propensity of neutral HBr release. [5] This work was supported by the National Science Centre, Poland, grant no. 2022/47/D/ST4/03286.

**Table 1**. Lowest resonance positions and widths for 1HBrT and 4HBrT calculated with analytical continuation barycentric approach [4].

| | Energy $E_r$ (meV) | Width $\Gamma$ (meV) |
|---|---|---|
| 1HBrT | 251 | 5 |
| 4HBrT | 201 | 0.1 |

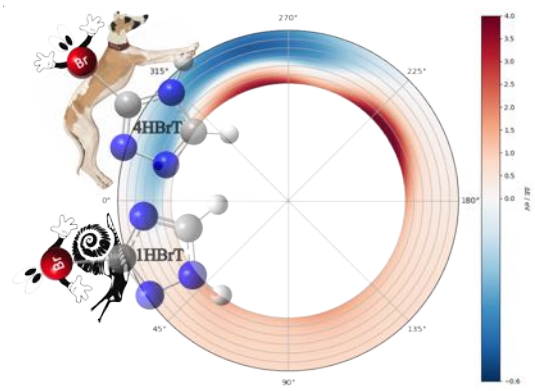


**Figure 1**. Bromine roaming around triazole ring

## References

[1] Bonandi E *et al.* 2017 *Drug Discov. Today* **22** 1572–1581
[2] Piekarski D G *et al.* 2020 *Chem. Eur. J.* **26** 17598–17603
[3] Sedmidubská B and Kočišek J 2024 *Phys. Chem. Chem. Phys.* **26** 9112–9136
[4] Čurík R and Horáček J 2025 *Comput. Phys. Commun.* **306** 109379
[5] Pataraprasitpon *et al.* 2025 *J. Am. Chem. Soc.* **147** 1337013376

*E-mail: dpiekarski@ichf.edu.pl

P-26

# Electronically resolved excitation in proton collisions with $H_2$

**C T Plowman[1]*, L H Scarlett[1], M C Zammit[2], I Bray[1] and D V Fursa[1]**

[1]Department of Physics, Curtin University, Perth, Western Australia 6102, Australia
[2]Theoretical Division, Los Alamos National Laboratory, Los Alamos, New Mexico 87545, USA

**Synopsis** We have extended the molecular convergent close-coupling (MCCC) method to proton collisions with $H_2$. Electronic excitation cross sections have been calculated for $H_2$ states up to $n = 3$ in the atomic limit. Since there are no experimental or theoretical cross sections available, current modelling relies on equivelocity scaled electron collision data. However, we find significant differences between our results and the scaled electron data, suggesting accurate *ab initio* calculations are required.

When galactic cosmic ray protons propagate through gas clouds in space they collide with atoms and molecules, transferring energy in the process. In order to calculate the photon flux produced as a result of these collisions knowledge of the rovibrationally resolved cross sections for excitation is required [1]. The most prevalent species in these environments is the hydrogen molecule. However, there is currently no data, experimental or theoretical, for electronically resolved excitation in p+$H_2$ collisions, let alone rovibrationally resolved, at keV energies where they are most significant. As a substitute, equivelocity scaling of the available data for electron collisions with $H_2$ [2] is currently used to estimate the p+$H_2$ cross sections [1].

We have extended the molecular convergent close-coupling (MCCC) method to tackle proton collisions with $H_2$ to solve this problem. The projectile motion is treated in the semi-classical approximation and the electronic dynamics are modelled quantum mechanically. Orientation-averaged results are obtained by analytically integrating over the angular coordinates of the internuclear vector [3]. Using the configuration-interaction expansion method developed for the MCCC approach to electron collisions [2], we are able to generate very accurate fixed-nuclei states for the hydrogen molecule. This enables us to determine electronically resolved cross sections for transitions into the excited states of $H_2$ up to $n = 3$ in the atomic limit. A sample of the results is shown in Figure 1 for the dipole-allowed transition $X\,^1\Sigma_g^+ \rightarrow B\,^1\Sigma_u^+$ (Lyman band). Comparison of the present calculations with the scaled electron cross sections reveals significant differences both around the centre of the peak (about 70 keV) and at lower energies where the scaled electron data falls to zero because the scaling also unphysically shifts the threshold. Our *ab initio* results for protons correctly incorporate the fact that at keV energies all bound excitation channels are open, resulting in a non-negligible cross section at these lower energies.

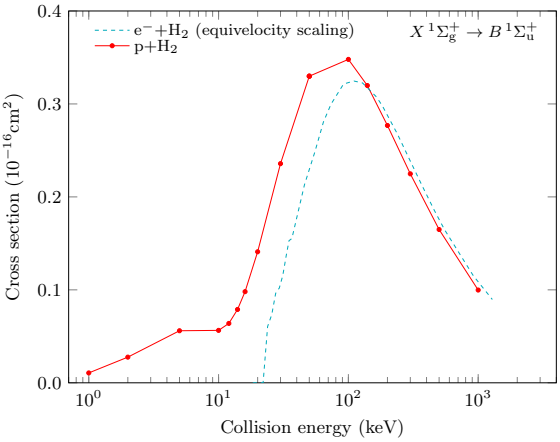


**Figure 1**. Excitation of the $B\,^1\Sigma_u^+$ state from the $X\,^1\Sigma_g^+$ ground state of $H_2$

The present results represent the first data for state-resolved electronic excitations in p+$H_2$ collisions and show that models relying on equivelocity electron cross sections will be underestimating the photon production rate from proton collisions.

## References

[1] Padovani M *et al.* 2024 *Astron. Astro.* **682** A131
[2] Scarlett L H *et al.* 2021 *Atom. Data Nucl. Data Tables* **137** 101361
[3] Abdurakhmanov I B *et al.* 2013 *Phys. Rev. Lett.* **111** 173201

*E-mail: corey.plowman@curtin.edu.au

P-27

# Evidence for the formation of excited fragments in the three body dissociation of methane

**C P Safvan[1]*, D Garg[1], A Cassimi[2], X Fléchard[3], J Rangama[2] and J Rajput[4]**

[1]Inter University Accelerator Centre, New Delhi 110067, India
[2]CIMAP, CEA-CNRS-ENSICAEN-UNICAEN, Normandie Université, F-14050 Caen Cedex 04, France
[3]Université de Caen Normandie, ENSICAEN, CNRS/IN2P3, LPC Caen UMR6534, F-14000 Caen, France
[4] Department of Physics and Astrophysics, University of Delhi, Delhi 110007, INDIA

**Synopsis** Evidence for the formation of hot fragments in the three body dissociation of methane dications is presented. Methane dications are formed in the interaction of neutral methane with energetic $Ar^{9+}$ and the momenta of the resulting recoil ionic fragments are measured using the technique of cold target recoil ion momentum spectroscopy. The dissociation channels ($H + H^+ + CH_2^+$) and ($H + H_2^+ + CH^+$) are studied. We show that the fragments are formed sequentially and the molecular intermediaries carry a few eVs of excess internal energy, part of which may be released when they emit an H atom.

Methane is one of the simplest hydrocarbon molecules found in the terrestrial as well as a wide range of astrophysical environments. The fragments formed from its dissociation like $CH_3^+$, $CH_2^+$, $CH^+$, $H_2^+$ are important contributors to interstellar and planetary chemistry as well as in combustion. Upon interaction with neutral species, these fragments may result in molecular growth to form higher hydrocarbons via ion-molecular reactions or through the hydrogen-abstraction-acetylene-addition (HACA) mechanism. It is well known that the rate coefficients for such association reactions are a strong function of the internal energy available in the molecular system [1].

$CH_4^{2+}$ formed upon a Frank-Condon transition from the ground electronic state of neutral methane has a tetrahedral geometry with $T_d$ symmetry. However, its minimum energy equilibrium structure is predicted to be planar (not square) with a $C_{2v}$ symmetry [2]. Thus the dication on its initial formation is expected to be vibrationally quite hot.

In this paper we follow the break up of the dication formed upon collision with an $Ar^{9+}$ ion. We show that the two dissociation channels leading to the fragments ($H + H^+ + CH_2^+$) and ($H + H_2^+ + CH^+$) proceed in a sequential manner with the charge separation preceding the neutral emission [3].

Utilising the native frames technique [4] for a three dimensional molecule, we investigate the kinetic energy release in the complete process, and the unimolecular breakup of the intermediate ion.

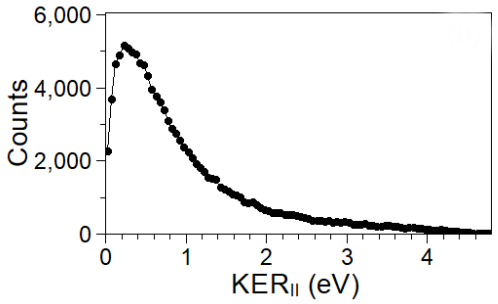


**Figure 1**. Distribution for $KER_{II}$ for the sequential three-body breakup of $CH_4^{2+}$ into ($H + H^+ + CH_2^+$). For a two-step breakup, $KER_{II}$ represents the kinetic energy release for $CH_3^+ \rightarrow CH_2^+ + H$.

Figure 1 shows the kinetic energy release for the breakup of the intermediate ion $CH_3^+$.

We show that the intermediate ions $CH_3^+$and $CH_2^+$ carry a large amount of internal energies (order of a few eV). Only a part of this may get dissipated in the second step of neutral emission and the final fragments are formed with significant internal energies.

## References

[1] Cernuto A *et al.* 2017 *J. Chem. Phys.* **147** 154302
[2] Wong M W and Radom L 1989 *J. Am. Chem. Soc.* **111** 1155
[3] Rajput J *et al.* 2023 *J. Chem. Phys.* **159** 184303
[4] Rajput J *et al.* 2018 *Phys. Rev. Letts* **120** 103001

*E-mail: cp.safvan@gmail.com

P-28

# Charge State Distributions of Ions Transmitted Through a Single-Layer Graphene Sheet under Fast $Li^+$ and $Li_2^+$ Ion Irradiation

**K. Saito[1] *, Y. Kumagai[2] and K. Ishii[2†]**

[1]Graduate School of Humanities and Sciences, Nara Women's University, Nara, 630-8506, Japan
[2] Department of Physics, Nara Women's University, Nara, 630-8506, Japan

**Synopsis** Graphene is well known as a functional material with high electron mobility, and refers to a single layer of carbon atoms with a honeycomb arrangement. To study the high electron mobility of graphene, we measured the charge-state distributions of fast lithium monomer and dimer ions transmitted through a graphene sheet. The charge-state distribution for the fast lithium monomer ions was reproduced by a simulation based on the Monte Carlo method, in order to discuss the high electron mobility of graphene. Moreover, we experimentally estimated the survival probability of lithium dimer ions after passing through the single graphene sheet to be a few percent.

Graphene refers to a single layer of carbon atoms with a honeycomb arrangement. The durability, electron mobility and thermal conductivity of graphene are anticipated to play a key role in the development of next-generation devices across various technological fields.

Monolayer graphene is an ideal object for studying fundamental ion–solid interactions through single scattering processes of fast ions due to its extreme thinness. In a previous study, the measured charge-state distributions after transmission through a single graphene layer with 60 and 135 keV $Xe^{30+}$ ions revealed the high electron mobility of graphene during collisions with highly charged ions [1]. Recently, by irradiating a graphene sheet with 0.5 MeV $C^+$ ions, we observed a rainbow scattering pattern, which is expected to be formed by the transmission of monochromatic fast ions through a two-dimensional regular potential [2]. The angular spread of the observed scattering was narrower than predicted by classical trajectory simulations, which indicates that the high electron mobility of graphene caused rapid neutralization of the fast ions.

Charge transfer between the carbon atoms of graphene and the incident ions is expected to be highly enhanced by the high electron mobility, which may strongly contribute to the charge distributions of the transmitted ions. Moreover, we expect that survival probability of lithium dimer ions ($Li_2^+$) transmitted through a graphene sheet is increased by the rapid neutralization. Because the internuclear distance of $Li_2^+$ is comparable to the diagonal distance between the carbon atoms in graphene, when their molecular axis is perpendicular to the graphene plane, they may be able to pass though without dissociation due to the charge exchange and the collisional ionization.

In order to elucidate the charge transfer between monolayer graphene and fast ions, we measured the charge-state distributions after the transmission of fast $Li^+$ and $Li_2^+$. We estimated the effective atomic charge of graphene carbon atoms during collisions with fast ions, as well as the survival probability of $Li_2^+$.

A pelletron accelerator at our labratory [3] provided $Li^+$ and $Li_2^+$ with kinetic energies of 0.5 and 1.0 MeV, respectively. Two slits with a width of 0.3 mm collimated the ion beam to the graphene sheet. An electrostatic deflector separated transmitted ions by charge state, and a movable photodiode detected them.

The yield ratios of $Li^0$, $Li^+$, and $Li^{2+}$ were 0.08, 0.52, and 0.30, respectively, after the transmission of fast $Li^+$ through the graphene sheet. We carried out Monte Carlo simulations based on the binary encounter model, to reproduce the experimental results. The simulation results indicated that the effective atomic charge of carbon atoms in graphene during collisions with fast ions is approximately 2. This low effective charge is considered to result from the high electron mobility.

We observed $Li_2^+$ after passing through the graphene sheet as well as its fragment ions. The estimated survival probability of $Li_2^+$ was a few percent.

This work was supported by the JST-Mirai Program (No. JPMJMI17A1).

## References

[1] E. Gruber *et al* 2016 *Nat. Commun.* **7** 13948
[2] N. Watanabe *et al* 2024 *NIMB.* **553** 165380
[3] N. Shiomi-Tsuda *et al* 1999 *NIMB.* **159** 123

* E-Mail: xak_saito@cc.nara-wu.ac.jp
† E-Mail: ishii@cc.nara-wu.ac.jp

P-29

# Experimental K-shell ionization cross sections by electron impact: a comprehensive database for $1 \leq Z \leq 92$

**S Segui[1] * S P Limandri[1], A C Carreras[1], J C Trincavelli[1], J A Guzmán[1], C C Montanari[2], D M Mitnik[2]**

[1]Instituto de Física Enrique Gaviola, CONICET, Universidad Nacional de Córdoba, 5000 Córdoba, Argentina
[2]Instituto de Astronomía y Física del Espacio, CONICET, Universidad de Buenos Aires, 1428 Buenos Aires, Argentina

**Synopsis** A new compilation of experimental ionization cross sections for K-shell induced by electron impact has been assembled, including results up to Dec. 2024. The data cover elements throughout the periodic table from H to U, and incident electron energies from eV to MeV. The statistical analysis allows to outline trends, evaluate number and dispersion of data, and to detect unexplored elements and energy ranges.

Despite the great effort devoted to determining ionization cross sections $\sigma$ of atomic inner shells for almost a century, its dependence on the atomic number and the incident electron energy cannot be fully described yet. Significant discrepancies persist among experimental datasets reported by different authors, as well as between experimental results and theoretical predictions [1]. A comprehensive and up-to-date database of experimental cross-sections is essential for evaluating theoretical models. In 1990, Long *et al.* [2] presented a compilation of $\sigma$ values for K-shell up to Dec. 1989, which was updated in 2000 by Liu *et al.* [3]. These reviews tabulate the numerical data reported, and also referenced additional values available only in graphical form. In 2014, an extensive work by Llovet *et al.* [1] expanded the K-shell ionization database with measurements reported up to Dec. 2013, and included data for L- and M-shells. However, while their work present comprehensive graphical data, no numerical tables were provided.

In the present work, an exhaustive search was conducted to gather experimental values of K-shell ionization cross sections by electron impact. As a result, a comprehensive database was assembled comprising data extracted from publications spanning the period 1930–2024. The collected information was organized into several tables –one for each element– and is available for public access upon request. A statistical analysis of the data was performed, taking into account their dispersion, uncertainties, methods and targets used, year of publication, etc. Taking the review by Llovet *et al.* [1] as the basis for the present work, the collected data can be divided into three groups:
(1) measurements surveyed by Llovet *et al.*,
(2) pre-2014 data not included in [1], and
(3) determinations reported from 2014 onwards.
Numerical values were retrieved directly from the original publications when available, or digitized from plots presented in [1] when necessary.

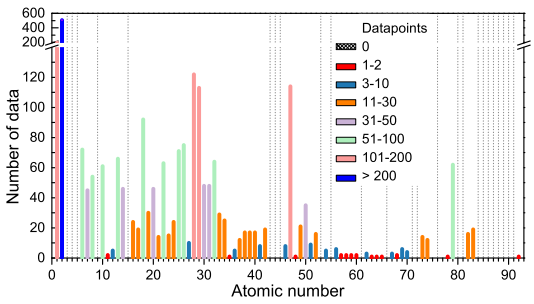


**Figure 1**. Number of K-shell ionization cross section measurements across the periodic table.

The database includes 2503 points for 65 elements from H to U across the energy range from 1.5 eV to 2 GeV, enlarging the previous compilation by 29%. Notably, ∼52% of the data correspond to just 8 elements, while 40 elements have fewer than three data points. Although research in this field has declined in recent years, there remain significant gaps (both in elemental coverage and energy range) that deserve further experimental investigations.

## References

[1] Llovet X *et al.* 2014 *J. Phys. Chem. Ref. Data* **43** 013102
[2] Long X *et al.* 1990 *At. D. Nucl. D. Tab.* **45** 353
[3] Liu M *et al.* 2000 *At. D. Nucl. D. Tab.* **76** 213

*E-mail: silvina.segui@mi.unc.edu.ar

P-30

# Coupled-channel calculations of FDCS for ionisation in 75 keV p + He collisions: Emission of low-energy electrons

**K. H. Spicer**[1]*, **N. W. Antonio**[1], **M. S. Schöffler**[2], **A. S. Kadyrov**[1,3]

[1]Curtin University, GPO Box U1987, Perth, Western Australia 6845, Australia
[2]Universität Frankfurt, 60438 Frankfurt, Germany
[3]Institute of Nuclear Physics, Ulugbek, Tashkent 100214, Uzbekistan

**Synopsis** The fully differential cross section for low-energy electrons emitted in collisions between 75 keV protons and helium is calculated using the wave-packet convergent close-coupling approach. Results are compared to recent measurements from the experimental group at Rolla, Missouri. Various discrepancies between the theoretical and experimental data in both shape and magnitude are found.

Despite decades of work amongst theorists and experimentalists, ionisation in even the simplest four-body collision systems is not fully understood. There has been progress toward this goal in measuring and calculating integrated, and singly and doubly differential cross sections, however, the most detailed quantity, the fully differential cross section (FDCS), remains a challenge. The recent measurements of Majumdar *et al.* [1] of the FDCS for electrons ejected with an energy of 1 eV for collisions of 75 keV protons with helium provide an opportunity for in-depth theoretical investigation. This is because the very low energy of the electrons suggests that the overwhelmingly dominant interaction will be between the ionised electron and residual helium ion. Therefore, simple single-centre methods should be valid, at least in this electron-energy region.

The wave-packet convergent close-coupling (WP-CCC) approach, unlike traditional close-coupling methods, has been developed to extract the transition amplitudes required to model differential ionisation. Thus far, it has been successfully applied to the calculation of integrated and various lowly differential cross sections for 75 keV p + He collisions. Here, it is employed to model the FDCS for 1 eV electrons as a function of the ejection angle at projectile scattering angles of 0.1, 0.3 and 0.5 mrad [2]. The results are presented in Fig. 1. Discrepancies between the WP-CCC and experimental data in terms of shape and magnitude are seen at all scattering angles. The high degree of alignment between the single-centre and two-centre implementations of the WP-CCC approach serves to reinforce the calculated FDCS. Further studies are needed to determine the source of the disparities.

*E-mail: kate.bain@postgrad.curtin.edu.au

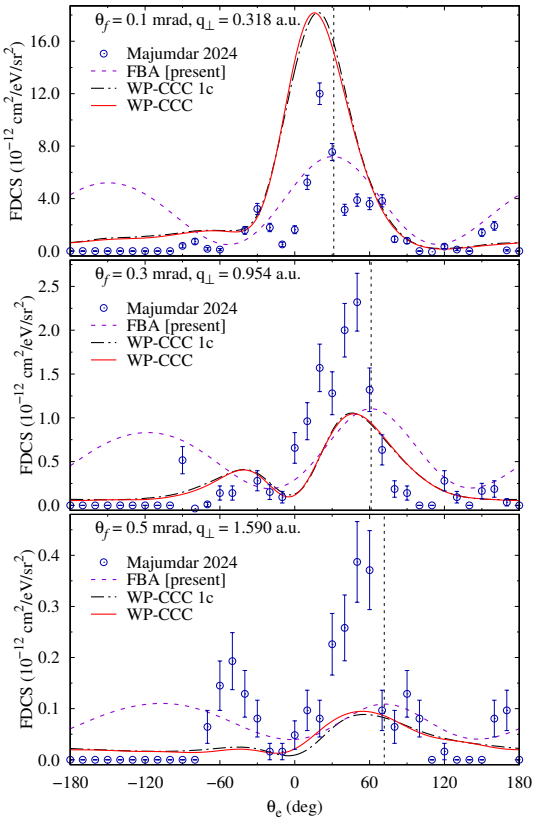


**Figure 1**. FDCS for 1 eV electrons ejected into the scattering plane in 75 keV p + He collisions as a function of electron ejection angle. The vertical dashed line indicates the direction of momentum transfer.

## References

[1] Majumdar S *et al.* 2024 *Phys. Rev. A* **110** 032814 **24** 3763
[2] Spicer K H *et al.* 2025 *Phys. Rev. A* submitted

P-31

# State selective charge-exchange cross sections in collisions between $C^{q+}$ ions with sodium atoms

**K. Tőkési[1,2*], B. G. Csillag[2], G. Anda[2], D. Dunai[2], D. Nagy[2], D. I. Réfy[2], M. Vécsei[3], S. Zoletnik[2]**

[1]HUN-REN Institute for Nuclear Research, Debrecen, Hungary
[2] HUN-REN Centre for Energy Research, Budapest, Hungary
[3]Max Planck Institute für Plasmaphysik, Greifswald, Germany

**Synopsis** The three-body classical trajectory Monte Carlo (CTMC) method was used to determine the principal quantum number ($n$) and the orbital angular momentum quantum number ($l$) dependent charge-exchange (CX) cross sections for sodium atom and carbon ion collisions. We found that higher the charge state higher value of $n$ shows the maximum cross sections.

The neutral alkali beams, such as lithium and sodium, were shown to be invaluable for measuring turbulence and electron density profiles in the boundary plasma [1]. These beams have also been proven to be useful for measuring local impurity properties using charge-exchange recombination spectroscopy [2]. The cross section calculations are vital to determine which spectral line can be significantly modulated by the charge-exchange (CX) processes between beam atoms and plasma ions.

In this work, the 3-body classical trajectory Monte Carlo (CTMC) method was used to determine the principal quantum number ($n$) and the orbital angular momentum quantum number ($l$) dependent CX cross sections for sodium atom and carbon ion collisions. The projectile carbon ion charge state was taken into account from the single charge till the fully stripped ion state. We performed the calculations for 35 keV and 50 keV impact energies. The CTMC method is a non-perturbative method, based on the calculation of a large number of individual particle trajectories when the initial atomic states are chosen randomly [3-4]. In the present work, the CTMC simulations were made in the three-body approximation, where the many-electron target atom was replaced by a one-electron atom and the projectile ion was taken into account as one particle. The three particles are characterized by their masses and charges and Coulomb force is acting between the colliding particles. The effective charge of the target core was calculated according to the Slater's rules [5]. The initial conditions of the individual collisions are chosen at sufficiently large inter-nuclear separations from the collision center, where the interactions among the particles are negligible. The classical equations of motion were integrated with respect to the time as independent variable by the standard Runge-Kutta method.

We found that higher the charge state higher value of $n$ shows the maximum cross sections. In the similar fashion, for high $n$ capture states the maximum $l$ capture cross sections also shift toward to higher values of $l$. Moreover, we found that the CTMC modelling and the experiments on the alkali beam of stellarator Wendelstein 7-X agree that for $q$=6 carbon ions the electron capture to the $n$=8 state occurs with the largest probability, while in case of the $q$=5 carbon ions the same holds for the $n$=7 states. The CTMC calculations indicate that in these cases the cross sections have a positive correlation with $l$.

This work has been carried out within the framework of the EUROfusion Consortium, funded by the European Union via the Euratom Research and Training Programme (GrantAgree ment No 101052200 — EUROfusion). Views and opinions expressed are however those of the author(s) only and do not necessarily reflect those of the European Union or the European Commission. Neither the European Union nor the European Commission can be held responsible for them.

**References**

[1] Zoletnik S *et al. Rev. Sci. Instrum.* 2018 **89** 063503
[2] Schorn R P *et al.* 1992 *Nuclear Fusion* **32** 351
[3] Tőkési K and Hock G 1994 *Nucl. Instrum. Meth.* B 86 201
[4] Tőkési K and Kövér Á J. Phys. B 2000 33 3067
[5] Slater J C 1930 Phys. Rev. **36** 57

* E-mail: tokesi@atomki.hu

P-32

# Energy loss function of samarium determined from the reflection electron energy loss spectroscopy spectra

**T.F. Yang[1], R.G. Zeng[2], L.H. Yang[1], A. Sulyok[3], M. Menyhárd[3], K. Tőkési[4#] and Z.J. Ding[1,5*]**

[1] *Department of Physics, University of Science and Technology of China, Hefei, Anhui 230026, People's Republic of China*
[2] *National Key Laboratory on Surface Physics and Chemistry, Institute of Materials, China Academy of Engineering Physics, P.O. Box 9071, Jiangyou, Sichuan 621907, People's Republic of China*
[3] *HUN-REN Research Institute for Technical Physics and Materials Science, Centre for Energy Research, ELKH, P.O. Box 49, H-1525 Budapest, Hungary*
[4] *HUN-REN Institute for Nuclear Research (ATOMKI), P.O. Box 51, Debrecen, Hungary*
[5] *Hefei National Research Center for Physical Sciences at the Microscale, University of Science and Technology of China, Hefei, Anhui 230026, People's Republic of China*

**Synopsis** We present a combined experimental and theoretical study to obtain a highly accurate energy loss function (ELF), or excitation spectrum, and consequently determine the dielectric function, refractive index, and extinction coefficient of samarium in the energy loss range of 3 eV to 200 eV. The accuracy of our results is validated using the *f*- and *ps*-sum rules. Our findings reveal a bulk plasmon mode centered at 14.2 eV with a peak width of approximately 6 eV, while the corresponding broadened surface plasmon mode appears in the energy range of 5–11 eV.

Lanthanides have nowadays become of vital importance in advanced materials and technology. Applications in laser science, solar cells, fluorescent lamps and a new organic light-emitting diodes components, as well as luminescent probes are strongly related with their optical and/or electronic properties. Samarium and its compounds are among the most frequently used lanthanides in the investigations during the last years. But the precise excitation property, especially the plasmon structure of samarium is still not known. It is not surprising because all lanthanides are highly reactive elements and interact strongly with oxygen and hydrogen. So, experimentally it is really a challenging to obtain accurate results.

Da et al. [1] developed a reverse Monte Carlo (RMC) method for the derivation of the energy loss function (ELF) and thereby the dielectric function and optical constants of solids in a much wider photon energy range than that of the usual optical measurements.

Our RMC technique was used to obtain the electron energy loss features buried in the REELS spectra of samarium [2]. The accuracy of the ELF was checked by applying sum rules. We found that the *ps*- and *f*-sum rules fulfils very accurately and reach the nominal values with 0.2% and 2.5% accuracy, respectively. We were able to separate the contribution from the bulk and the surface excitations. We show the detailed excitation characteristic in the optical data in the energy range between 3 and 60 eV.

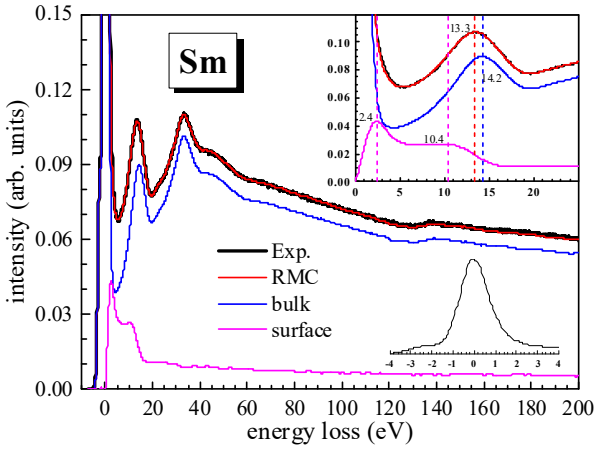


Fig. 1. Comparison of simulated spectrum and experimental spectrum.

This work was supported by Fund for Bilateral Relationships Between China and Hungary in Science and Technology (S&T) (2021-1.2.4-TÉT-2021-00055).

**References**

[1] Da B *et.al.* Journal of Applied Physics 2013 **113** 214303
[2] Yang TF *et.al.* Scientific Reports 2023 13:3909

* E-mail: zjding@ustc.edu.cn
‡ E-mail: tokesi@atomki.hu

P-33

# Electron capture cross sections in $Ne^{8+}$ ions collision with $H_2$ and He

**K. Tőkési[1,2*] and Y. Wu[3,4,5†]**

[1] *HUN-REN Institute for Nuclear Research (ATOMKI), 4026 Debrecen, Hungary*
[2] *HUN-REN Centre for Energy Research, 1121 Budapest, Hungary*
[3] *Institute of Applied Physics and Computational Mathematics, Beijing 100088, China*
[4] *School of Physics and Information Technology, Shaanxi Normal University, Xi'an, Shaanxi 710119, China*
[5] *HEDPS, Center for Applied Physics and Technology, Peking University, Beijing 100084, China*

**Synopsis** We present single electron capture cross sections for $Ne^{8+}$ ions interacting with neutral $H_2$ and He targets. The calculations were performed classically using the three-body CTMC approximation. We provide a detailed comparison and analyze the similarities and differences between our experimental and theoretical data.

Electron capture (EC) of highly charged ions (HCIs) with neutral atoms and molecular species is a fundamental process occurring in various plasma environments. It affects the ionization balance and leads to X-ray emissions in astrophysical regions and fusion devices. For example, Neon ions are among the main impurities appearing at various relative energies in different ionization stages within plasmas. Moreover, EC between the $Ne^{8+}$ ion and neutral gases is the dominant collision process in the solar wind (SW). Consequently, there is a strong demand for accurate data on the cross sections of EC for these applications.

In this work, we present absolute total and n-resolved state-selective cross sections for single electron capture (SEC) between $Ne^{8+}$ ions and neutral H2, as well as He targets. The experimental cross sections are compared with our current classical trajectory Monte Carlo (CTMC) simulations.

The experiment was conducted on the 150 kV highly charged ion collision platform at Fudan University to measure the total and state-selective EC cross sections. The HCI beam produced by an ECR ion source collides with neutral gases in a gas cell to measure the total EC cross sections. The cross sections were measured in the energy range of 2.8 to 40 keV/u.

The CTMC simulations are based on calculations involving a large number of individual particle trajectories, with the initial atomic states chosen randomly. The CTMC calculations were performed using a three-body approximation with two versions of the model. In both cases, the many-electron target atom was simplified to a one-electron atom, treating the projectile ion as a single particle. The difference between the two models lies in their treatment of the other electrons in the target. In the first case, the Coulomb force acts between the colliding particles, and we calculate the effective charge of the valence electron using Slater's rules. In the second approach, a central model potential is employed to describe the interaction between the active target electron and the target core. We present a detailed comparison and analyze the similarities and differences between our experimental and theoretical data.

This work has been carried out within the framework of the EUROfusion Consortium, funded by the European Union via the Euratom Research and Training Programme (GrantAgree ment No 101052200 — EUROfusion). Views and opinions expressed are however those of the author(s) only and do not necessarily reflect those of the European Union or the European Commission. Neither the European Union nor the European Commission can be held responsible for them.

## References

[1] Han J et al., APJS. 2021 **253** 6
[2] Meng T et al., New J. Phys. 2023 **25** 093026
[3] Tőkési K and Hock G Nucl. Instrum. Meth. B 1994 **86** 201
[4] Slater, J C Phys. Rev. 1930 **36** 57
[5] Garvey R H et al., Phys. Rev. 1975 A**12** 1144

* E-mail: tokesi@atomki.hu
† E-mail: wu_yong@iapcm.ac.cn

P-34

# Ionization of Noble Gases by Collisions with Fast Molecular Ions Depending on the Molecular Axis Orientation

**M Umemura[1*], Y Kumagai[2], K Ishii[2†]**

[1]Graduate School of Humanities and Sciences, Nara Women's University, Nara, 630-8506, Japan
[2]Department of Physics, Nara Women's University, Nara, 630-8506, Japan

**Synopsis** Collisional ionization with fast molecular ions is of fundamental interest, as the orientation of molecular-ion axis is expected to strongly affect the ionization probability. To investigate this effect, we measured ion yields for each charge state after collisions with fast molecular ions as a function of the angle between the molecular-ion axis and the incident beam axis. The experiments were conducted by irradiating noble gases, He and Ar, with lithium dimer ions ($Li_2^+$) with a kinetic energy of 1 MeV. The orientation of the $Li_2^+$ axis strongly influenced the ratios of $Ar^{n+}$ ($n$ = 1-5) ion yields, but had no effect on those of He ions. We simulated the ion yields as a function of molecular-axis orientation based on the binary encounter model, which qualitatively reproduced the experimental results.

Collisions of fast ions primary cause ionization of atoms and molecules. For the past few decades, the collisional processes of atoms and molecules with atomic ions have been studied, and the elementary processes such as collisional ionization and charge transfer have come to be well understood. However, when it comes to fast molecular ions, most collisional processes, even ionization, remain unclear. In particular, the orientation of molecular ions relative to the incident axis is expected to strongly affect the probabilities of collisional ionization and charge transfer. In other words, understanding the collisional processes with fast molecular ions requires incorporating the effects of their orientation.

A noble gas is one of the simplest systems for studying collisional processes with fast ions. Therefore, we have studied the dependence of collisional ionization for noble gases on the orientation of fast molecular ions relative to the incident axis. We measured the charge-state distributions of He and Ar ions produced by irradiation with lithium dimer ions ($Li_2^+$) as a function of the angle between the $Li_2^+$ axis and the incident beam axis, to reveal the effect of molecular-axis orientation on ionization probabilities.

A Pelletron accelerator at Nara Women's University [1] provided $Li_2^+$ with a kinetic energy of 1 MeV. To distinguish the orientation of $Li_2^+$ during collisions with noble gases, we recoreded the momentum distribution of fragment ions ($Li^+$) produced by the dissociation of the incident molecular ions, simultaneously with time-of-flight spectroscopy of the ionized noble gases.

We observed singly and doubly charged He ions produced by the collisions of $Li_2^+$. The singly charged ions are the primary products, as the $He^+$ yield was approximately 20 times higher than the $He^{2+}$ yield. On the other hand, highly charged states of Ar ions, up to the quintuply charged state, were generated by collisional ionization. Moreover, the ratios of $Ar^{n+}$ ($n$ = 1–5) ion yields to the total ion yield showed a dependence on the orientation of $Li_2^+$, while the yield ratio between $He^+$ and $He^{2+}$ ions remained approximately constant regardless of the orientation. To be more specific, the ratios for $n \geq 3$ increased when the molecular axis was parallel to the beam axis, while those for $n \leq 2$ decreased.

We attempted to reproduce the observed orientation dependence by developing a simulation method based on the binary encounter model. The electron densit s y distributions of noble gases were calculated using the ZBL potential. The simulated ionization probabilities of He and Ar for each charge state as a function of the angle of the $Li_2^+$ axis qualitatively reproduced the experimental results. Yet, the simulated charge distributions did not agree with the experimental results. One possible reason for the discrepancies is that the simulations did not include inner-shell ionization followed by the creation of multiply charged states via Auger–Meitner decay.

This work was supported by the JST-Mirai Program (No. JPMJMI17A1).

## References

[1] Shiomi-Tsuda N. *et al*. 1999 *Nucl. Instrum. Methods*. **B** 129 1

*E-mail: xam_umemura@cc.nara -wu.ac.jp
†E-mail: ishii@cc.nara-wu.ac.jp

P-35

# Collision-induced atomic alignment and magnetic-substate ionization of medium- and high-$Z_t$ elements

**X Wang[1]*, Y Liu[1], J Ren[1], X Ren[1], Y Zhao[1], Z Xu[1], R Cheng[2] and G Xiao[2]**

[1]Xi'an Jiaotong University, Xi'an, 710049, China
[2]Institute of Modern Physics, Chinese Academy of Sciences, Lanzhou, 730000, China

**Synopsis** Perturbation on atomic alignment by multiple ionization for heavy ion impact is demonstrated. Magnetic-substate ionization are well understood with probability density distribution of the orbital electrons.

Many-body systems possessing excess internal energy undergo relaxation toward lower-energy states through the reorganization of atomic structure. Inner-shell atomic spectroscopy serves as a powerful tool, offering detailed insights into the properties and dynamics of the collision system under investigation [1,2].

Alignment property of electron vacancies produced by ions $^1H^+$, $^4He^{2+}$, $^{40}Ar^{12+}$ and $^{129}Xe^{30+}$ respectively, is investigated within energy region from $100\times q$ keV to $250\times q$ keV. Here $q$ is the charge state of incident ion. Angular dependence of differential intensity ratios $L_\alpha/L_{\beta1}$ and $L_{\beta2}/L_{\beta1}$ has been studied as a function of the second-order Legendre polynomial $P_2(\cos\theta)$. This approach effectively minimized experimental uncertainties. Subsequently, the anisotropy parameter $\beta$ was transformed into the alignment parameter $\mathscr{A}_{20}$ by incorporating the CK correction coefficient and the anisotropy coefficient.

In order to compare the experimental alignment in different collision processes, the projectile energy is customarily converted to the scaled incident velocity $V = v_p/v_{L_3}$. Here $v_p$ is the projectile velocity and $v_{L_3} = (2E_{L_3}/m_e)^{1/2}$ is the velocity of orbital electron as calculated with electron mass $m_L$ and the binding energy $E_{L_3}$. The results are compared with both experimental data from other studies and theoretical predictions derived using a semiclassical approximation [3]. Notably, excellent agreement was observed only for proton-impact scenarios. Whereas the measured atomic alignment becomes smaller with the increasing of atomic number, as presented in Figure 1. The dealignment coefficient $G_K$ is derived to be 0.98, 0.71 and 0.30 for $^4He^{2+}$, $^{40}Ar^{12+}$ and $^{129}Xe^{30+}$ ions impact, respectively, at $V^2 = 0.011$. Strong dealignment, especially for heavy ions impact (i.e. $^{129}Xe^{30+}$), is demonstrated in experiment due to multiple ionization in target atom [4].

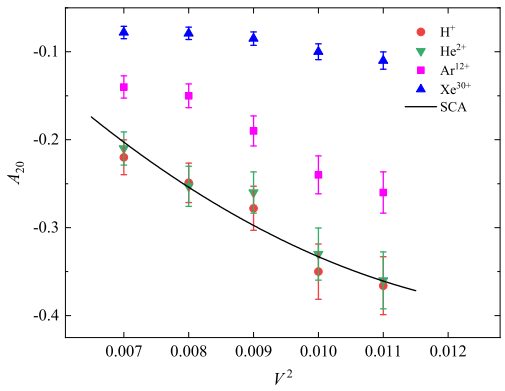


**Figure 1**. Alignment parameter $\mathscr{A}_{20}$ of Ag as a function of the square of scaled projectile velocity $V$. The solid curve is the theoretical prediction by SCA model for $^1H^+$ impact, and the symbols with error bars are the experimental results for $^1H^+$(●), $^4He^{2+}$(▼), $^{40}Ar^{12+}$(■) and $^{129}Xe^{30+}$(▲) ions impact, respectively.

Ionization cross sections $\sigma(\frac{3}{2},\frac{1}{2})$ and $\sigma(\frac{3}{2},\frac{3}{2})$ for high-$Z_t$ targets exhibits a more remarkable increase rate with the increase of incident energy. In addition, the correlation between the ionization cross section $\sigma(\frac{3}{2},\frac{3}{2})$ and $\frac{1}{Z_t^2}$ are manifested ($Z_t$ is the atomic number of the target nucleus). Experimental results are well understood by taking account of probability density distribution of the orbital electrons [5].

## References

[1] Drescher M *et al.* 2002 *Nature* **419** 803
[2] Wang X *et al.* 2023 *Results Phys.* **44** 106196
[3] Wang X *et al.* 2022 *Phys. Rev. A* **105** 052807
[4] Wang X *et al.* 2023 *Phys. Lett. A* **480** 128967
[5] Liu Y *et al.* 2025 *Phys. Lett. A* **541** 130417

*E-mail: wangxingcn@xjtu.edu.cn

P-36

# Vicinage effect on convoy electrons from carbon foils under heteronuclear diatomic ion bombardment

**Y. Yano[1*], U. Ozeki[1], T. Takahashi[2], S. Ishii[2], K. Sasa[1, 2], S. Tomita[1†]**

[1]Institute of Pure and Applied Sciences, University of Tsukuba, Tsukuba, Ibaraki 305-8573, Japan
[2]Tandem Accelerator Complex, CRiES, University of Tsukuba, Tsukuba, Ibaraki 305-8577, Japan

**Synopsis** This study reports the vicinage effect on convoy electron yield from carbon foils under $OH^+$ bombardment at 120 keV/u. A substantial enhancement was observed for $OH^+$ vs $O^+$, with the difference being almost 5 times larger than the $H^+$ yield.

Convoy electrons are forward-emitted electrons with velocities matching emerging projectiles from solid targets. Previous investigations using $C_n^+$ molecular ions demonstrated a substantial enhancement in convoy electron yield compared to the sum of that of constituent atomic ions [1,2]. This molecular effect, termed the vicinage effect [3], stems from the close distances and small relative velocities between the constituent atomic ions dissociated from the molecular ion within the solid target.

The prior studies focused only on homonuclear molecular ions. In these cases, the dissociated constituent atomic ions from molecular ions are identical, resulting in nearly equivalent velocities within the solid. For heteronuclear molecular ions, the relative velocities between the constituent atomic ions increase due to differences in their stopping powers as the target thickness increases. Therefore, the investigation for heteronuclear ions will shed light on the importance of velocity matching between constituent ions. However, vicinage effects in heteronuclear molecular ions remain less explored.

Fig. 1 shows the electron energy spectra obtained for a 4.7 μg/cm² carbon thin film under $OH^+$, $O^+$, and $H^+$ irradiation with energy of 120 keV/u. The yields were normalized to the number of incident molecular, atomic ions. A pronounced peak near 60 eV, matching the incident ion velocity, is attributed to convoy electrons. Fig. 1 reveals a significant enhancement in $OH^+$ over $O^+$ that is larger than the $H^+$ yield. The convoy electron yields were obtained by integrating over the convoy electron peaks. The difference could originate from the existence of an $H^+$ ion moving together with an $O^+$ ion. The difference $Y(OH^+) - Y(O^+)$ is almost 5 times larger than $Y(H^+)$.

The impurity of the $^{17}O^+$ ion in the $OH^+$ beam was monitored according to the ratio of the backscattering yield of O and H from a thin Au target measured on the same ion beam [4]. The obtained impurity of $^{17}O^+$ was 12.5% in the $OH^+$ ion beam. Assuming the same convoy electron yield for $^{17}O^+$ as $^{16}O^+$, the existence of impurity of $^{17}O^+$ would give only 2.2% increase in convoy electron yield of $OH^+$ ions. Thus, the substantial enhancement of $Y(OH^+)$ originates from the existence of an $O^+$ ion moving together with a $H^+$ ion at close distance and nearly the same velocity.

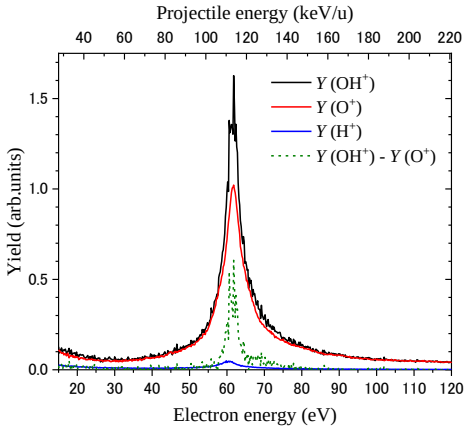


**Fig. 1 The energy spectra obtained for 4.7 μg/cm² carbon thin film under $OH^+$, $O^+$, and $H^+$ irradiation with energy of 120 keV/u, along with the difference between the $OH^+$ and $O^+$ spectra.**

## References

[1] S. Tomita *et al* 2006 Phys. Rev. A 73 060901(R).
[2] Y. Shiina *et al* 2024 Phys. Rev. A 110 062826.
[3] W. Brandt *et al* 1974 Phys. Rev. Lett. 33 1325.
[4] Y. Yano *et al* 2024 UTTAC Annu. Rep. 2023 UTTAC-93 11–12

* E-mail: yano@ilab.bk.tsukuba.ac.jp
† E-mail: tomita@tac.tsukuba.ac.jp

P-37

# Influence of plasma ion state and epitaxial atoms in sputtering system

**Gui-Sheng Zeng**[1] * **and Sheng-Hui Chen**[2] †

[1]National Center for Instrumentation Research, National Institutes of Applied Research, 20 R&D Rd. VI, Hsinchu Science Park, Hsinchu, Taiwan
[2]Department of Optics and Photonics, National Central University, 300 Chung-da Road, Chung-Li, Taoyuan, Taiwan

**Synopsis** The open plasma of the sputtering system will bombard the atoms on the substrate and the film surface, reducing the quality of the epitaxial film. By exploring the relationship between the high-density plasma ion state compressed by the applied voltage and the quality of the film epitaxial film, the best sputtering epitaxial process parameters can be optimized.

In recent years, there has been a marked increase in epitaxial research using sputtering systems for emerging materials such as IGZO, GaN, $Ga_2O_3$, and 2D-$MoS_2$ [1,2]. However, plasma bombardment is a major challenge faced by sputtering systems during epitaxy. This study will explore the relationship between the high-density plasma ion state compressed by an applied voltage and the epitaxial quality of the film layer. Significantly reducing the collision between ions and atoms will effectively improve the epitaxial quality.

Figure 1 shows the change of plasma ion state when voltage is applied. As the voltage increases, the plasma range is significantly concentrated and compressed to avoid plasma bombardment of the substrate surface.

Figure 2 shows XRD measurement, and the results show that the epitaxial quality is significantly improved. However, when the voltage is increased to 98V, the shorter average free path causes the germanium atoms that have left the target surface to be bombarded by argon ions in all directions, causing the germanium atoms to fly away and the epitaxial quality to drop significantly.

Figure 3 shows the oblique incidence of visible light on the sample surface. Due to the Rayleigh scattering principle, the sample with poor epitaxial growth will see short-wavelength blue light preferential scattering due to the presence of too many tiny grains in the film layer, especially at the corners of the epitaxial substrate.

This study proves that by applying appropriate voltage to the chamber, shaft, and bias plate, the plasma ion state can be greatly changed to greatly reduce ion bombardment, which will effectively improve the epitaxial quality.

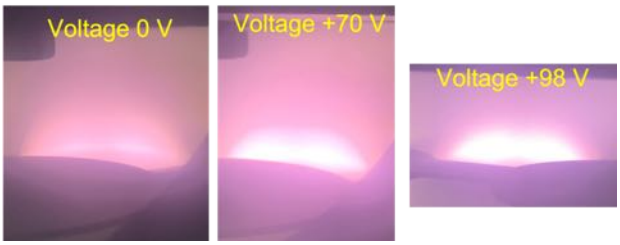


**Figure 1. plasma ion state in sputtering system.**

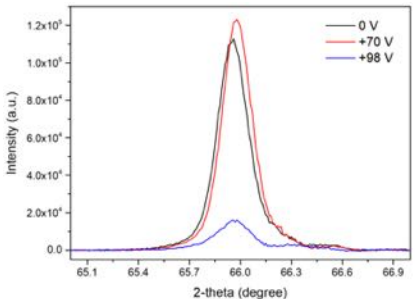


**Figure 2. XRD measurement**.


**Figure 3. oblique incidence of visible light on the sample**.

## References

[1] D. Gupta et al 2022 Inorg. Chem. Commun. 144 109848
[2] D. Pyngrope et al 2024 Mater. Sci. Semicond. Process. 174 108243

* E-mail: 2309241@narlabs.org.tw
† E-mail: ericchen@dop.ncu.edu.tw

# HIGH VOLTAGE ENGINEERING EUROPA B.V.

**The Largest and Most Diverse Designer and Manufacturer of Electrostatic Particle Accelerators for Scientific and Industrial Applications**

## Ion Accelerators

- Air-insulated Ion Accelerators with TV up to 500 kV
- $SF_6$-insulated Singletron Single-ended Ion Accelerators with TV up to 6.0 MV
- $SF_6$-insulated Tandetron Tandem Ion Accelerators with TV up to 6.0 MV
- Vacuum-insulated Tandem Ion Accelerators with TV up to 300 kV

## Electron Accelerators

- Singletron Electron Accelerators with TV up to 6.0 MV/TV

## Ion Implanters

- Beam energies 10 - 60 MeV and higher
- Beam powers up to 25 kW

## Ion Beam Analysis Systems

- Rutherford Backscattering Spectroscopy (RBS)
- Particle Induced X-ray Emission (PIXE)
- Particle Induced Gamma-ray Emission (PIGE)
- Nuclear Reaction Analysis (NRA)
- Elastic Recoil Detection (ERD)
- Medium Energy Ionscattering Spectroscopy (MEIS)

## Accelerator Mass Spectrometers

Vacuum-insulated Tandem and $SF_6$-insulated Tandetron based Systems for the measurement of $^{3}H$, $^{10}Be$, $^{14}C$, $^{26}Al$, $^{36}Cl$, $^{41}Ca$, $^{129}I$ and actinides for application in

- Archeology
- Oceanography
- Geosciences
- Material sciences
- Biomedicine
- Etc.

## Ion Microbeam Systems

- Tandetron and Singletron based Systems

## Neutron Generator Systems

- Air-insulated, Tandetron and Singletron based DC and Pulsed-beam Systems

## Components

Ion and Electron Accelerator Tubes, Ion and Electron Sources,
Beam Handling & Monitoring Equipment, Etc.

**MORE ENERGY FOR RESEARCH**

KYOKUTO BOEKI KAISHA, LTD.
TOKYO, JAPAN
産業インフラソリューショングループ第3ユニット
TEL:03-3244-3525 Email: kbk.acc.team@kbk.co.jp

National Electrostatics Corp.

# A WORLD LEADER IN ION BEAM ANALYSIS SYSTEMS

## National Electrostatics Corp.

National Electrostatics Corp.（NEC）は、1965年にウィスコンシン州ミドルトンで設立された、静電型加速器(ペレトロン）のリーディングカンパニーです。
同社は、75,000平方フィートを超える敷地でCNC加工、金属/セラミック接合、真空部品や電気部品の製作組立から、ペレトロン加速器システム全体のテストまで一貫して行っています。
自社で製作を行っている機器は、製造終了になる事はほぼ無く、寿命の長い加速器として世界中のユーザーに高い評価を頂いています。

■国内導入例

・東京大学　・神戸大学　・東京都市大学　・京都大学　・東北大学　・理化学研究所　・筑波大学
・山形大学　・産業技術総合研究所(AIST)　・奈良女子大学　・神奈川大学　・日本原子力研究開発機構(JAEA)
・東京工業大学　・国立環境研究所　・核融合科学研究所　・量子科学技術研究開発機構(QST)　・民間企業　他

## AMS 専用機

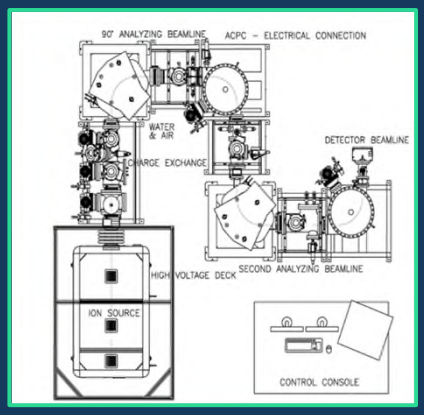


**PIMS(Positive Ion Mass Spectrometry)**

簡便測定(操作性・ワークフロー統合)
ECRイオン源採用(セルフクリーニング可能)
CO2ガスから直接ビーム生成可能
グラファイト、Cs、カソードが不要
従来のAMS装置に比べ非常に省スペース(5 x 5m以内)

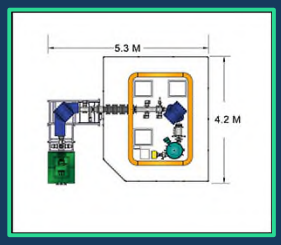


**SSAMS**
加速エネルギー:250kV
測定可能核種：炭素(C)

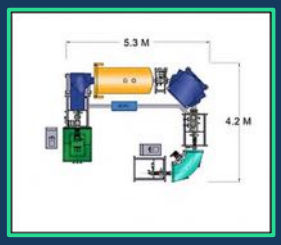


**CAMS**
加速エネルギー:500kV
測定可能核種：炭素(C)

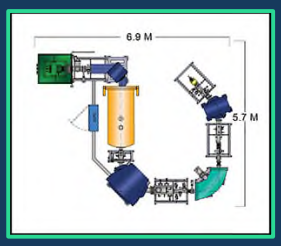


**XCAMS**
加速エネルギー:500kV
測定可能核種：C, Be, Al

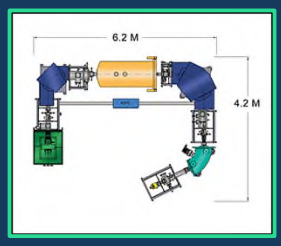


**ICAMS**
加速エネルギー:500kV
測定可能核種：C, I

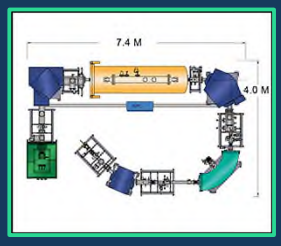


**UAMS**
加速エネルギー:1MV
測定可能核種：C, Be, Al, I, Ca

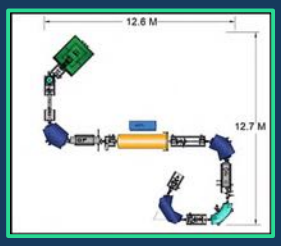


**Actinide AMS**
加速エネルギー:1MV
測定可能核種：C, Be, Al, Ca, アクチノイド

## IBA 専用機

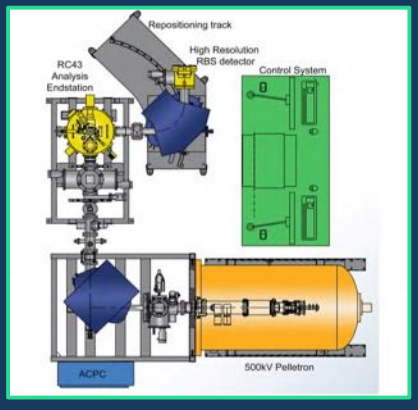


**CARBS(Compact Automated RBS)**

加速エネルギー:500kV
コンパクトレイアウト 4mx3.5m
自動分析機能
優れたビーム安定性(<50eV)
簡単にアップグレード可能(1-2MeV)

## Versatile (AMS & IBA)

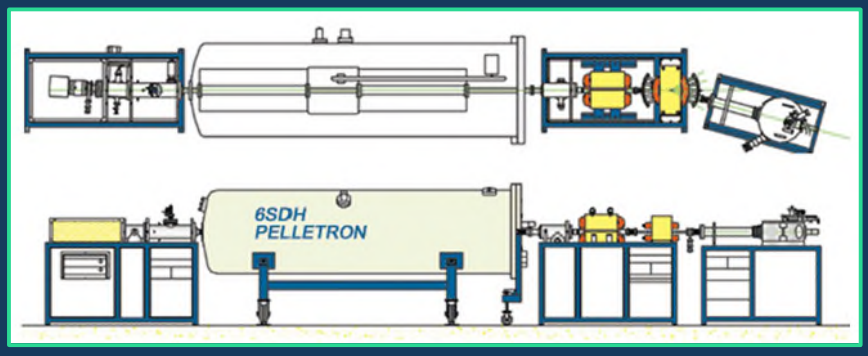


**S-Series**

加速エネルギー:3SDH(1MV), 5SDH(1.7MV), 6SDH(2MV), 9SDH(3MV), 12SDH(4MV), 18SDH(6MV)
AMS、IBAのどちらの用途でも使用可能な汎用モデル
イオン源やビームラインなどカスタマイズ可能


日本総代理店
**伯東株式会社**
住所:東京都新宿区新宿1-1-13
Mail: G5@Hakuto.co.jp
TEL:03-3225-8052


**【取扱い製品】**
・National Electrostatics Corporation
・BUCKLEY SYSTEMS LIMITED
・Group 3 Technologies Ltd.
・D-PACE, Inc

WEBサイトQRコード

真空機器の未来と歩む

# Navatec

**各種真空設備のトータルプランを**
**お客様のニーズに合わせご提供いたします。**

TURBO MOLECULAR PUMP

DRY PUMP(ECO DRY)

TURBO LAB

HELIUM LEAK DETECTOR

VACUUM GAUGE

DRY PUMP(NEODRY)

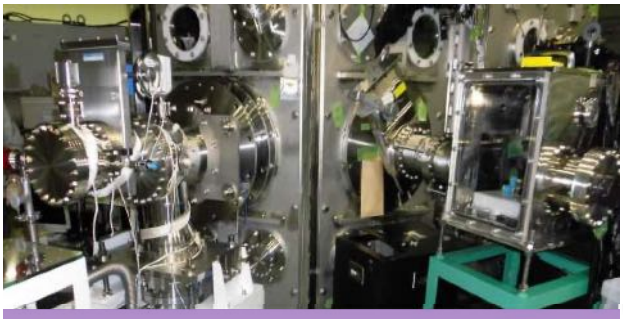

CHAMBER SYSTEM

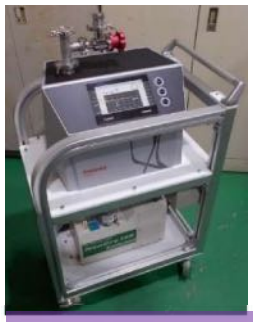

TURBO･DRY PUMP SYSTEM

| PRODUCT　LINE | |
|---|---|
| **真空機器販売** | ターボ分子ポンプ・ドライ真空ポンプ・ヘリウムリークディテクタ<br>油回転ポンプ・油拡散ポンプ・ルーツポンプ・真空計　など |
| **真空排気装置・真空容器等<br>設計製作** | ＴＭＰ高真空排気装置・補助排気系付きリーク検査装置<br>超高真空対応真空チャンバー・角型真空容器　など |
| **真空機器メンテナンス** | 油回転ポンプ・ルーツポンプ・ドライ真空ポンプ<br>油拡散ポンプ・真空バルブ・ヘリウムリークディテクタ　など |
| **真空部品類販売** | 真空フランジ・継手・フレキシブルチューブ・真空グリス<br>真空ポンプ用オイル（鉱物油、合成油、フッ素油）　など |


Navatec

**株式会社ナバテック**

〒583-0841
大阪府羽曳野市駒ヶ谷 39-1

TEL　：072-957-7107
FAX　：072-957-7102
E-mail：navatec@cyber.ocn.ne.jp

ナバテック　検索